RECONSTRUCTION OF PAST PRECIPITATION IN SOUTH-WEST TÜRKİYE FROM VARVED SEDIMENTS OF KÖYCEĞİZ LAKE

A THESIS SUBMITTED TO
THE GRADUATE SCHOOL OF NATURAL AND APPLIED SCIENCES
OF
MIDDLE EAST TECHNICAL UNIVERSITY

BY

ORHAN KARAMAN

IN PARTIAL FULFILLMENT OF THE REQUIREMENTS
FOR
THE DEGREE OF MASTER OF SCIENCE
IN
GEOLOGICAL ENGINEERING

NOVEMBER 2025

Approval of the thesis:

RECONSTRUCTION OF PAST PRECIPITATION IN SOUTH-WEST TÜRKİYE FROM VARVED SEDIMENTS OF KÖYCEĞİZ LAKE

submitted by **ORHAN KARAMAN** in partial fulfillment of the requirements for the degree of **Master of Science** i**n Geological Engineering, Middle East Technical University** by,

Prof. Dr. Naci Emre Altun
Dean, **Graduate School of Natural and Applied Sciences** _____

Prof. Dr. Erdin Bozkurt
Head of the Department, **Geological Engineering** _____

Assoc. Prof. Dr. Ulaş Avşar
Supervisor, **Geological Engineering, METU** _____

Examining Committee Members:

Assoc. Prof. Dr. Atilla Arda Özacar
Geological Eng, METU _____

Assoc. Prof. Dr. Ulaş Avşar
Geological Eng., METU _____

Assoc. Prof. Dr. Fatma Toksoy Köksal
Geological Eng., METU _____

Prof. Dr. Mustafa Tuğrul Yılmaz
Civil Eng., METU _____

Assoc. Prof. Dr. Şule Gürboğa
Geological Eng., ITU _____

Date: 27.11.2025

I hereby declare that all information in this document has been obtained and presented in accordance with academic rules and ethical conduct. I also declare that, as required by these rules and conduct, I have fully cited and referenced all material and results that are not original to this work.

Name Last name : Orhan Karaman

Signature :

ABSTRACT

RECONSTRUCTION OF PAST PRECIPITATION IN SOUTH-WEST TÜRKİYE FROM VARVED SEDIMENTS OF KÖYCEĞİZ LAKE

Karaman, Orhan
Master of Science, Geological Engineering
Supervisor : Assoc. Prof. Dr. Ulaş Avşar

November 2025, 94 pages

High-resolution paleoclimate records offer valuable insights into historical climate changes and current climate trends that extend beyond the scope of instrumental data. Among various paleoclimate records, annually laminated lacustrine sediments, known as varves, allow for the extraction of finely resolved climate proxies and provide precise chronological control. This study aims to construct a high-resolution past precipitation reconstruction from the varved sediments of Köyceğiz Lake in southwestern Türkiye. A 124.95 cm-long gravity core was analyzed using ITRAX micro-XRF core scanning at a 0.2 mm resolution. Varve counting determined that the sedimentary record spans a total of 609 years. The ITRAX data, corresponding to winter-spring laminae, examined for potential correlations with precipitation measurements from meteorological stations in Muğla, Köyceğiz, Dalaman and Marmaris. Due to the natural interdependencies between geochemical variables, five Principal Components (PC) were created using Principal Component Analysis (PCA) on the dataset. Subsequently, these components were used in a Multiple Linear Regression (MLR) model to create a precipitation reconstruction spanning

approximately 500 years. The resulting paleoclimate trend was compared with 3 different reconstructions, created with different methods obtained from different studies, across Türkiye. In conclusion, the reconstruction generated within this study was shown to exhibit the same trend as other reconstructions obtained from the three other studies. It is concluded that the precipitation reconstruction generated in this study is consistent with both historical records and existing paleoclimatic studies.

Keywords: Paleoclimatology, Precipitation Reconstruction, Varve, Principal Component Analysis (PCA), Multiple Linear Regression (MLR).

ÖZ

TÜRKİYE'NİN GÜNEYBATISINDA BULUNAN KÖYCEĞİZ GÖLÜNÜN VARV SEDİMANLARINDAN GEÇMİŞ YAĞIŞ VERİLERİNİN OLUŞTURULMASI

Karaman, Orhan
Yüksek Lisans, Jeoloji Mühendisliği
Tez Yöneticisi: Doç. Dr. Ulaş Avşar

Kasım 2025, 94 sayfa

Yüksek çözünürlüklü paleoiklim kayıtları, tarihsel iklim değişiklikleri ve enstrümantal verilerin ötesinde güncel iklim eğilimleri hakkında değerli bilgiler sunar. Çeşitli paleoiklim kayıtları arasında, varv olarak bilinen yıllık tabakalar halinde bulunan gölsel tortulları, yüksek çözünürlükte iklim göstergeleri elde edilmesine ve hassas ölçüde kronolojik kontrol sağlanmasına olanak tanır. Bu çalışma, Türkiye'nin güneybatısında bulunan Köyceğiz Gölündeki varv sedimanlarından yüksek çözünürlüklü paleo-yağış verileri çıkarmayı amaçlamaktadır. 124.95 cm uzunluğundaki bir gravite karotiyerinden alınan karotlar, 0.2 mm çözünürlükte ITRAX mikro-XRF karot taraması kullanılarak analiz edilmiştir. Varv sayımı, sediman kayıtlarının toplamda 609 yıla yayıldığını belirlemiştir. Kış-ilkbahar tabakaları ile ilişkili ITRAX verileri, Muğla, Köyceğiz, Dalaman ve Marmaris'teki meteorolojik istasyonlardan alınan yağış ölçümleri ile potansiyel korelasyonlar açısından incelenmiştir. Jeokimyasal değişkenler arasındaki doğal karşılıklı bağımlılıklar nedeniyle, veri seti üzerinde Temel Bileşen Analizi (PCA) uygulanarak beş Temel Bileşen (PC) oluşturulmuştur. Daha sonra, bu bileşenler Çoklu Doğrusal Regresyon (MLR) modelinde kullanılarak yaklaşık 500 yıllık bir yağış rekonstrüksiyonu oluşturulmuştur. Elde edilen bu paleoiklim trendi,

Türkiye genelinde farklı yöntemlerle yapılmış üç farklı rekonstrüksiyon ile karşılaştırılmıştır. Sonuç olarak, bu çalışma kapsamında üretilen rekonstrüksiyonun, diğer üç çalışmadan elde edilen rekonstrüksiyonlarla aynı trendi sergilediği gösterilmiştir. Bu çalışmada oluşturulan yağış rekonstrüksiyonunun hem tarihsel kayıtlarla hem de mevcut paleoiklim çalışmalarla tutarlı olduğu sonucuna varılmıştır.

Anahtar Kelimeler: Paleoiklim, Yağış Rekonstrüksiyonu, Varv, Temel Bileşen Analizi (PCA), Çoklu Doğrusal Regresyon (MLR).

To My Parents, Seza and Cahit...

ACKNOWLEDGMENTS

This study uses data obtained within the scope of the project titled “Köyceğiz Gölü (Muğla) Varvlı Sedimanlarında Sedimanter Deprem Kayıtlarının İncelenmesi”, which was funded by the Scientific and Technological Research Council of Türkiye (TÜBİTAK, Project No: 117C021).

Firstly, I would like to express my deepest gratitude to my supervisor, Assoc. Prof. Ulaş Avşar, for his invaluable guidance, constant encouragement, and insightful feedback throughout this research.

I am also grateful to the members of my thesis committee, Assoc. Prof. A. Arda Özacar, Assoc. Prof. Fatma Toksoy Köksal, Prof. Dr. M. Tuğrul Yılmaz and Assoc. Prof. Şule Gürboğa for their constructive comments and suggestions that helped refine the scope of this work. I would like to express my profound gratitude to Prof. Dr. M. Lütfi Süzen for his invaluable life and academic guidance since my undergraduate years.

I would like to express my sincere gratitude to my brothers, Alper Al and Ozan Uysal, who never failed to provide me with unshakable and endless support during the most challenging stages of this journey. I also express my deepest gratitude to Hilal Ergili, who laid the foundation for my current academic path with her uninterrupted academic guidance and friendship since my first year of university. I also extend my sincere thanks to Hakan Bora Okay and Mert İnanç Örge. Beyond the invaluable technical expertise, they provided during the thesis process, their mentorship and friendship have been the cornerstones of my progress. Finally, I would like to thank Kaan Onat and Ozan Sinoplu, who have constantly encouraged and supported me despite the great distance and continents between us.

Last but certainly not least, I am eternally grateful to my family for their endless support, patience, and love during the long and often challenging process of writing this thesis. This work is dedicated to them.

TABLE OF CONTENTS

ABSTRACT v

ÖZ vii

ACKNOWLEDGMENTS x

TABLE OF CONTENTS xi

LIST OF FIGURES xiii

CHAPTERS

1 INTRODUCTION 1

1.1 Study Area 4

1.2 Climate Proxy Records of Lacustrine Sediments 6

1.3 Literature Review of Paleoclimatic Studies 7

1.3.1 Paleoclimatic Studies based on Lacustrine Sediments 8

1.3.2 Paleoclimatic Studies Based on Tree Rings and Caves 12

1.3.3 Paleoclimatic Reconstructions Based on Advanced Statistical Methods 15

2 MATERIALS AND METHODS 17

2.1 Bathymetric Survey, Sediment Coring and Core Splitting 17

2.2 ITRAX Micro-XRF Core Scanning 17

2.3 Varve Chronology Construction 18

2.4 Multiple Linear Regression Analysis 20

2.5 Principal Component Analysis 22

3 RESULTS 23

3.1 Optical Image and ITRAX Micro-XRF Data 23

3.2 Varve Chronology and Meteorological Station Data Correlation 25

4 DISCUSSION 43
4.1 Element-ratio Profiles for the Past Precipitation Reconstruction 43
4.2 Multiple Regression Analysis for the Past Precipitation Reconstruction 45
4.3 Principal Component Analysis and Multiple Regression Analysis for the Past Precipitation Reconstruction 63
5 CONCLUSION AND RECOMMENDATIONS 77
REFERENCES 79
APPENDICES 85

LIST OF FIGURES

Figure 1.1 a) Location of Köyceğiz Lake in Türkiye. J is Jsibeli Forest and N is Nar Lake. b) Topography (relief-shaded) and geological units located in the catchment are of the lake (Modified from Avşar et al., 2016). The locations of KYC-J core used in this study and G04 core used in Akçer-Ön study (2017). c) Meteorological stations which are located near the study area. 6
Figure 3.1. Close-up view of 3 examples from winter seasons. Yellow lines indicating depressions in Ca/Ti ratio and showing the level of winter seasons (Taken from Karadaş, 2022). 24
Figure 3.2. a) Age-depth model of the core KYC-J based on the varve construction. b) Varve thickness variation along the core based on the determined thickness according to the constructed varve chronology. 25
Figure 3.3. Graph shows the average precipitation amounts for every month for 4 meteorological stations. “Summer” months are the months in yellow part, “winter” months are the months in the darker part. 26
Figure 3.4. Gray lines indicating raw data (Ca/Ti ratio from varve chronology) and black lines are showing the trend derived from 21 point moving average calculation. 27
Figure 3.5. The figure shows the correlation between precipitation data and corresponding geochemical data obtained from Ti/Ca ratio. Blue lines are showing the precipitation data and black lines are showing the Ti/Ca ratio. 29
Figure 3.6. Matrixes showing R^2 values of all possible elemental and non-elemental ratios with winter precipitation records of Muğla station. a) matrix shows annual geochemical data vs meteorological station b) matrix shows 7-point moving average values vs meteorological station. The color scale used in all matrices is same. Green color shows higher and red color shows lower R^2 values. 31
Figure 3.7. Matrixes showing R^2 values of all possible elemental and non-elemental ratios with winter precipitation records of Köyceğiz station. a) matrix shows annual

geochemical data vs meteorological station b) matrix shows 7-point moving average values vs meteorological station. The color scale used in all matrices is same. Green color shows higher and red color shows lower R^2 values. 32
Figure 3.8. Matrixes showing R2 values of all possible elemental and non-elemental ratios with winter precipitation records of Marmaris station. a) matrix shows annual geochemical data vs meteorological station b) matrix shows 7-point moving average values vs meteorological station. The color scale used in all matrices is same. Green color shows higher and red color shows lower R^2 values.33
Figure 3.9. Matrixes showing R^2 values of all possible elemental and non-elemental ratios with winter precipitation records of Dalaman station. a) matrix shows annual geochemical data vs meteorological station b) matrix shows 7-point moving average values vs meteorological station. The color scale used in all matrices is same. Green color shows higher and red color shows lower R^2 values. 34
Figure 3.10. Graphs showing the correlation of rainfall data with smooth and unsmooth ratios prepared for 4 meteorological stations. The top row of the two rows prepared for each station shows the correlations for unsmooth, while the bottom line shows the correlations for smooth. The blue lines in the graphs represent precipitation, while the black lines represent the ratio data. The value written below each ratio shows the R^2 value of that ratio. The values written below the R^2 show the p-test result for that ratio, and the color of the result indicates whether the ratio is significant (green) or insignificant (red). Note that negative signs in the ratios mean negative correlation. 36
Figure 3.11. A matrix constructed by taking the average of all ratios produced separately for all meteorological stations using the 7-points moving average method (matrices in Figure 3.6 to Figure 3.9). The color scale is the same as the scale in the matrices above. The 16 ratios with the highest R^2 values and geochemically meaningful results are marked with a black frame. 38
Figure 3.12. Precipitation reconstruction curves derived from the 16 ratios. Black lines are indicating Marmaris, brown colored lines belong to Köyceğiz, red lines are indicating Muğla and blue lines are showing the Dalaman meteorological

station. Yellow horizontal lines indicating with “D1, D2, etc.” are dry purple lines with “W1, W2, etc.” periods are indicating wet periods implied by the curves. 40
Figure 4.1. Results of PCA on 16 elemental ratios and winter precipitation of Muğla station. a) Precipitation reconstructions constructed by using single variable regression derived from PCs. Note that y-axis shows years while x-axis shows the precipitation amount. b) Correlation coefficients of each elemental ratios with 5 PCs. 44
Figure 4.2. Results of MLR analysis for 4 meteorological stations’ “winter precipitation data and “winter” geochemical data (17 elemental and 3 non-elemental data) and varve thicknesses. Blue lines are indication “winter” precipitations recorded in meteorological stations. Black lines are the trends created after MLR. The precipitation and geochemical data are not smoothed with 7-points moving average. 46
Figure 4.3. Precipitation reconstructions for 4 meteorological stations derived from the formulas obtained with MLR. Red horizontal layers are example periods which indicate the inconsistencies between trends and green horizontal layers are example periods which show a consistent period of the trends. Y- axis shows years and x-axis shows precipitation amount in mm. Note that Marmaris’ trend is reaching negative precipitation values. 47
Figure 4.4. Upper Lower Operation results for Muğla and Köyceğiz stations. a) The upper half of the instrumental data is used for deriving equation, and the lower half is used for precipitation prediction for Muğla station. c) The lower half of the instrumental data is used for eqaution, and the upper half is predicted for Muğla station. b) The upper half of the instrumental data is used for equation, and the lower half is used for precipitation prediction for Köyceğiz station. d) The lower half of the instrumental data is used for equation, and the upper half is predicted for Köyceğiz station. Note that negative precipitation in a and d. 48
Figure 4.5. Graphs and R^2 values of the graphs are showing the results of “Odd Even Operation” performed for Muğla meteorological station’s “winter” precipitation data. Blue lines are representing actual “winter” precipitation and

black lines are showing the MLR results of the operation. X-axis and y-axis show precipitation (mm) and years respectively. 51
Figure 4.6. Graph showing the predicted trend derived from “Odd Even Operation” for Muğla station. Trend on the left (dark blue) representing the reconstruction derived from the formula obtained from even years (called as “by even years”) and right trend (light blue) resulted from odd year’s equation (called as “by odd years”). Time periods a, b and c are showing examples of inconsistencies between two trends. 52
Figure 4.7. Graphs and R^2 values of the graphs are showing the results of “Odd Even Operation” performed for Köyceğiz meteorological station’s “winter” precipitation data. Blue lines are representing actual “winter” precipitation and black lines are showing the MLR results of the operation. X-axis and y-axis show precipitation (mm) and years respectively. 54
Figure 4.8. Graph showing the predicted trend derived from “Odd Even Operation” for Köyceğiz station. Trend on the left (dark blue) representing the reconstruction derived from the formula obtained from even years (called as “by even years”) and right trend (light blue) resulted from odd year’s equation (called as “by odd years”). Note that precipitation values implied by "by even years" trend has negative values. 55
Figure 4.9. Graphs and R^2 values of the graphs are showing the results of “Odd Even Operation” performed for Muğla meteorological station’s “winter” precipitation data. Note that the precipitation, geochemical and varve thickness data is smoothed with 7-point moving average method. Blue lines are representing actual “winter” precipitation and black lines are showing the MLR results of the operation. X-axis and y-axis show precipitation (mm) and years respectively..... 56
Figure 4.10. Graph showing the predicted trend derived from “Odd Even Operation” for Muğla station. Trend on the left (dark blue) representing the reconstruction derived from the formula obtained from smoothed even years (called as “by even years”) and right trend (light blue) resulted from smoothed odd year’s equation (called as “by odd years”). 58

Figure 4.11. Graphs and R2 values of the graphs are showing the results of “Odd Even Operation” performed for Köyceğiz meteorological station’s “winter” precipitation data. Note that the precipitation, geochemical and varve thickness data is smoothed with 7-point moving average method. Blue lines are representing actual “winter” precipitation and black lines are showing the MLR results of the operation. X-axis and y-axis show precipitation (mm) and years respectively. 59
Figure 4.12. Graph showing the predicted trend derived from “Odd Even Operation” for Köyceğiz station. Trend on the left (dark blue) representing the reconstruction derived from the formula obtained from smoothed even years (called as “by even years”) and right trend (light blue) resulted from smoothed odd year’s equation (called as “by odd years”). Note that precipitation values implied by "by even years" trend has negative values. 61
Figure 4.13. Component Coefficients for the 5 principal components derived from PCA. This table displays the correlation between each of the original 20 variables (elemental and non-elemental proxies) and the constructed PCs. High absolute values (highlighted in green) indicate a strong statistical relationship between the variable and the corresponding principal component. Note that cps is counts per second, “W_S” is the ratio of Winter/Summer thickness of the varves and “TW” is winter varve thickness..... 64
Figure 4.14. Graphs showing the PCs and their correlations with most dominant components. Black lines are PCs’ trends and gray lines are component’s trends. . 64
Figure 4.15. Upper Lower Operation results for Muğla and Köyceğiz stations. The operation is conducted with PCs and equations are derived from MLR. a) The upper half of the instrumental data is used for deriving equation, and the lower half is used for precipitation prediction for Muğla station. c) The lower half of the instrumental data is used for equation, and the upper half is predicted for Muğla station. b) The upper half of the instrumental data is used for equation, and the lower half is used for precipitation prediction for Köyceğiz station. d) The lower half of the instrumental data is used for equation, and the upper half is predicted for Köyceğiz station..... 65

Figure 4.16. Graphs and R^2 values of the graphs are showing the results of "Odd Even Operation" performed for Muğla meteorological station's smoothed "winter" precipitation data with PCs. Blue lines are representing actual "winter" precipitation and black lines are showing the MLR results of the operation. X-axis and y-axis show precipitation (mm) and years respectively. 67
Figure 4.17. Graph showing the predicted trend derived from "Odd Even Operation" between PCs and Muğla station. Trend on the left (dark blue) representing the reconstruction derived from the formula obtained from smoothed even years (called as "by even years") and right trend (light blue) resulted from smoothed odd year's equation (called as "by odd years"). 69
Figure 4.18. Graphs and R^2 values of the graphs are showing the results of "Odd Even Operation" performed for Köyceğiz meteorological station's smoothed "winter" precipitation data with PCs. Blue lines are representing actual "winter" precipitation and black lines are showing the MLR results of the operation. X-axis and y-axis show precipitation (mm) and years respectively. 70
Figure 4.19. Graph showing the predicted trend derived from "Odd Even Operation" between PCs and Köyceğiz station. Trend on the left (dark blue) representing the reconstruction derived from the formula obtained from smoothed even years (called as "by even years") and right trend (light blue) resulted from smoothed odd year's equation (called as "by odd years"). 71
Figure 4.20. Table of element coefficients from the equation generated by element-based MLR and table of PC coefficients from the equation generated by PC-based MLR for 5 different precipitation data from 5 different meteorological stations. .. 72
Figure 4.21. Figure showing the comparison of Element-based MLR and PC-based MLR methodologies applied to varve thickness and geochemical data to obtain long term precipitation reconstructions for 5 different meteorological stations. Note that negative precipitation values are implied by Element-based MLR results. Tables below the graphs show R^2 values of the correlations between reconstructions produced for different stations using the same methodology. 73

Figure 4.22. The figure compares 4 precipitation reconstructions that have been conducted in Türkiye. The reconstruction labeled Nar Lake originates from a varved lake study, utilizing the O^{18} ratio (Jones et al., 2006). The Sofular Cave record was obtained from a speleothem study dated using C^{13} (Fleitmann et al., 2009). The trend labeled Köyceğiz Lake represents a prior paleoclimate study carried out at Köyceğiz (Akçer-Ön, 2017). Red lines indicate similar events implied by different trends. Note that drier and wetter axis are reversed in Nar Lake graph. 74

CHAPTER 1

INTRODUCTION

Climate is a crucial determinant for humankind because it directly influences human life in terms of essential activities, such as agricultural practices and architectural designs. The climate is currently changing due to multiple factors, and humanity must be prepared to adapt to these shifts to survive and thrive. Therefore, critical climatic elements, like the precipitation regime and temperature, must be accurately recorded and analyzed to properly understand changes occurring over time. However, instrumental precipitation and temperature records typically do not exceed 300 years (NWS, n.d.), creating a major limitation in long-term climate assessment. The limited coverage of instrumental records restricts obtaining more comprehensive knowledge of past climate regimes. Thus, geological archives allow scientists to obtain climate records covering more timeline than instrumental records. These main archives can be listed as ice cores, dendrochronology, corals, speleothems and lacustrine sediments.

Ice cores, obtained from polar and mountain glaciers, provide a high-resolution vertical climate chronology extending more than 750,000 years. These cores provide records of paleo-temperatures with stable oxygen isotopes, past atmospheric gas composition from trapped air bubbles, and accumulation rates from layer thicknesses. While ice cores are critical for understanding glacial cycles, their spatial coverage is restricted with high latitudes and altitudes. Therefore, this method has more temporal coverage but less spatial coverage than the instrumental records (NASA Earth Observatory, 2005).

Another crucial non-instrumental archive can be provided by dendrochronology study, which is defined as the scientific study of tree ring growth. Trees annually produce a new ring and the ring's width, and density reflect the environmental conditions of that season in which that ring is growth. Since climate (temperature

and precipitation amount) plays a significant role on tree's growth, the patterns within these rings serve as high-resolution proxy data for local and regional paleoclimate. While a single tree can provide limited information, cross-dating and collecting thousands of samples can establish robust chronologies, such as the 12,500-year sequence for oak. Although the method can be used for limited areas where specific, long-lived tree species exist, dendrochronology is important because it has high resolution annual chronology. Consequently, it provides a useful tool for reconstructing paleo-precipitation and understanding pre-historical drought times and extreme temperatures (Environmental Science, n.d.).

Corals (specifically their calcium carbonate skeletons) provide an archive for reconstructing tropical ocean climate variability. As corals grow, seasonal changes in water temperature, light, and nutrient conditions lead to variations in skeletal density which is creating annual growth bands similar to those that existed in trees. This precise annual banding allows scientists to date samples to an exact year and season. Chemical analysis of the trapped oxygen isotopes within these bands provides information for estimating seasonal ocean temperatures and rainfall through time. Critically, corals are highly sensitive to climatic stress, such as ocean acidification and temperature changes, enabling paleoclimatologists to determine past extreme climate conditions (NOAA NCEI, n.d.).

Speleothems are cave formations such as stalactites, stalagmites, and flowstones and they provide a valuable archive for terrestrial climate reconstruction because they are located deep underground and thus protected from erosion and surface weathering that can compromise other land-based records. They are formed when mineral-rich groundwater drips into a cave, calcium carbonate is deposited as thin, successive layers. The thickness of these accumulated growth layers directly reflects the amount of water infiltrating through the cave. Rapid growth often suggests high precipitation, while little growth may indicate drought conditions. Scientists can determine the age of the layers using Uranium-Thorium radioisotopic dating by measuring the predictable decay of uranium into thorium. Furthermore, the oxygen isotope ratios preserved in the calcite rock provide crucial clues about the climate at

the time of formation, including air temperature and the amount or origin of local precipitation. Since caves are distributed across the globe, speleothems have the potential to provide a comprehensive land-based record of past climate. (NASA Earth Observatory, 2005)

Lacustrine sediments are regarded as highly valuable continental archives for reconstructing past climatic and environmental conditions, especially at decadal and even annual timescales. They capture a wide range of environmental signals that reflect both changes in the water column and within the lake's surrounding catchment. To explore these signals, researchers employ a combination of geochemical, sedimentological, and biological techniques. The resulting data, which is known as climate proxies, are essential for interpreting historical climate variability as well as human-induced impacts on both the lake and its watershed. Unlike some other natural archives, lake sediments are more widespread and can be found in diverse environmental contexts. When these sediments are analyzed using high-resolution methods and robust dating techniques, they offer more comprehensive insights into past climates than other continuous terrestrial records such as speleothems or tree rings (Zolitschka and Enters, 2009). If fine laminae are identified within these lake sediments and confirmed to represent annual layers, they are classified as varved sediments (Zolitschka, 1991). The formation of these annual layers is predominantly driven by seasonal variations in temperature and precipitation. Depending on the lake's geographic location, geomorphology, and underlying geology, several types of varves may develop, including clastic, organic/biogenic, endogenic, or mixed forms (O'Sullivan, 1983; Zolitschka et al., 2015). Each varve typically consists of two or more thin seasonal sub-layers that differ in color, composition, texture, structure, and thickness. The alternating light and dark layers within a varve represent one full year of sediment deposition. Two key conditions are necessary for varve preservation: first, a seasonal rhythm in sediment deposition must exist; second, the lake bottom must be oxygen-depleted to prevent bioturbation by benthic organisms, which would otherwise disrupt the laminated structure (Weinheimer and Biondi, 2003). Most notably, varves provide

unparalleled chronological control. By counting individual annual layers within a sediment core, researchers can establish a precise calendar-year timeline. This combination of seasonal resolution and exact dating makes varved sequences exceptionally valuable as high-resolution climate archives (Zolitschka, 2003; Tylmann et al., 2013; Zolitschka et al., 2015). As discussed above, such natural archives preserve climate proxies-indicators of past environmental and climatic conditions-which are highly sensitive to a range of ecological and atmospheric influences.

The study of paleoclimatological records preserved in lake varves is essential for understanding the dynamics of past climate systems. As annually laminated sediments, varves offer one of the most precise natural archives, capturing environmental changes with a resolution that few other records can provide. The notion that “the present is the key to the past, and the present lights the way to the future” emphasizes the value of these archives: observations of present-day processes allow us to decode the imprints of past variability, while at the same time informing our expectations of future change. In the context of this study, the proxies obtained from lacustrine sediments will be briefly introduced in the following sections.

1.1 Study Area

Köyceğiz Lake is located in the southwestern part of Türkiye, within the Eastern Mediterranean region, specifically in Muğla Province (Figure 1.1). With a surface area of approximately 52 km², it ranks among the 20 largest lakes in the country. The lake's catchment area extends over 875 km² and features an elevation gradient reaching up to 2200 meters above sea level (Avşar et al., 2016; Avşar and Kurtuluş, 2017). The main tributaries feeding the lake are the Yuvarlak, Namnam, and Köyceğiz streams. Its outflow occurs through the Dalyan Channel, which connects the lake to the Mediterranean Sea. The region experiences a typical Mediterranean climate, characterized by hot, dry summers and mild, wet winters. Köyceğiz Lake

has been classified as a meromictic lake, indicating that its bottom waters remain permanently anoxic (Kazancı et al., 1992; Bayarı et al., 1995; Kazancı et al., 2008). In such systems, water column mixing during seasonal turnover is limited to the upper layers, leaving deeper waters isolated from atmospheric oxygen (Anderson et al., 1985). A study by Avşar et al. (Avşar et al., 2016) reported the presence of carbonaceous-organic varved sediments in Köyceğiz Lake. These annual varves consist of alternating layers: a light-colored, calcium-rich lamina deposited during the summer, and darker, clastic and organic-rich layers formed during the autumn and winter seasons. The lake is composed of two distinct sub-basins: the Köyceğiz Basin in the north and the Sultaniye Basin in the south (Kazancı et al., 1992). According to bathymetric data presented by Avşar et al. (2016), the maximum depth reaches 26 meters in the northern basin and 32 meters in the southern basin (Figure 1.1b). Geologically, southwestern Anatolia is dominated by the Lycian Nappes and Quaternary alluvial deposits. The Lycian Nappes are stratigraphically divided into three main units from bottom to top: the Yeşilbarak, carbonate, and Marmaris nappes. The Yeşilbarak Nappe, dating from the Late Lutetian to Early Burdigalian, primarily consists of shales and sandstones. All regional formations are overlain by the Lower Cretaceous-aged Marmaris Nappe (Şenel, 1997; Kurtuluş et al., 2019). Within the lake's catchment area, peridotites represent the dominant lithology, accounting for approximately 60% of the geological composition (Avşar et al., 2016).

The aim of this thesis is to reconstruct past precipitation patterns in the Köyceğiz Lake region (SW Türkiye) by analyzing varved lake sediments. This study utilizes geochemical data obtained from an ITRAX micro-XRF core scanner along a single, undisturbed gravity core, allowing for high-resolution examination of sediment composition. By interpreting variations in elemental concentrations and their relationship to hydrological and climatic processes, the research seeks to provide insights into long-term rainfall variability and its potential drivers. Ultimately, the findings aim to improve our understanding of past regional climate dynamics and

contribute to broader discussions on how precipitation patterns have changed over time in response to natural and possibly anthropogenic influences.

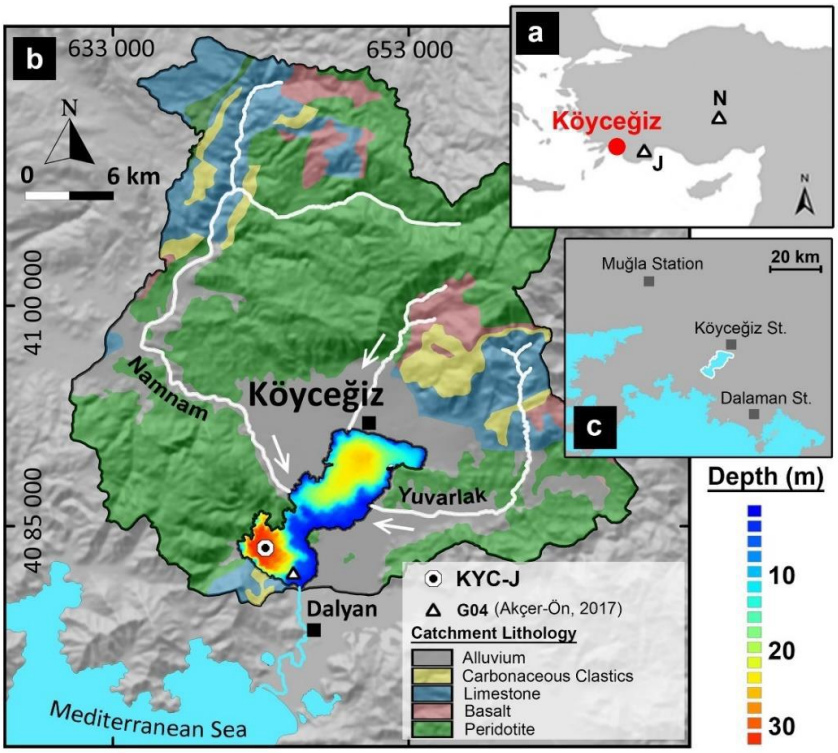

Figure 1.1 a) Location of Köyceğiz Lake in Türkiye. J is Jsibeli Forest and N is Nar Lake. b) Topography (relief-shaded) and geological units located in the catchment are of the lake (Modified from Avşar et al., 2016). The locations of KYC-J core used in this study and G04 core used in Akçer-Ön study (2017). c) Meteorological stations which are located near the study area.

1.2 Climate Proxy Records of Lacustrine Sediments

Lacustrine sediments serve as invaluable archives of past environmental and climatic conditions, offering high-resolution records that extend back thousands to even millions of years. Unlike marine or ice core records, lake sediments often provide more regionally sensitive insights into climatic variability, making them especially useful for reconstructing local paleoenvironments. These sediments accumulate in stratified layers over time, each layer potentially preserving a snapshot of the

surrounding climate and catchment conditions at the time of its deposition. Through the analysis of various proxies-such as biogenic components (e.g., pollen, diatoms, ostracods), geochemical signatures (e.g., stable isotopes, elemental ratios), and sedimentological features (e.g., grain size, varve structure) researchers can reconstruct parameters like temperature, precipitation, hydrology, vegetation dynamics, and even anthropogenic impacts. The reliability of lacustrine proxies depends on their sensitivity to environmental change and the fidelity with which they are preserved in the sediment record. In particular, closed-basin lakes or those with limited catchment disturbance often provide some of the most continuous and interpretable archives. Additionally, advances in dating methods such as radiocarbon dating, varve counting, and tephrochronology have greatly improved the chronological control of lake sediment sequences. As climate continues to change understanding long-term natural variability becomes more crucial. Lake sediment proxies not only enhance our understanding of past climate dynamics but also inform predictive models by offering analogues for current and future changes. In this sense, they bridge the gap between natural archives and societal relevance, transforming passive sedimentary records into active tools for understanding Earth's climate system.

1.3 Literature Review of Paleoclimatic Studies

Various paleoclimatic studies have been conducted with different techniques in Anatolia in the last decades. Most of the studies are conducted based on proxies such as lacustrine sediments, speleothems and dendrochronology in Anatolia and the neighboring area of the study area. These studies' most recent ones (studies after 2000) were summarized below.

1.3.1 Paleoclimatic Studies based on Lacustrine Sediments

Wick et al. (2003) conducted a study on Lake Van, which is a varved lake and it is in eastern part of Anatolia. Based on the study's constructed varve chronology, varve span is about 1300 years. Sediment cores are examined by using multiple proxies of geochemical, stable-isotopic, pollen and charcoal analyses.

In a study conducted by Eastwood et al. (2007), Gölhisar Lake, that is located in southwest of Türkiye, was studied for understanding Holocene climate change by using stable isotope and pollen data obtained from the lake. The study was conducted by comparing present and past oxygen and hydrogen isotope composition of the lake water with $^{18}O/^{16}O$ ratios in calcite which is precipitated during the summer months.

Ülgen et al. (2012) studied the sediments record of İznik Lake which is located in northwestern Anatolia, to understand the climate change. 4700 years sedimentary record was examined in multiple proxy analyses which include geochemistry, magnetic susceptibility with micro XRF core scanner, palynology and mineralogy.

In a study conducted by Ocakoğlu et al. (2015), Lake Çubuk which is located in the northwest Türkiye was examined. The core examined during the study corresponds to 2800 years ago to present and sedimentology, trace element geochemistry, pollen, stable isotopes, diatoms and ostracods proxies were used.

Şimşek and Çağatay (2018) conducted a study on Lake Van by using multiple proxies such as stable isotopes of oxygen and carbon, ostracod counts and micro-XRF elemental (geochemical analyses) to understand the climate changes. Since the lake is a varved lake they produce a varve chronology for past 3500 years from one core. As a result of the study, the climate records of Lake Van are conformable with Sofular speleothem and Lake Nar.

In a study conducted by El Ouahabi et al. (2017-2018), Amuq Lake was examined by using radiocarbon dating with ostracods, shells and charcoals, to understand the climate variability with human occupation. In addition to the age study (4000 years

from present), magnetic susceptibility, clay mineralogy and geochemistry (XRF scanning) were used as proxies.

In a study conducted by Ön et al. (2018), Lake Hazar which is located in eastern Anatolia, a statistical method named independent component analysis (ICA) was implied to the micro-XRF element data. The ICA was used to extract statistically independent climate related signals from the geochemical multi element data of a core taken from the lake. In addition, ostracod shells were used for oxygen and carbon isotopes. For the Independent Component Analysis (ICA) method, distance correlation was used to measure the similarity between past climate records and independent components. As past climate records, they selected the high-resolution and well-dated oxygen isotope record from the North Greenland Ice Project (NGRIP) and the carbon isotope record from Sofular Cave. Based on distance correlation similarity, they selected two of the six independent components. They proposed that these two components are related to temperature and precipitation-evaporation processes.

In a study conducted by Danladi and Akçer-Ön (2018), Salda Lake which is located in southwest Anatolia, was examined to understand the relationship between solar forcing and climate variability. In the study, 4 cores were used and high-resolution multiple proxies which are magnetic susceptibility, geochemical data (micro-XRF scanner), organic and inorganic carbon, carbon and oxygen isotopes. As a result of the radiocarbon measurements from ostracod shells, it was determined that the cores contain 1400 years. It was stated that dry periods correspond to low solar activity period, wet periods are conformable with high solar activity period.

Avşar et al. (2019) studied the sediments of Amuq Valley to reveal the paleoenvironmental changes resulting from human activities and the climatic change over the las 31 kyr. Piston coring method was used to extract the sediments, and the sediments were examined by using ITRAX micro-XRF core scanning for geochemical analyses and radiocarbon dating was used with charcoal samples. It was

concluded that the interpretations will be improved with several cores taken from different areas of the valley.

In another study conducted by Danladi et al. (2021), Gölcük Lake which is located in southwest Anatolia, was examined to understand the temperature and precipitation changes from 1730. Two cores were taken and magnetic susceptibility, geochemical analyses (with micro-XRF core scanner) are used as multiple proxies. It was concluded that wet periods are associated with low solar activity and dry periods are conformable with high solar activity.

Lake Nar, which is located in the Cappadocia region of Central Anatolia, is one of Türkiye's varved lakes and has been studied by multiple research teams (Jones et al., 2005 and Jones et al., 2006; Dean et al., 2015; Roberts et al., 2018). Jones et al. (2005, 2006) published high-resolution measurements of stable oxygen isotopes (^{18}O) from a 3.76-meter sedimentary core recovered from the lake. Each annual layer (varve) comprises a lighter-colored carbonate layer deposited during the summer and a darker, organic matter-rich layer. Thus, the varve chronology was constructed by counting these layers. The core has the last 1700 years of sediment, and its isotope measurements were conducted for precipitation and evaporation changes.

Another study conducted on Nar Lake has been done by England et al. (2008). Pollen analyses were conducted on a sedimentary core that had been previously studied in the area (Jones et al., 2005; 2006). The derived pollen data were then integrated with the existing stable isotope record constructed by Jones et al., (2005; 2006), in addition to the archaeological and historical documentation. This combination was used to interpret the role of various human and natural factors in changing the Late Holocene landscape of Cappadocia. A key observation was made that the vegetation and land-use shifts indicated by the pollen data were not directly correlated with the fluctuations observed in the stable isotope record.

Dean et al. (2015) focused on revealing centennial-scale climate changes and major shifts throughout the Holocene by presenting a high-resolution record of stable oxygen and carbon isotopes and carbonate mineralogy from Lake Nar. Three cores

were retrieved from the deepest part of the lake for the analysis. The sediment chronology was established through a combination of varve counting and uranium-thorium dating method. As a result, it was stated that the Eastern Mediterranean hydroclimate is influenced by additional controls.

The erosion history of the Lake Nar catchment in Central Türkiye was reconstructed by Roberts et al. (2018). Three cores were retrieved, and micro-XRF scanning measurements were performed along the split cores and oxygen isotope and pollen proxies were also used. Clastic laminations were identified using ITRAX data. It was observed that these clastic laminations were well defined by high Titanium and Potassium concentrations, while low concentration of Calcium.

In a study conducted by Akçer-Ön (2017), the sedimentary record of Köyceğiz Lake was examined to understand climatic changes in western Türkiye by using multiple proxies (magnetic susceptibility, geochemical data obtained from micro-XRF core scanning and carbon and oxygen stable isotope measurements). Three sediment cores were retrieved for this study: two from the northern and one from the southern basins of the lake, along with an additional core recovered from the ridge separating the two basins. The chronology for the sedimentary record, which spans approximately the last 500 years, was established using radiocarbon dating on shell fragments. Geochemical data and magnetic susceptibility were measured at 5 mm resolution. For stable isotope analysis, a coarser resolution of 20 mm intervals was used. As a result, three main correlations were obtained from the analyses: Firstly; Titanium, Potassium and Iron were inversely correlated with Calcium and Strontium. Secondly, Manganese was noted to indicate redox conditions, while Calcium was shown to reflect biological and/or chemical precipitation in the sediment. Lastly, there is an inverse relationship between Titanium, Potassium, and Iron and the Incremental/Coherent ratio, which is considered a proxy for total organic carbon. This was interpreted as the enrichment of total organic carbon during drier and colder periods. For the purposes of the study, Iron was utilized for detrital input, and Calcium was used for carbonate precipitation. A decrease in carbonate precipitation and an increase in clastic input was found to occur during warmer and wetter periods.

1.3.2 Paleoclimatic Studies Based on Tree Rings and Caves

Southwestern Anatolia was studied by Touchan et al. (2003, 2007) and Köse et al. (2013), where May-June precipitation was reconstructed utilizing tree ring data (dendrochronology). A preliminary study was conducted by Touchan et al. (2003), and a 660-year record, spanning from 1339 to 1998 AD in the Burdur and Antalya districts, was created. The reconstruction of May-June precipitation in the Mersin and Antalya districts was later developed by Touchan et al. (2007); their study covered the last 900 years (between 1097-2000 AD). For both investigations, response function analyses were employed for the correlation between monthly temperature and precipitation data and the established tree ring chronology. In addition to these studies, May-June precipitation for southwestern Anatolia was reconstructed by Köse et al. (2013), spanning the years 1692 to 2004 AD. Their purpose was stated as understanding the region's rainfall regime and examining the connection between reconstructed precipitation patterns and significant volcanic eruptions. Tree ring data were calibrated with meteorological data. For the final reconstruction, three tree ring chronologies were built, and four previously published tree ring chronologies were also utilized. It was found that wet conditions were developed after major volcanic eruptions.

A preliminary study on the reconstruction of March-June precipitation in the western Black Sea region of Anatolia was conducted by Akkemik et al. (2005), covering the years 1635 to 2000 AD. The widths of trees were examined to figure out drought patterns, especially patterns of wet and dry years. As a preliminary step in the reconstruction, the relation between tree ring indicators and monthly precipitation data was investigated by using simple correlation coefficients. It was observed that historical drought records in Türkiye and neighboring countries confirmed the data provided by tree ring widths.

A study on the April-August precipitation reconstruction was presented by Akkemik and Aras (2005), utilizing tree rings in the southern part of Central Anatolia. The purpose was stated as revealing the wet and dry years and their durations in the region

from 1689 to 1994 AD. The chronology was established by a linear regression. It was found that the distribution of wet and dry years was not regular, and the interval between two dry periods was less than six years.

A reconstruction of May-June precipitation for the western Black Sea region of northwestern Anatolia was presented by Akkemik et al. (2008), spanning from 1650-2000 AD. A spring-summer (May-August) streamflow reconstruction was also described for the first time, distinguishing it from other dendroclimatological studies in Türkiye. Tree ring widths were correlated with gridded monthly precipitation data. It was stated that since the region is mostly humid, dry events are observed to have shorter duration compared to other regions.

Past wet and dry events for Western Anatolia were examined by Köse et al. (2011) through the development of spatial and local May-June precipitation reconstructions. It was concluded that a significant overlap is observed between dry years and the years of agricultural famine.

In the study conducted by Heinrich et al. (2013), reconstructed the January-May temperatures chronology (1125 AD to present) in southwest Türkiye by using stable carbon isotope beside the tree ring from Jsibeli (Antalya). It was stated that the study is the first isotope record based on tree rings from Türkiye, so its utility for future paleoclimatological studies was evaluated. The aim was to detect high and low frequency climatic signals from the record. However, the warming trend of the 20th century observed in other studies could not be observed in their proxy record and the relevant meteorological data used for their study.

A reconstruction of March-April Spring temperatures was also presented by Köse et al. (2017), using 23 tree ring chronologies from Türkiye. Study covered the period between 1800 and 2002. The findings were compared to previous precipitation and temperature reconstructions to allow for a clearer knowledge of climate conditions during the nineteenth and twentieth centuries. The study area is located in western Anatolia, Marmara, and the western parts of the Mediterranean and Black Sea regions. In addition to the 15 chronologies produced by previous studies, tree ring

chronologies were developed for 8 study areas. Widths of tree rings were measured, and they were cross dated visually. After that, the climate was reconstructed by using the principal components of the 23 chronologies. It was concluded that, beside precipitation signals, temperature signals obtained from tree rings and both parameters are climate indicators while reconstructing past temperature changes.

The stalagmite record of Sofular Cave in Northwestern Anatolia was studied by Fleitmann et al. (2009). Their purpose was to understand the time of abrupt climatic oscillations, which are termed as Greenland Interstadials, that occurred during the last glacial period. Three active, large stalagmites were collected from the cave. The stable isotopes of oxygen and carbon were measured at about twenty-year resolutions. According to their findings, it was concluded that clear evidence of a rapid ecosystem and climate response to Greenland Interstadials in the Eastern Mediterranean is provided by the Sofular Cave stalagmite record.

A 500-year stalagmite record from Akçakale Cave in northeast Türkiye was studied by Jex et al. (2011). Winter precipitation was reconstructed by extrapolating a relationship between the stalagmite's oxygen isotope record and the observed winter precipitation data from Gümüşhane. It was concluded from isotope record and meteorological data that pressure fields over the Caspian Sea and Western Russia influence winter precipitation variability in northeastern Türkiye.

A highly resolved, late Holocene record from Kocain Cave in southwest Türkiye was presented by Jacobson et al. (2021). To reveal variations in past climate, multiple proxy measurements were conducted on a stalagmite that was actively growing. These analyses involved measuring trace metals, carbon, and oxygen isotope ratios. It was suggested that wetter climatic intervals in southwest Türkiye are indicated by increasing P/Ca ratios alongside decreasing Sr/Ca and Mg/Ca ratios.

The present study represents a novel contribution to existing literature. Specifically, a correlation analysis utilizing instrumental precipitation data obtained from meteorological stations and geochemical data derived from varved lake sediments has not been previously attempted in the literature.

1.3.3 Paleoclimatic Reconstructions Based on Advanced Statistical Methods

Kalugin et al. (2007) reconstructed a high-resolution, 800-year record (AD 1210–1991) of annual air temperature and precipitation in southern Western Siberia by analyzing laminated sediments from Teletskoye Lake using Synchrotron Radiation X-Ray Fluorescence (SR-XRF). To translate geochemical proxies specifically Bromine (Br) for biogenic productivity linked to temperature, X-ray density (XRD) for precipitation-driven sediment flux, and Sr/Rb ratios for grain-size variations, into quantitative climate data, the researchers employed Artificial Neural Networks (ANN) rather than standard linear regression. The statistical calibration was performed using instrumental data from the nearby Barnaul weather station covering the period AD 1840–1991.

Another study was conducted by Karadaş in 2022 by using statistical methods called Principal Component Analysis (PCA) and Multiple Linear Regression (MLR). This study aims to reconstruct high-resolution paleotemperature records using varved sediments from Lake Köyceğiz (SW Turkey). Analysis of a 124.95 cm gravity core via ITRAX micro-XRF scanning at 0.2 mm resolution, combined with visual varve counting and Ca/Ti ratios, yielded a 609-year sedimentary record. Using ITRAX data specifically from summer-deposited carbonaceous laminae, the ratios of Br, Cl, and Zr to clastic elements showed significant correlations with instrumental summer temperatures from regional meteorological stations. To provide a quantitative paleotemperature reconstruction, a multiple linear regression model was developed after determining the Principal Components via PCA for eliminate multicollinearity problem occurred while using MLR, which effectively captures the recent global warming trend and aligns with the Global Average Temperature Change (GATC).

Another study conducted by Meydan in 2024 by using only Multiple Regression Analysis. This study presents a high-resolution paleoenvironmental reconstruction of Eastern Anatolia over the last millennium, utilizing annually laminated (varved) sediments from Lake Van and Lake Erçek. The researchers employed Synchrotron

Radiation X-Ray Fluorescence (SR-XRF) scanning. To translate these raw geochemical data into quantitative climate records, the team applied the "Calibration In Time" (CIT) approach, utilizing Multiple Linear Regression (MLR). The researchers first established a calibration period using instrumental weather data spanning from 1949 to 2015. A feature selection process was used to retain only those elements that significantly minimized error; for instance, the temperature model for Lake Van relied on Calcium, Copper, Gallium, and Arsenic, while Lake Erçek's model utilized Titanium, Copper, and Bromine. Notably, the study employed a cross-lake regression strategy, using the geochemical data from Lake Erçek to reconstruct the water levels of Lake Van.

CHAPTER 2

MATERIALS AND METHODS

2.1 Bathymetric Survey, Sediment Coring and Core Splitting

A detailed bathymetric survey of Köyceğiz Lake was carried out by Avşar et al. (2016). The bathymetric map was produced using the floating research platform "JEOLODTÜ," operated by the Department of Geological Engineering at Middle East Technical University (METU). The results revealed that the lake consists of two distinct sub-basins, with maximum water depths of 26 meters in the northern basin and 32 meters in the southern basin. Following the generation of the bathymetric map, the coring location was carefully selected. The sediment core was retrieved from the deepest and flattest part of the southern basin, based on two primary considerations. First, cores collected from sloped areas of the basin are more likely to be affected by mass-wasting processes, which can disrupt the continuity of sediment accumulation and lead to stratigraphic gaps. Second, sedimentation rates tend to be lower in the deepest, more stable central parts of the basin compared to the margins, resulting in a longer and more continuous sedimentary record. Therefore, selecting such a location increases the likelihood of obtaining an undisturbed, high-resolution archive of past environmental and climatic changes

2.2 ITRAX Micro-XRF Core Scanning

As part of this study, the sediment core was scanned at the Marine Research Laboratory, which operates under the Marine Research Department of the General

Directorate of Mineral Research and Exploration (MTA) in Türkiye. The core, composed of finely laminated varved sediments, was scanned at a resolution of 0.02 cm. X-ray fluorescence (XRF) measurements were conducted using a molybdenum (Mo) tube with an exposure time of 5 seconds per measurement point. During scanning, the ITRAX system generates an XRF spectrum for each measurement position along the core. These spectra represent the photon emission intensity (in counts per second, cps) as a function of incident X-ray energy (in keV). Each element is detected based on its characteristic energy levels required to emit photons, and the height of each peak in the spectrum reflects the relative concentration of that element within the sample. The ITRAX software automatically identifies spectral peaks and calculates their areas, enabling semi-quantitative geochemical profiling of the sediment sequence with high spatial resolution.

Although every data point acquired via the ITRAX system is quantitatively expressed in counts per second (cps), the inherent magnitudes of these measurements vary considerably. Consequently, the entire dataset requires standardization to ensure that comparisons between different proxies are valid, effectively removing the influence of these differing magnitudes. For this standardization, the mean and standard deviation (sigma) are first computed for every single element. Subsequently, the standard score (z) for any given measurement point is obtained by dividing the deviation of that data value from its mean (mu) by its calculated standard deviation (sigma). The process of calculating the standard scores (z) for all variables produces a new dataset characterized by a mean value of 0 and a standard deviation of 1, which ensures all elements are scaled appropriately across the sedimentary record for comparable analysis.

2.3 Varve Chronology Construction

The Ca/Ti ratio is a widely utilized geochemical proxy for defining the seasonal stratification within annually laminated (varved) lacustrine sediments. This methodology relies on the contrasting mobility and sources of the two elements

within the hydrological cycle. Titanium (Ti) is a lithogenic element, resistant to weathering, making its concentration a reliable indicator of allochthonous clastic input (terrigenous material delivered by runoff). Consequently, high Ti levels typically correspond to the wet season (winter/spring) when precipitation and snowmelt are highest, increasing surface runoff and erosion. Conversely, Calcium (Ca) is primarily associated with autochthonous carbonate precipitation (e.g., calcite or aragonite) that occurs within the lake water column. This precipitation is maximized during the dry season (summer) when water temperatures are warmest, evaporation rates are highest, and CO_2 solubility decreases. Therefore, a high Ca/Ti ratio marks the summer layer, signifying a period dominated by chemical/biogenic sedimentation and low clastic dilution. A low Ca/Ti ratio or high Ti peak is characteristic of the winter/spring layer, signifying high clastic input. This inverse relationship allows researchers to accurately delineate the annual boundary and reconstruct the seasonal intensity of past precipitation and temperature regimes.

The utilization of Titanium (Ti) and Calcium (Ca) in the Les Echets sediment sequence analysis provides distinct insights into the catchment's physical and chemical paleoclimate history. Titanium (Ti) functions primarily as a normalization element and a proxy for minerogenic and detrital input into the lake. It is strongly associated with clay mineral assemblages and the fine size fractions of sediments. Ti is chosen for data normalization because of its conservative nature during transport and weathering, its abundance, and its non-biological importance. Consequently, increases in Ti peak areas (or normalized proxies like Ti) typically signal an increase in fine-grained detrital material input. In contrast, Calcium (Ca) relates to both external (allogenic) input from the carbonate-rich bedrock and, more crucially, to authigenic (in-lake) precipitation of Calcium Carbonate ($CaCO_3$). Ca variations, especially when examined through the Ca/Ti ratio and correlated with Strontium (Sr), are used to decipher lake level and productivity changes. High Ca signals suggest the lake waters reached carbonate saturation, a condition often met when lake levels drop, and the water become concentrated (Kylander et al., 2011).

Due to the semi-quantitative nature of the geochemical data generated by ITRAX, the absolute concentrations of individual elements are typically not employed directly in paleoclimate interpretation. The raw ITRAX output can be significantly affected by matrix effects, which include variations in organic matter, water content, grain size, and sediment density. Consequently, reliable environmental inference requires that elements be normalized to a stable reference element. Utilizing the ratios of elements- rather than their absolute peak areas- effectively mitigates these physical matrix effects, allowing for the isolation of geochemical variations driven primarily by past climatic and environmental changes. Thus, the elemental data produced by ITRAX, relative changes in the elemental profile are more useful than the element's absolute concentration in paleoclimatology (Kylander et al., 2011). Using ratio of the elemental data ensures that the reconstructed proxy signals accurately reflect shifts in detrital input, chemical precipitation, or weathering processes.

In this study, varve chronology was established based on multiple parameters derived from the ITRAX micro-XRF core scanning data. Specifically, the elemental ratios of calcium to titanium (Ca/Ti), along with the identification and counting of peak layers in the optical core image, were used to construct an annual-scale sedimentation framework. In addition to these geochemical indicators, Red-Green-Blue (RGB) color spectrum ratios were employed to assist in identifying the lighter (white) laminae within the sediment sequence, providing further support for the visual and geochemical varve interpretation.

2.4 Multiple Linear Regression Analysis

Multiple Linear Regression (MLR) is a widely utilized multivariate model that builds upon simple linear regression by extending it to include more than one explanatory variable (X_1, X_2, …). Linear regression itself is a modeling technique used for analyzing data to make predictions. The fundamental structure of the MLR model assumes that the response variable (y) is directly related to a linear combination of

the explanatory variables. The equation for MLR is represented by the following formula: $Y=a+\beta_1 X_1+\beta_2 X_2+\beta_3 X_3+\cdots etc$, where is a the constant (the predicted value of Y when all explanatory variables are 0), and each explanatory variable receives its own β coefficient. This technique allows for the discussion of model building, assumptions, and interpreting results to gain meaningful understanding from the data. MLR analysis allows researchers to investigate how a set of explanatory variables is associated with a response variable of interest. It is a widely used method within social sciences research and practice. Examples of its application include predicting an individual's income given several socio-economic characteristics or estimating systolic or diastolic blood pressure based on a variety of behavioral characteristics. However, a critical aspect of interpretation is distinguishing between correlation and causation. A good model fit merely confirms a statistical association; the analysis, while investigating association, does not provide grounds for causal inference. This caution is vital because, statistically speaking, one could build an equally good model using the response variable to predict the explanatory variables, which often makes no substantive sense.

To interpret an MLR model and understand its limitations, it is important to consider the underlying assumptions of linear regression. Key requirements include that the response variable must be continuous (able to take any value between its minimum and maximum), and the relationship between the outcome and explanatory variables must be linear. Furthermore, the model assumes that the residuals (error terms) are normally distributed and homoscedastic (possessing constant variance regardless of the explanatory variables). A crucial assumption is that there is no more than limited multicollinearity. Violations of this limited multicollinearity assumption, where two or more explanatory variables are highly correlated (collinear), can cause the model to become unstable, making the estimation of β coefficients less precise.

2.5 Principal Component Analysis

Principal Component Analysis (PCA) is widely considered the most popular multivariate statistical technique, utilized extensively across almost all scientific disciplines. PCA is designed to analyze a data table where the observations are described by several inter-correlated quantitative dependent variables. The primary goals of this method are threefold: to extract the important information from the data set, to compress the size of the data set by retaining only this crucial information, and to simplify the description and analyze the structure of the observations and variables. By achieving these goals, PCA allows researchers to process complex data and reduce its intrinsic dimensionality. To accomplish this simplification, PCA computes new variables called principal components, which are obtained as linear combinations of the original variables. Crucially, these new components are mathematically constrained to be orthogonal (uncorrelated) to one another. The first principal component is constructed specifically to possess the largest possible variance (or inertia), meaning it is the component that extracts the largest part of the total inertia from the data table. Subsequent components are then sequentially computed to be orthogonal to all preceding components while still maximizing the remaining variance in the data. The numerical values of these new variables for the individual observations are known as factor scores.

The output of a PCA is a comprehensive representation that includes the geometric display of similarity patterns. PCA aims to display the pattern of similarity of the observations and of the variables as points in maps. Mathematically, PCA relies on the eigen-decomposition of positive semi-definite matrices (like covariance or correlation matrices) and the Singular Value Decomposition (SVD) of rectangular matrices to find these optimal components. The importance of a component is quantified by its inertia or the percentage of the total inertia that it explains. The quality of the overall PCA model can further be evaluated using computer-based resampling techniques, such as the bootstrap and cross-validation techniques like the jackknife.

CHAPTER 3

RESULTS

3.1 Optical Image and ITRAX Micro-XRF Data

Varve chronology was established by counting the lighter, carbonate-rich laminae (named as whitish) that are interpreted as summer layers. These layers are characterized by distinct anomalies in both the Red/Green (R/G) color ratio and the Ca/Ti elemental ratio-indicators of more whitish hues and increased carbonate content, respectively. To enhance the identification of laminae that meet both criteria simultaneously (i.e., those that are both yellowish and carbonate-rich), a new proxy was created by multiplying the R/G and Ca/Ti profiles. This combined index helps to determine the varve layers more clearly. In addition to the carbonate-rich "whitish" laminae, clastic-rich laminae (named as brownish) that are interpreted as winter layers. "Brownish" layers are marked with the help of Fe/Ca elemental ratio's indicators, and these layers appear as brownish dark in color.

Each identified varve-corresponding to "whitish" with red bars across the R/G, Ca/Ti, and [R/G] × [Ca/Ti] profiles. These markers are also displayed on the optical image of the core along the LS (longitudinal section), providing visual confirmation of the stratigraphic positions. The complete varve sequence for core KYC-J is presented in Appendix A. In addition to "whitish" layers, "brownish" layers are also marked with using Ca/Ti ratio's depression, Fe/Ca ratio's peak depths.

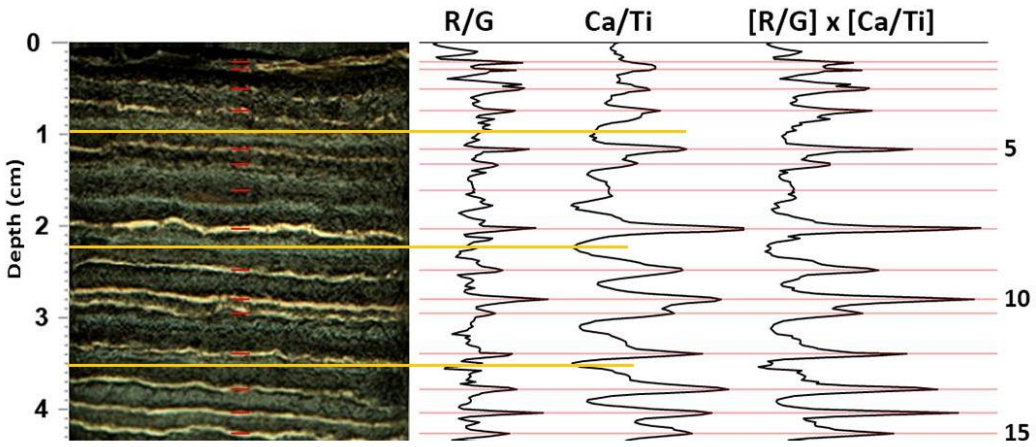

Figure 3.1. Close-up view of 3 examples from winter seasons. Yellow lines indicating depressions in Ca/Ti ratio and showing the level of winter seasons (Taken from Karadaş, 2022).

"Brownish" winter layers were detected by using Ca/Ti ratio's depression levels and Fe/Ca ratio's peak levels (Figure 3.1). During the varve counting both optical core image, element ratios obtained from ITRAX data and R/G ratios were used.

Avşar et al. (2016) documented distinct anomalies within the $[Cr/Ni]_{av}/[Ti,K,Fe]_{av}$ profile following earthquakes that generated peak ground acceleration (PGA) values exceeding 70 cm/s². These anomalies were interpreted as a reflection of increased erosion within the lake's catchment triggered by strong seismic activity, which subsequently led to enhanced sediment delivery to the basin, referred to as Catchment Response (CR). Given that the catchment of Köyceğiz Lake is primarily composed of peridotites, earthquake-induced landslides remobilized sediments derived from these ultramafic lithologies. This process resulted in Ni and Cr-rich sediment deposition persisting for approximately 5 to 10 years. Evidence of such a CR associated with the 1959 earthquake is distinctly observed in the KYC-J core.

3.2 Varve Chronology and Meteorological Station Data Correlation

According to rules determined and used on the optical image of the core and geochemical data, varve chronology was constructed, and the constructed age-depth model of the core is presented in Figure 3.2a.

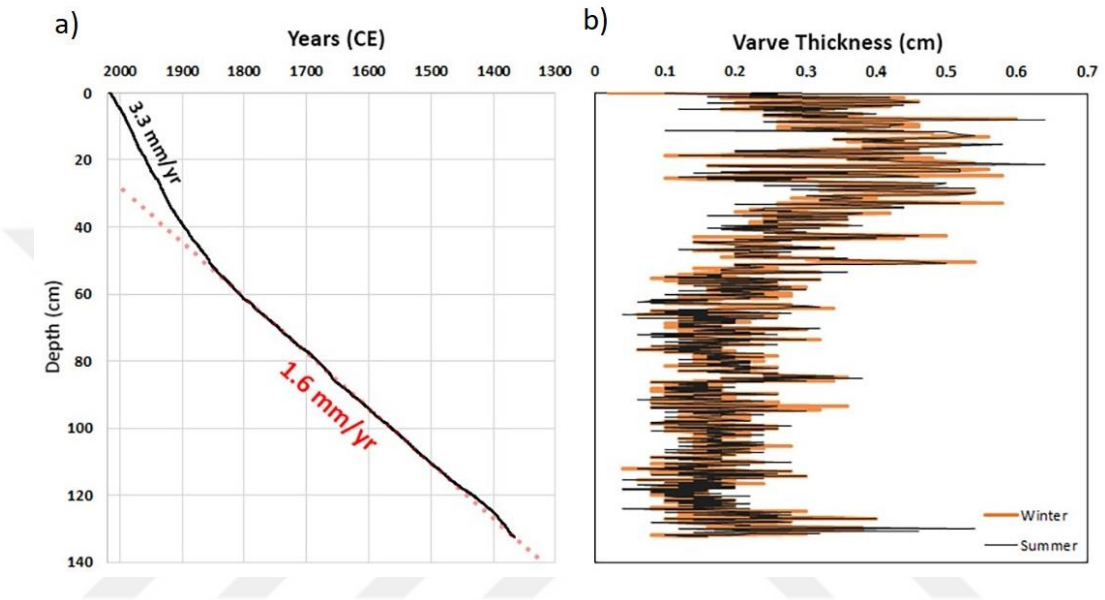

Figure 3.2. a) Age-depth model of the core KYC-J based on the varve construction. b) Varve thickness variation along the core based on the determined thickness according to the constructed varve chronology.

After the varve construction was completed, varve thickness was measured according to the summer and winter level's differences. In other words, carbonate rich white layers' thickness was measured, and these are noted as summer thicknesses, clastic rich dark layers are measured as winter thicknesses. The thickness variation along the core can be seen in Figure 3.2.

2 different sedimentation rates can be observed in Figure 3.2a; before the year 1850 the sedimentation rate is 3.3 mm/year and after the year 1850 the sedimentation rate is decreased to 1.6 mm/year. This change may result from compaction effect because the deeper part of the core is more compacted than the shallow part. Although the change in the sedimentation rate around the 1850s appears abrupt, it is an artifact of

the logarithmic compaction effect which intensifies with increasing core depth. If the core had been longer, intervals where the sedimentation rate was below the 1.6 mm/year threshold could have been observed below a certain depth.

Once the winter and summer layer thicknesses were determined, the instrumental precipitation data obtained from meteorological stations were examined to identify the corresponding months to be assigned as "winter" and "summer" for correlation with the established varve chronology. 4 meteorological stations located near Köyceğiz Lake with long-term data records were selected for this study. These stations are Muğla, Dalaman, Marmaris and Köyceğiz meteorological stations. The data coverage periods for these stations are as follows: the Muğla station spans 1935-2016, the Dalaman station covers 1957-2011, the Marmaris station from 1959-2016, and the Köyceğiz station from 1959-2011. The monthly averages for all years within the data set were calculated for each station. The months having the highest precipitation amount (October, November, December, January, February, March) were grouped under the group "winter," while those with the lowest precipitation amount (April, May, June, July, August, September) were collected under the group "summer" (Figure 3.3).

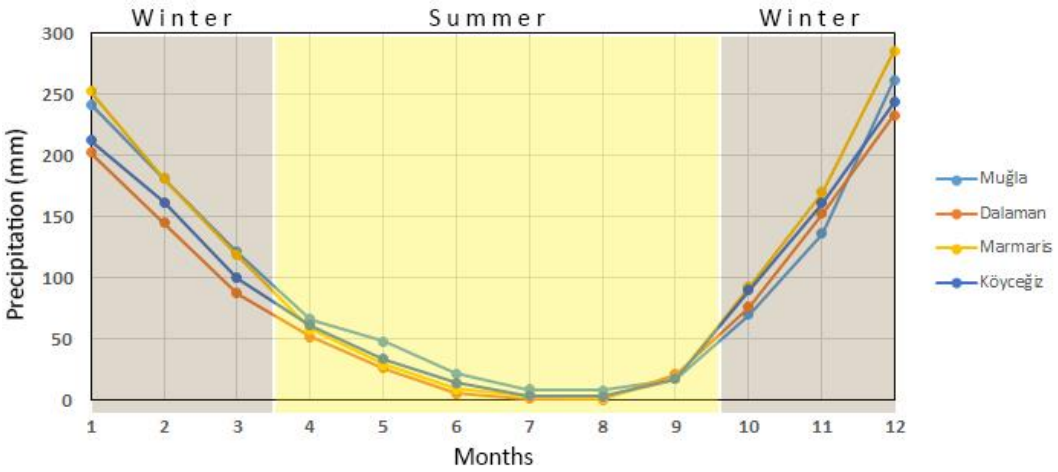

Figure 3.3. Graph shows the average precipitation amounts for every month for 4 meteorological stations. “Summer” months are the months in yellow part, “winter” months are the months in the darker part.

As mentioned in the previous chapter that the Ca/Ti ratio is a fundamental geochemical proxy for hydroclimatic reconstruction in annually laminated (varved) lake sediments. This ratio shows the balance between allochthonous (terrigenous) input and autochthonous (in-lake water column chemical) precipitation. Titanium (Ti) is utilized as the normalization element, as its concentration primarily signals clastic material input delivered by winter/spring runoff and surface erosion. In contrast, Calcium (Ca) is typically linked to carbonate precipitation, a process enhanced during dry summer months due to warmer temperatures alnd increased evaporation. Consequently, a high Ca/Ti ratio indicates a period dominated by summer chemical sedimentation and relative aridity, while a low Ca/Ti ratio signifies high clastic dilution driven by increased winter/spring precipitation and runoff. This inverse elemental signaling allows the Ca/Ti ratio to use as a reliable indicator of the seasonal hydrological balance captured within the varve structure.

To understand whether winter or summer depths' Ca/Ti ratio represent the general trend of geochemical data, 21-point average was applied to the geochemical data (Figure 3.4).

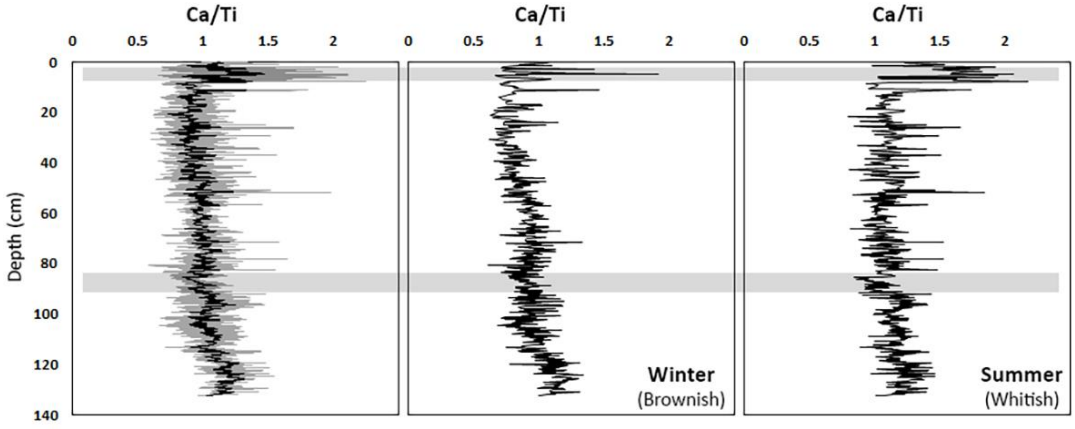

Figure 3.4. Gray lines indicating raw data (Ca/Ti ratio from varve chronology) and black lines are showing the trend derived from 21 point moving average calculation.

8 different graphs were constructed to understand the correlation between precipitation and the most frequently utilized paleoclimatological proxy, the Ti/Ca ratio. The Ti/Ca ratio was employed instead of the standard Ca/Ti ratio because precipitation exhibits a negative correlation with the Ca/Ti ratio. The "Winter" Ti/Ca ratio was obtained from the depths of the winter layers derived during varve construction, and the "Summer" ratio was taken from the Ti/Ca values corresponding to the depths of the white carbonate layers. Subsequently, the geochemical data (Ti/Ca ratio) from the depths determined for both the summer and winter layers during varve counting were compared with the instrumental data collected from four different meteorological stations (Muğla, Dalaman, Marmaris and Marmaris meteorological stations) (Figure 3.5).

The winter months (which account for the highest precipitation) were selected to understand the relationship between geochemistry and rainfall, as consistent correlation findings for the Ti/Ca ratio with summer or winter precipitation could not be established. In other words, winter months (decided and explained in previous chapter as October, November, December, January, February and March) have more precipitation values than summer months (decided and explained in previous chapter as April, May, June, Jully, August and September). Thus, winter geochemical data is selected for the further investigations mentioned below.

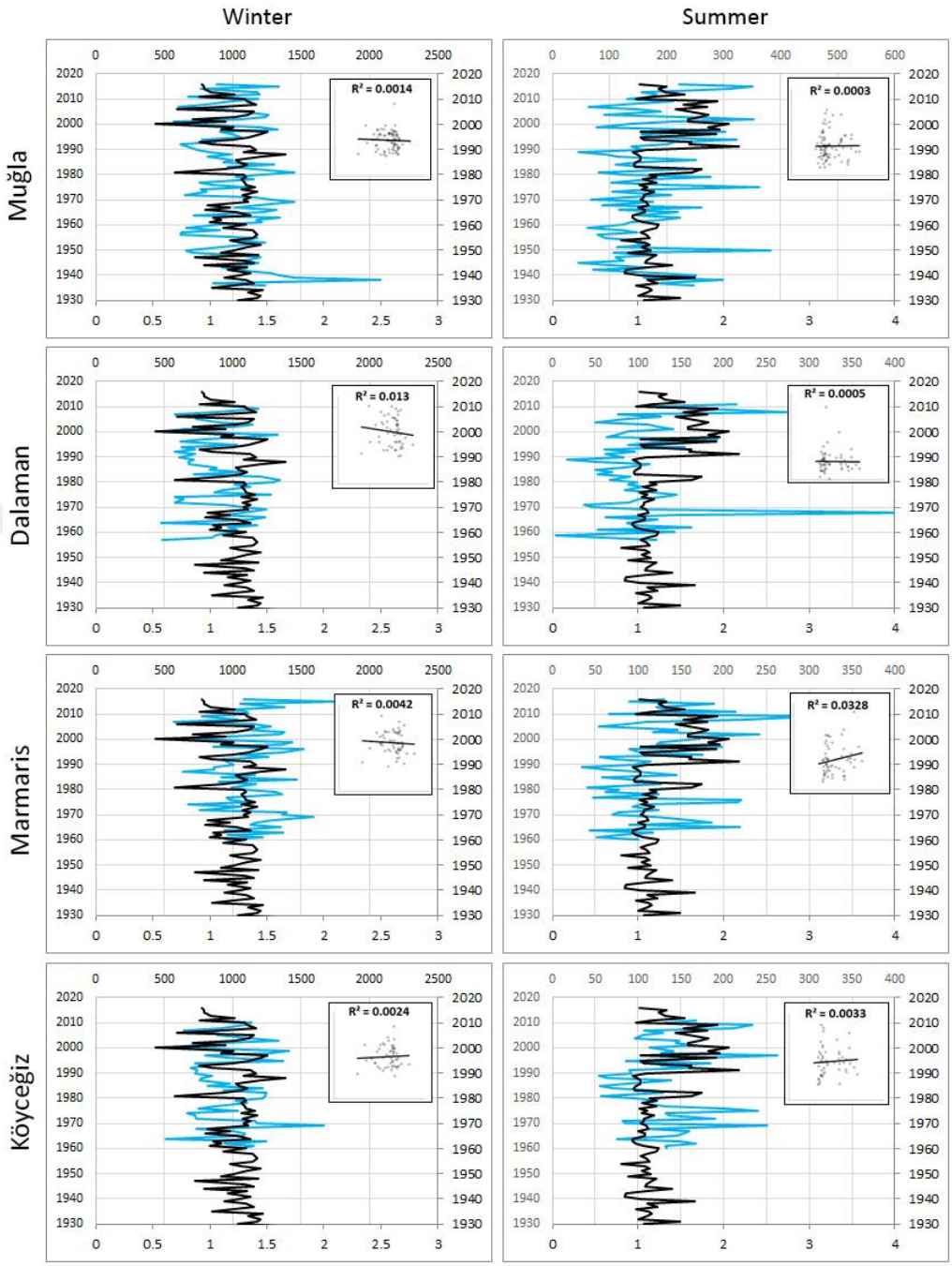

Figure 3.5. The figure shows the correlation between precipitation data and corresponding geochemical data obtained from Ti/Ca ratio. Blue lines are showing the precipitation data and black lines are showing the Ti/Ca ratio.

When the Ti/Ca ratio alone was compared with precipitation data, the resulting R^2 values were found to be quite low, and this ratio failed to demonstrate any success

in tracking precipitation trends. This situation leads to searching for alternative elemental ratios that could show a higher correlation with precipitation, compared to the Ti/Ca ratio. To detect another ratio, all elements and non-elemental data from the ITRAX geochemical data were systematically ratioed against each other, and the resulting R^2 values correlating with the precipitation data were subsequently calculated (Figure 3.6).

However, since these ratios showed low R^2 values in the correlation between annual precipitation data and geochemical data, the dataset was subsequently corrected using a 7-point moving average. This adjustment process resulted in an increase in the R^2 values. After using this method, the average R^2 value increased for all ratios in the matrix, and the R^2 values of some ratios showed increases that could be considered significant at some meteorological stations. In other words, significant increases in specific R^2 values were observed for different element ratios at different stations. These specific increases are clearly visible in the green squares in the right-hand column of the Figure 3.6.

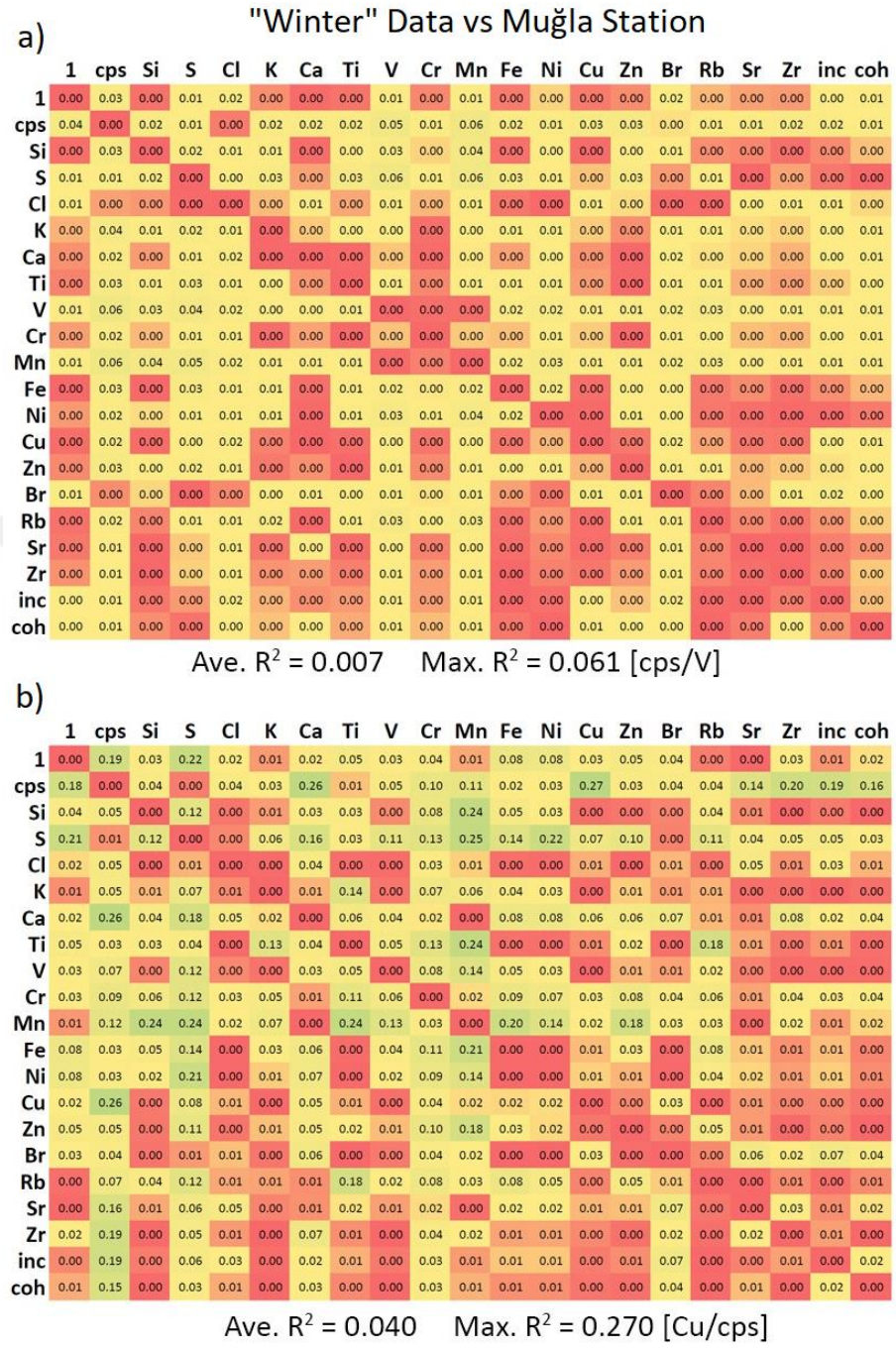

Figure 3.6. Matrixes showing R^2 values of all possible elemental and non-elemental ratios with winter precipitation records of Muğla station. a) matrix shows annual geochemical data vs meteorological station b) matrix shows 7-point moving average values vs meteorological station. The color scale used in all matrices is same. Green color shows higher and red color shows lower R^2 values.

a) "Winter" Data vs Köyceğiz Station

	1	cps	Si	S	Cl	K	Ca	Ti	V	Cr	Mn	Fe	Ni	Cu	Zn	Br	Rb	Sr	Zr	inc	coh
1	0.00	0.00	0.00	0.00	0.01	0.01	0.02	0.00	0.01	0.00	0.00	0.00	0.00	0.00	0.00	0.00	0.00	0.01	0.02	0.00	0.00
cps	0.01	0.00	0.01	0.00	0.00	0.02	0.00	0.01	0.03	0.00	0.01	0.02	0.01	0.00	0.00	0.00	0.01	0.00	0.00	0.00	0.01
Si	0.00	0.02	0.00	0.00	0.01	0.02	0.01	0.01	0.01	0.00	0.00	0.01	0.00	0.00	0.02	0.00	0.00	0.01	0.01	0.00	0.00
S	0.00	0.01	0.00	0.00	0.01	0.02	0.01	0.02	0.02	0.00	0.00	0.04	0.01	0.00	0.00	0.00	0.00	0.01	0.01	0.00	0.00
Cl	0.01	0.00	0.00	0.00	0.00	0.00	0.00	0.00	0.01	0.00	0.00	0.00	0.00	0.01	0.00	0.01	0.00	0.00	0.00	0.01	0.01
K	0.01	0.03	0.02	0.02	0.02	0.00	0.02	0.00	0.00	0.00	0.01	0.00	0.01	0.01	0.05	0.01	0.01	0.02	0.02	0.01	0.01
Ca	0.01	0.00	0.00	0.00	0.00	0.01	0.00	0.00	0.01	0.00	0.00	0.00	0.00	0.00	0.00	0.00	0.00	0.01	0.00	0.00	0.01
Ti	0.01	0.03	0.01	0.02	0.02	0.00	0.02	0.00	0.00	0.00	0.01	0.00	0.01	0.01	0.04	0.01	0.01	0.02	0.02	0.01	0.01
V	0.02	0.04	0.01	0.02	0.02	0.00	0.02	0.00	0.00	0.00	0.02	0.00	0.01	0.02	0.04	0.01	0.01	0.02	0.03	0.01	0.01
Cr	0.00	0.01	0.00	0.00	0.01	0.00	0.01	0.00	0.00	0.00	0.00	0.00	0.00	0.00	0.00	0.00	0.00	0.01	0.01	0.00	0.00
Mn	0.01	0.02	0.00	0.00	0.01	0.01	0.01	0.00	0.01	0.00	0.00	0.00	0.00	0.01	0.01	0.01	0.00	0.01	0.02	0.00	0.00
Fe	0.01	0.03	0.01	0.04	0.01	0.00	0.02	0.00	0.00	0.00	0.00	0.00	0.03	0.01	0.03	0.01	0.00	0.01	0.02	0.01	0.00
Ni	0.00	0.02	0.00	0.01	0.01	0.01	0.01	0.01	0.01	0.00	0.00	0.03	0.00	0.00	0.01	0.00	0.00	0.01	0.01	0.00	0.00
Cu	0.00	0.01	0.00	0.00	0.01	0.00	0.01	0.00	0.00	0.00	0.00	0.00	0.00	0.00	0.00	0.00	0.00	0.01	0.01	0.00	0.00
Zn	0.00	0.00	0.01	0.00	0.00	0.05	0.00	0.03	0.04	0.00	0.01	0.02	0.01	0.00	0.00	0.00	0.01	0.01	0.01	0.00	0.00
Br	0.00	0.00	0.00	0.00	0.02	0.00	0.01	0.00	0.00	0.00	0.00	0.00	0.00	0.00	0.00	0.00	0.00	0.01	0.01	0.00	0.00
Rb	0.00	0.01	0.00	0.00	0.01	0.01	0.01	0.01	0.01	0.00	0.00	0.00	0.00	0.00	0.02	0.00	0.00	0.01	0.01	0.00	0.00
Sr	0.01	0.00	0.00	0.00	0.00	0.01	0.01	0.00	0.01	0.00	0.00	0.00	0.00	0.01	0.00	0.00	0.00	0.00	0.00	0.01	0.01
Zr	0.01	0.00	0.01	0.00	0.00	0.01	0.00	0.01	0.02	0.00	0.01	0.01	0.00	0.01	0.00	0.00	0.01	0.00	0.00	0.01	0.03
inc	0.00	0.01	0.00	0.00	0.02	0.00	0.01	0.00	0.00	0.00	0.00	0.00	0.00	0.00	0.00	0.00	0.00	0.01	0.01	0.00	0.00
coh	0.00	0.01	0.00	0.00	0.02	0.00	0.01	0.00	0.00	0.00	0.00	0.00	0.00	0.00	0.00	0.01	0.00	0.01	0.02	0.00	0.00

Ave. R^2 = 0.007 Max. R^2 = 0.051 [Zn/K]

b)

	1	cps	Si	S	Cl	K	Ca	Ti	V	Cr	Mn	Fe	Ni	Cu	Zn	Br	Rb	Sr	Zr	inc	coh
1	0.00	0.25	0.28	0.39	0.01	0.08	0.09	0.18	0.16	0.01	0.11	0.26	0.30	0.13	0.19	0.02	0.01	0.06	0.02	0.01	0.03
cps	0.25	0.00	0.04	0.00	0.18	0.06	0.45	0.03	0.10	0.07	0.09	0.02	0.01	0.20	0.06	0.24	0.07	0.37	0.28	0.27	0.29
Si	0.27	0.04	0.00	0.14	0.01	0.15	0.18	0.00	0.14	0.08	0.09	0.04	0.08	0.01	0.03	0.01	0.18	0.12	0.03	0.07	0.02
S	0.37	0.00	0.14	0.00	0.04	0.16	0.31	0.11	0.25	0.10	0.16	0.18	0.12	0.10	0.18	0.06	0.18	0.20	0.14	0.17	0.11
Cl	0.01	0.20	0.01	0.06	0.00	0.00	0.10	0.01	0.00	0.01	0.00	0.02	0.03	0.01	0.01	0.00	0.00	0.25	0.00	0.01	0.00
K	0.08	0.07	0.15	0.18	0.00	0.00	0.09	0.30	0.00	0.06	0.00	0.13	0.14	0.00	0.03	0.00	0.11	0.07	0.00	0.01	0.00
Ca	0.10	0.44	0.21	0.34	0.11	0.11	0.00	0.17	0.15	0.00	0.12	0.22	0.27	0.27	0.19	0.13	0.04	0.05	0.19	0.11	0.16
Ti	0.18	0.04	0.01	0.12	0.01	0.30	0.15	0.00	0.11	0.08	0.06	0.04	0.07	0.00	0.01	0.01	0.25	0.10	0.02	0.04	0.01
V	0.16	0.11	0.15	0.29	0.00	0.00	0.13	0.11	0.00	0.04	0.00	0.17	0.19	0.01	0.04	0.00	0.02	0.09	0.00	0.01	0.00
Cr	0.01	0.07	0.07	0.10	0.01	0.05	0.00	0.08	0.03	0.00	0.05	0.08	0.09	0.03	0.06	0.01	0.03	0.01	0.01	0.01	0.02
Mn	0.12	0.08	0.09	0.18	0.00	0.00	0.11	0.06	0.00	0.06	0.00	0.10	0.12	0.00	0.03	0.00	0.02	0.08	0.00	0.02	0.00
Fe	0.24	0.02	0.04	0.18	0.01	0.13	0.19	0.04	0.15	0.08	0.09	0.00	0.12	0.02	0.08	0.02	0.17	0.13	0.05	0.08	0.04
Ni	0.27	0.01	0.08	0.12	0.03	0.13	0.23	0.07	0.16	0.08	0.11	0.12	0.00	0.05	0.12	0.03	0.16	0.15	0.08	0.11	0.06
Cu	0.12	0.18	0.01	0.11	0.01	0.00	0.25	0.01	0.00	0.03	0.00	0.03	0.05	0.00	0.00	0.01	0.01	0.17	0.08	0.17	0.08
Zn	0.19	0.06	0.03	0.18	0.00	0.03	0.17	0.01	0.04	0.06	0.03	0.09	0.13	0.00	0.00	0.00	0.08	0.11	0.02	0.04	0.01
Br	0.01	0.25	0.01	0.07	0.00	0.00	0.12	0.01	0.00	0.02	0.00	0.02	0.04	0.01	0.01	0.00	0.00	0.21	0.00	0.01	0.00
Rb	0.01	0.09	0.19	0.20	0.00	0.11	0.04	0.25	0.02	0.04	0.03	0.19	0.19	0.02	0.09	0.00	0.00	0.04	0.00	0.00	0.00
Sr	0.08	0.41	0.15	0.25	0.24	0.09	0.05	0.13	0.11	0.00	0.09	0.17	0.20	0.20	0.13	0.22	0.05	0.00	0.21	0.10	0.16
Zr	0.02	0.25	0.04	0.15	0.00	0.00	0.18	0.03	0.01	0.02	0.00	0.06	0.09	0.08	0.02	0.00	0.00	0.18	0.00	0.00	0.00
inc	0.01	0.28	0.07	0.19	0.00	0.01	0.10	0.05	0.02	0.02	0.02	0.09	0.12	0.17	0.04	0.01	0.00	0.09	0.00	0.00	0.03
coh	0.02	0.30	0.03	0.12	0.00	0.00	0.14	0.02	0.00	0.02	0.00	0.04	0.07	0.08	0.01	0.00	0.00	0.14	0.00	0.03	0.00

Ave. R^2 = 0.083 Max. R^2 = 0.449 [Ca/cps]

Figure 3.7. Matrixes showing R^2 values of all possible elemental and non-elemental ratios with winter precipitation records of Köyceğiz station. a) matrix shows annual geochemical data vs meteorological station b) matrix shows 7-point moving average values vs meteorological station. The color scale used in all matrices is same. Green color shows higher and red color shows lower R^2 values.

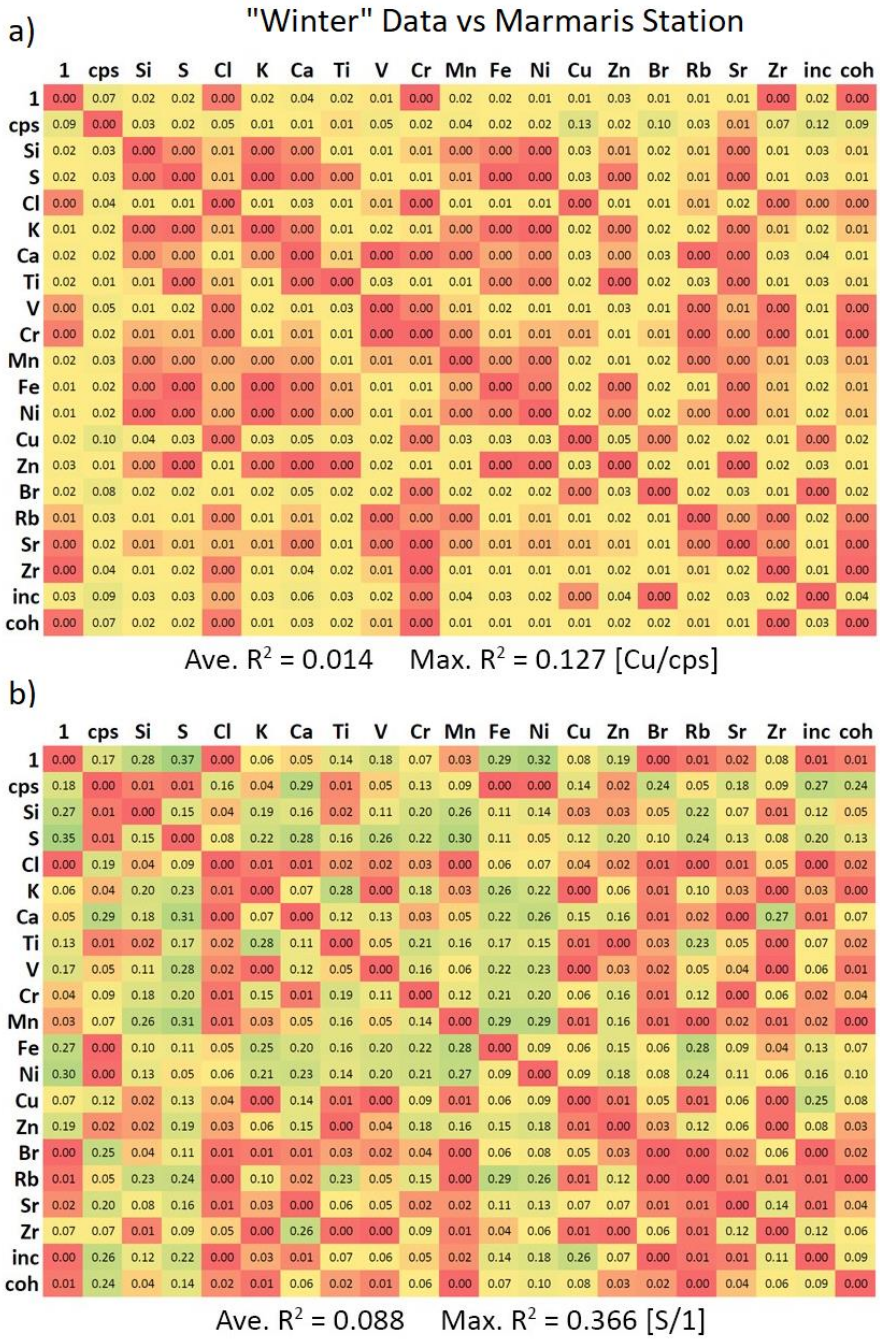

Figure 3.8. Matrixes showing R2 values of all possible elemental and non-elemental ratios with winter precipitation records of Marmaris station. a) matrix shows annual geochemical data vs meteorological station b) matrix shows 7-point moving average values vs meteorological station. The color scale used in all matrices is same. Green color shows higher and red color shows lower R^2 values.

a)

"Winter" Data vs Dalaman Station

	1	cps	Si	S	Cl	K	Ca	Ti	V	Cr	Mn	Fe	Ni	Cu	Zn	Br	Rb	Sr	Zr	inc	coh
1	0.00	0.05	0.02	0.04	0.00	0.01	0.00	0.01	0.01	0.00	0.00	0.02	0.03	0.00	0.04	0.00	0.01	0.00	0.02	0.01	0.00
cps	0.05	0.00	0.01	0.00	0.01	0.01	0.02	0.00	0.02	0.01	0.03	0.00	0.00	0.04	0.00	0.04	0.00	0.01	0.01	0.07	0.08
Si	0.01	0.02	0.00	0.03	0.00	0.00	0.00	0.00	0.01	0.00	0.03	0.01	0.02	0.00	0.01	0.00	0.00	0.00	0.00	0.02	0.01
S	0.03	0.00	0.03	0.00	0.00	0.02	0.00	0.01	0.04	0.01	0.06	0.02	0.00	0.01	0.00	0.01	0.01	0.00	0.00	0.03	0.02
Cl	0.00	0.03	0.01	0.02	0.00	0.01	0.00	0.01	0.00	0.00	0.00	0.01	0.01	0.00	0.02	0.00	0.01	0.00	0.01	0.01	0.00
K	0.00	0.02	0.01	0.03	0.00	0.00	0.00	0.03	0.00	0.00	0.00	0.02	0.02	0.00	0.03	0.00	0.01	0.00	0.00	0.00	0.00
Ca	0.00	0.02	0.01	0.02	0.00	0.00	0.00	0.01	0.00	0.00	0.00	0.01	0.02	0.00	0.02	0.00	0.01	0.00	0.02	0.01	0.00
Ti	0.01	0.01	0.00	0.02	0.00	0.03	0.00	0.00	0.01	0.00	0.02	0.00	0.01	0.00	0.01	0.00	0.00	0.00	0.00	0.01	0.00
V	0.00	0.03	0.01	0.04	0.00	0.00	0.00	0.01	0.00	0.00	0.00	0.02	0.02	0.00	0.03	0.00	0.01	0.00	0.00	0.00	0.00
Cr	0.00	0.01	0.00	0.01	0.00	0.00	0.00	0.00	0.00	0.00	0.00	0.01	0.01	0.00	0.01	0.00	0.00	0.00	0.00	0.00	0.00
Mn	0.00	0.05	0.03	0.06	0.00	0.00	0.00	0.02	0.00	0.00	0.00	0.03	0.04	0.00	0.05	0.00	0.02	0.00	0.01	0.00	0.00
Fe	0.01	0.01	0.00	0.02	0.00	0.01	0.00	0.00	0.02	0.00	0.03	0.00	0.02	0.00	0.00	0.00	0.00	0.00	0.00	0.01	0.01
Ni	0.02	0.00	0.01	0.00	0.00	0.01	0.00	0.01	0.02	0.01	0.04	0.02	0.00	0.01	0.00	0.01	0.01	0.00	0.00	0.02	0.01
Cu	0.00	0.04	0.01	0.03	0.00	0.00	0.00	0.01	0.00	0.00	0.00	0.01	0.02	0.00	0.03	0.00	0.01	0.00	0.01	0.02	0.01
Zn	0.03	0.00	0.01	0.00	0.00	0.02	0.00	0.00	0.03	0.01	0.04	0.00	0.00	0.01	0.00	0.01	0.01	0.00	0.00	0.02	0.02
Br	0.00	0.05	0.01	0.03	0.01	0.01	0.01	0.01	0.01	0.00	0.01	0.02	0.02	0.00	0.02	0.00	0.01	0.00	0.02	0.01	0.00
Rb	0.01	0.01	0.00	0.01	0.00	0.01	0.00	0.00	0.01	0.00	0.01	0.00	0.01	0.00	0.01	0.00	0.00	0.00	0.00	0.01	0.01
Sr	0.00	0.02	0.01	0.02	0.00	0.00	0.00	0.01	0.00	0.00	0.00	0.01	0.01	0.00	0.01	0.00	0.01	0.00	0.01	0.00	0.00
Zr	0.01	0.01	0.00	0.01	0.00	0.00	0.00	0.00	0.00	0.00	0.00	0.00	0.01	0.01	0.01	0.02	0.00	0.00	0.00	0.04	0.05
inc	0.02	0.07	0.03	0.04	0.01	0.01	0.01	0.02	0.02	0.01	0.02	0.03	0.03	0.03	0.04	0.01	0.02	0.00	0.04	0.00	0.00
coh	0.01	0.08	0.03	0.04	0.01	0.02	0.01	0.02	0.02	0.01	0.01	0.03	0.03	0.02	0.04	0.00	0.02	0.00	0.05	0.00	0.00

Ave. R^2 = 0.011 Max. R^2 = 0.080 [cps/coh]

b)

	1	cps	Si	S	Cl	K	Ca	Ti	V	Cr	Mn	Fe	Ni	Cu	Zn	Br	Rb	Sr	Zr	inc	coh
1	0.00	0.54	0.18	0.42	0.14	0.00	0.01	0.08	0.03	0.10	0.05	0.21	0.28	0.33	0.15	0.14	0.02	0.00	0.12	0.08	0.17
cps	0.54	0.00	0.21	0.08	0.12	0.26	0.63	0.19	0.32	0.24	0.28	0.16	0.11	0.37	0.21	0.24	0.29	0.38	0.43	0.48	0.40
Si	0.18	0.23	0.00	0.26	0.02	0.30	0.06	0.04	0.15	0.20	0.08	0.06	0.14	0.01	0.01	0.01	0.43	0.03	0.00	0.01	0.00
S	0.41	0.08	0.25	0.00	0.00	0.30	0.23	0.22	0.32	0.23	0.24	0.40	0.14	0.05	0.24	0.01	0.38	0.10	0.07	0.14	0.05
Cl	0.13	0.13	0.02	0.00	0.00	0.05	0.28	0.02	0.05	0.12	0.04	0.00	0.00	0.02	0.02	0.05	0.07	0.31	0.06	0.12	0.05
K	0.00	0.29	0.31	0.32	0.06	0.00	0.00	0.47	0.01	0.15	0.03	0.21	0.23	0.09	0.15	0.06	0.20	0.00	0.03	0.01	0.05
Ca	0.01	0.62	0.08	0.26	0.29	0.01	0.00	0.05	0.02	0.06	0.03	0.12	0.18	0.27	0.08	0.28	0.00	0.00	0.23	0.08	0.21
Ti	0.08	0.22	0.04	0.24	0.03	0.47	0.04	0.00	0.08	0.20	0.03	0.09	0.14	0.02	0.00	0.02	0.51	0.02	0.00	0.00	0.01
V	0.03	0.35	0.16	0.36	0.07	0.02	0.02	0.08	0.00	0.14	0.01	0.17	0.21	0.10	0.09	0.06	0.11	0.01	0.03	0.01	0.05
Cr	0.08	0.26	0.21	0.25	0.13	0.14	0.04	0.21	0.13	0.00	0.21	0.21	0.23	0.17	0.20	0.13	0.09	0.02	0.11	0.12	0.15
Mn	0.05	0.28	0.08	0.25	0.05	0.04	0.02	0.02	0.01	0.20	0.00	0.10	0.15	0.08	0.05	0.05	0.15	0.01	0.02	0.00	0.04
Fe	0.20	0.17	0.06	0.41	0.01	0.20	0.10	0.09	0.15	0.20	0.10	0.00	0.23	0.00	0.07	0.00	0.34	0.04	0.00	0.03	0.00
Ni	0.27	0.11	0.13	0.14	0.00	0.20	0.16	0.13	0.18	0.21	0.15	0.21	0.00	0.01	0.14	0.00	0.32	0.07	0.03	0.07	0.02
Cu	0.32	0.36	0.01	0.05	0.02	0.07	0.24	0.02	0.09	0.16	0.07	0.00	0.01	0.00	0.02	0.01	0.12	0.09	0.04	0.26	0.02
Zn	0.16	0.24	0.01	0.25	0.03	0.15	0.07	0.00	0.09	0.20	0.05	0.07	0.15	0.02	0.00	0.02	0.30	0.03	0.00	0.01	0.01
Br	0.12	0.24	0.01	0.01	0.05	0.04	0.26	0.01	0.05	0.12	0.04	0.00	0.00	0.01	0.01	0.00	0.07	0.21	0.04	0.12	0.04
Rb	0.02	0.31	0.44	0.40	0.09	0.19	0.00	0.51	0.11	0.11	0.16	0.36	0.35	0.14	0.30	0.09	0.00	0.00	0.07	0.05	0.09
Sr	0.01	0.42	0.04	0.14	0.31	0.00	0.00	0.03	0.01	0.03	0.01	0.06	0.10	0.12	0.04	0.22	0.00	0.00	0.12	0.03	0.10
Zr	0.11	0.42	0.00	0.08	0.06	0.03	0.21	0.00	0.03	0.12	0.02	0.01	0.03	0.05	0.00	0.04	0.06	0.10	0.00	0.02	0.01
inc	0.07	0.49	0.01	0.14	0.11	0.01	0.07	0.00	0.01	0.11	0.00	0.03	0.07	0.27	0.01	0.12	0.04	0.02	0.03	0.00	0.20
coh	0.15	0.40	0.00	0.05	0.05	0.04	0.19	0.01	0.04	0.13	0.03	0.00	0.02	0.02	0.00	0.04	0.07	0.08	0.01	0.20	0.00

Ave. R^2 = 0.117 Max. R^2 = 0.632 [Ca/cps]

Figure 3.9. Matrixes showing R^2 values of all possible elemental and non-elemental ratios with winter precipitation records of Dalaman station. a) matrix shows annual geochemical data vs meteorological station b) matrix shows 7-point moving average values vs meteorological station. The color scale used in all matrices is same. Green color shows higher and red color shows lower R^2 values.

Figure 3.6 to Figure 3.9 show the results of the systematic correlation analysis designed to find the optimal proxy ratio for precipitation reconstruction before (annual raw data without smoothing) and after the computation of 7-years moving average (smoothing). Figures (Figure 3.6.a, Figure 3.7.a, Figure 3.8.a Figure 3.9.a) show matrices derived from the unsmoothed annual data, where the Average R^2 values were low, ranging from a minimum of 0.007 (Köyceğiz and Muğla) to a maximum of 0.014 (Marmaris). Figures (Figure 3.6.b, Figure 3.7.b, Figure 3.8.b Figure 3.9.b), however, displays the significant impact of the smoothing procedure (7-point moving average). The Average R^2 values increased substantially for all stations, rising to a maximum average of 0.117 for Dalaman. The analysis also reveals the most effective elemental pairs after the smoothing operations for each location: The highest maximum R^2 value for Muğla was found to be 0.270 using the Cu/cps ratio for Marmaris, the maximum correlation reached 0.449 with the Ca/cps ratio for Köyceğiz, a maximum R^2 of 0.366 was observed using the S/1 ratio and for Dalaman, the highest R^2 value was 0.632 with the Ca/cps ratio.

From the 8 matrices shown in Figure 3.6 to Figure 3.9, the highest 8 R^2 values from each matrix were selected. These specific element ratios were then used to create graphs showing the correlation between these optimal proxy ratios and the instrumental precipitation data (Figure 3.10).

P-test was applied to both unsmoothed and smoothed ratios selected from the matrices from Figure 3.6 to Figure 3.9. As a result of this test, ratios selected from unsmoothed ratios are mostly insignificant ($p > 0.05$), but all smoothed ratios are significant ($p < 0.05$). The fact that correlations made with smoothed data yield higher R^2 scores than correlations made with unsmoothed data may be due to the lake's slow response to environmental conditions. As a result, the correlation between precipitation data and element ratios obtained from geochemistry yields a higher R^2 value in the smoothed version produced using a 7-year moving average, valid for all stations.

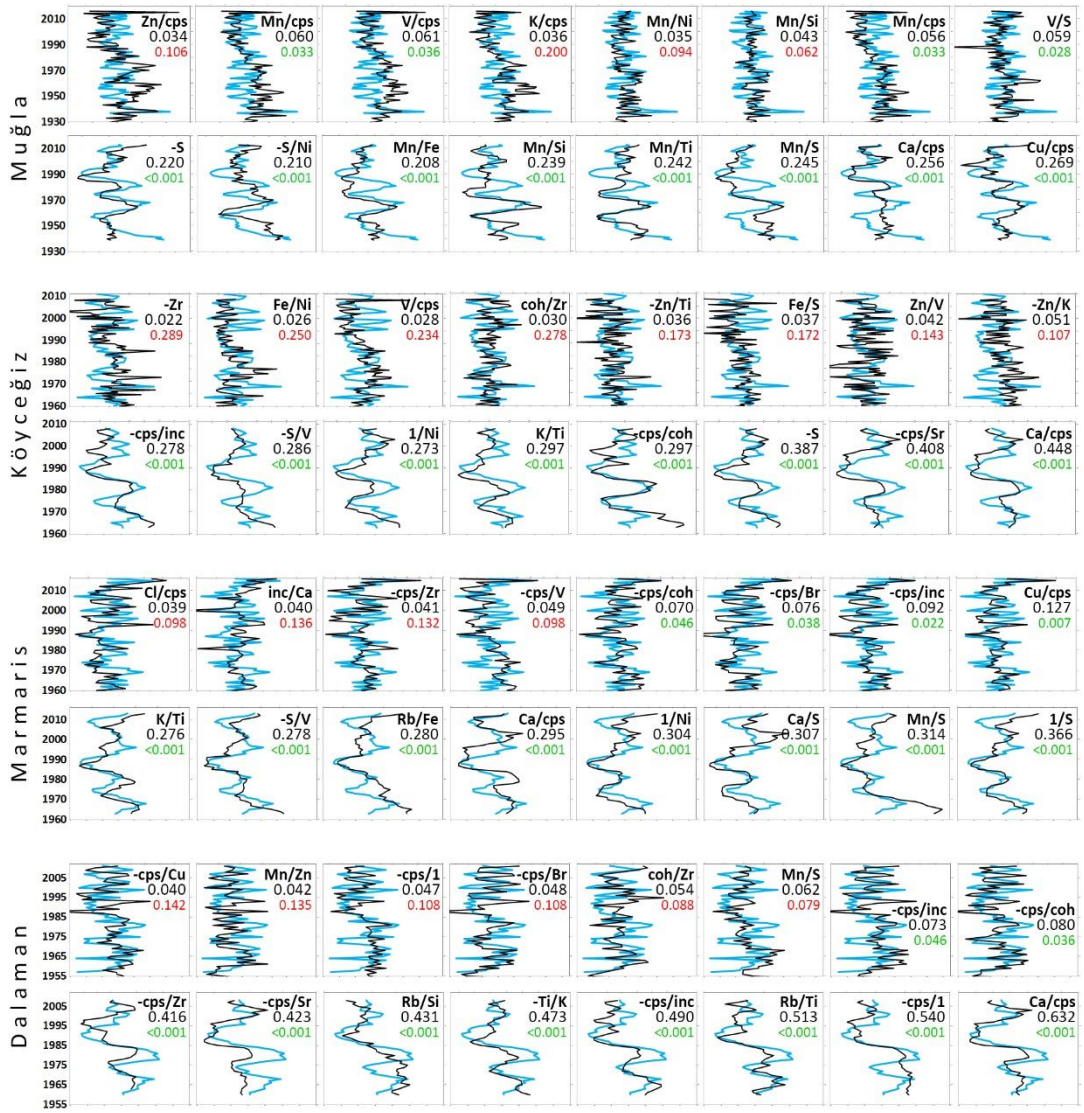

Figure 3.10. Graphs showing the correlation of rainfall data with smooth and unsmooth ratios prepared for 4 meteorological stations. The top row of the two rows prepared for each station shows the correlations for unsmooth, while the bottom line shows the correlations for smooth. The blue lines in the graphs represent precipitation, while the black lines represent the ratio data. The value written below each ratio shows the R^2 value of that ratio. The values written below the R^2 show the p-test result for that ratio, and the color of the result indicates whether the ratio is significant (green) or insignificant (red). Note that negative signs in the ratios mean negative correlation.

The expected outcome was that the unsmoothed ratios would show a lower R^2 compared to the smoothed ones. Such a situation was observed, yet the main concern here lies in the lack of consistency, as the ratios that produce the maximum R^2 values differ significantly between the raw (unsmoothed) and the treated (smoothed) data. In other words, at least similar pattern is expected for both unsmoothed and smoothed ratios. For example, for Köyceğiz station, highest R^2 value is observed at "Ca/cps" ratio from smoothed ratios, but the ratio did not even rank among the 8 highest correlations observed within the unsmoothed annual dataset. Element ratios which are showing high R^2 scores showed inconsistencies between different meteorological stations. Furthermore, inconsistencies were also observed within the same station: even between unsmoothed (annual) data and smoothed data (smoothed by using a 7-point moving average), there were significant differences between specific ratios showing the highest correlations. Although some ratios yield high R^2 scores, for these ratios to be used as proxies, they must also be geologically and geochemically meaningful ratios. Some ratios yielding high R^2 scores in statistical analysis are not geologically or geochemically meaningful. This issue can be seen in non-elemental parameters: for example, the ratios of "-cps/Inc ($R^2 = 0.54$)" and "-cps/1 ($R^2 = 0.49$)" for Dalaman and the ratio of "cps/coh ($R^2 = 0.3$)" for Köyceğiz (from smoothed ratios) have no geochemical significance. Furthermore, this problem is also observed in unsmoothed (annual) data; some of the highest R^2 ratios, including "-cps/coh" and "-cps/inc" for Dalaman and "-cps/inc" for Marmaris, are similarly difficult to interpret geochemically.

When the results obtained from these procedures were far from the expected outcomes, so that another method was employed to find a proxy from elemental ratio that can be used for all stations. In this method, all the ratios created by using 7-points moving average were averaged by using 4 meteorological station's ratios and a new matrix is formed (Figure 3.11). "cps, inc, coh" values are obtained from the measurements which are not geochemical values but, only the cps is a geologically meaningful parameter when it is used for a ratio. Thus, from the new matrix constructed, both the highest R^2 value and the geochemically significant 16 ratio

were selected. These ratios are S/1, Ca/cps, Ca/S, Ti/K, Mn/S, Fe/1, Fe/S, Ni/1, Ni/Ca, Cu/cps, Rb/Si, Rb/S, Rb/Ti, Rb/Fe, Sr/cps and Zr/cps.

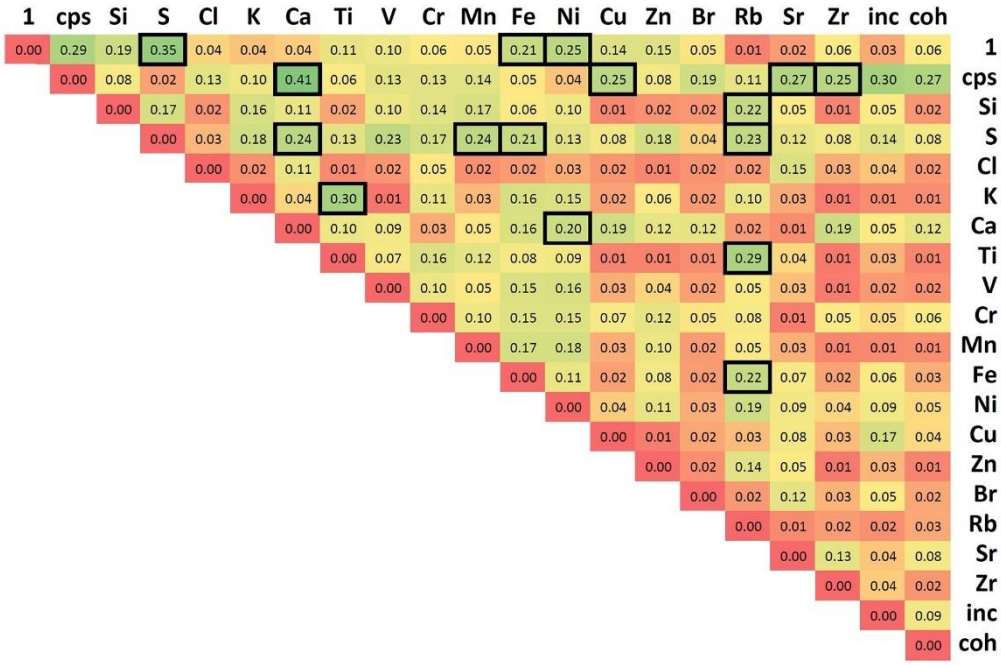

Figure 3.11. A matrix constructed by taking the average of all ratios produced separately for all meteorological stations using the 7-points moving average method (matrices in Figure 3.6 to Figure 3.9). The color scale is the same as the scale in the matrices above. The 16 ratios with the highest R^2 values and geochemically meaningful results are marked with a black frame.

These 16 ratios from Figure 3.11 are marked as possible proxies for the precipitation reconstruction. To create reconstruction curves, these steps were followed: First, a formula was developed using the established correlation between instrumental rainfall data and the element ratios. After that, this formula was applied to the element ratios to reconstruct precipitation for the unrecorded periods (the precipitation beyond the instrumental data limit). This procedure is repeated for 16 ratios for each 4 meteorological stations (Figure 3.12).

When precipitation reconstruction curves were examined, it was observed that the curves produced from four meteorological stations showed approximately the same trend for the same ratio, except for the Rb/Si ratio (Dalaman station's curve for Rb/Si diverges from other stations at the bottom).

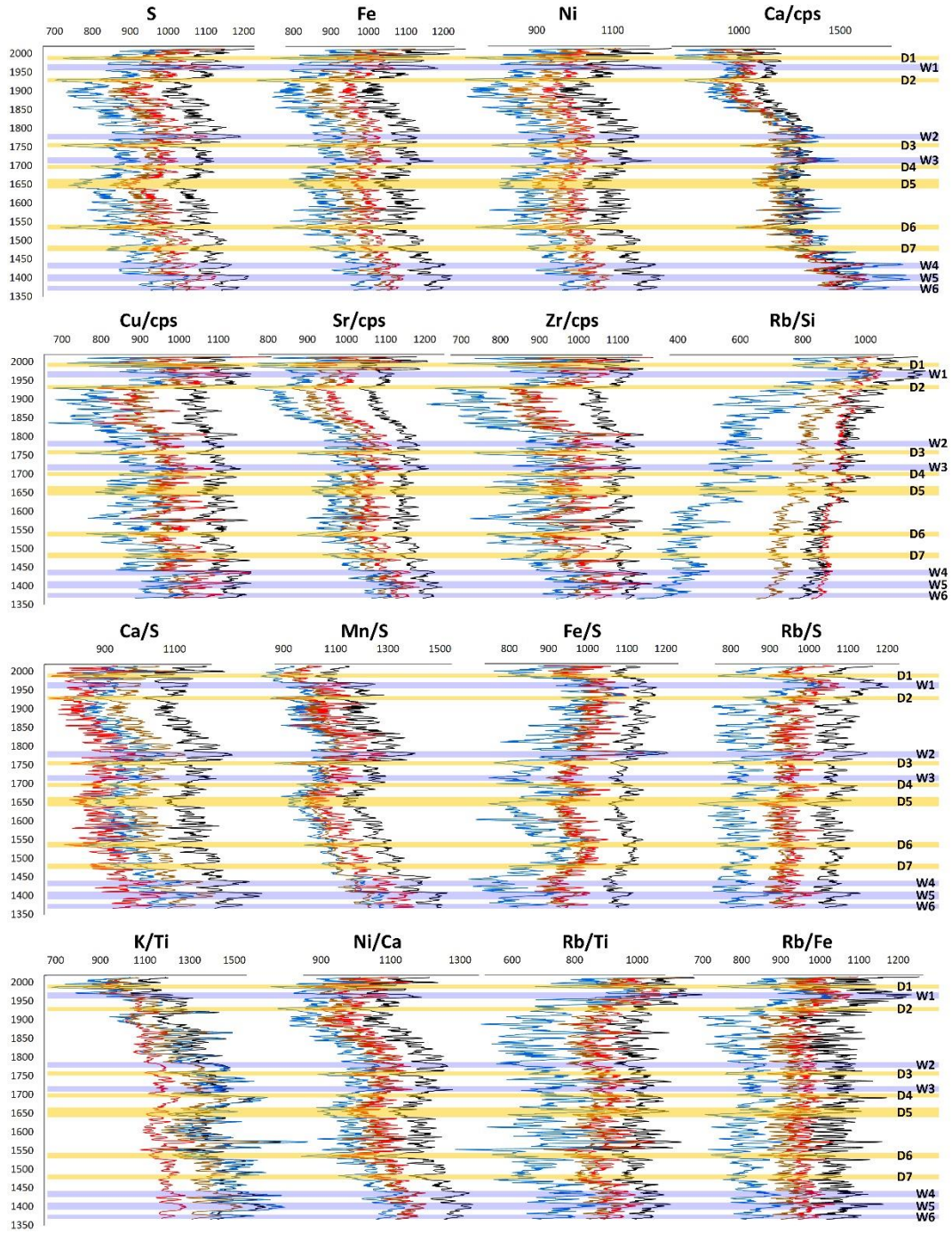

Figure 3.12. Precipitation reconstruction curves derived from the 16 ratios. Black lines are indicating Marmaris, brown colored lines belong to Köyceğiz, red lines are indicating Muğla and blue lines are showing the Dalaman meteorological station. Yellow horizontal lines indicating with “D1, D2, etc.” are dry purple lines with “W1, W2, etc.” periods are indicating wet periods implied by the curves.

The stations are ordered from highest to lowest precipitation amount for most element ratios: Marmaris (black), Muğla (red), Köyceğiz (brown), and Dalaman (blue). This situation is an expected outcome, as a similar ranking in terms of precipitation amount is observed within the instrumental station measurements (Figure 3.3). Yet, the order is different in Rb/Si, Ca/S and K/Ti.

Highest R^2 values were the ratios "Ca/cps" ($R^2 = 0.41$) and "S/1" ($R^2 = 0.35$). When the precipitation reconstructions created from these two ratios are examined, it can be concluded that the Ca/cps ratio implies a steady drop in precipitation over the last 600 years. On the other hand, although the S/1 ratio shows that rainfall trends fluctuated intermittently over these six centuries, it did not imply any significant change in total precipitation. This situation introduces several questions; for instance, if two ratios have the highest R^2 value can produce different reconstructions, what specific level of R^2 should be considered reliable.

Another inconsistency is observed when comparing the reconstructions derived from the Ca/Cps and K/Ti ratios. Despite both ratios correlating positively with instrumental precipitation, their reconstructions frequently show different implications across various periods. For instance, during the D2 dry period, the Ca/Cps ratio indicates dry period, an observation that is not supported by the K/Ti ratio. Similarly, the wet period (W3) clearly visible in the Ca/Cps reconstruction cannot be observed in the K/Ti record. Furthermore, Ca/cps ratio should be negatively correlated with precipitation.

The dry (D) and wet (W) periods highlighted in the Figure 3.12 are examples selected for demonstration and do not represent the full records of dry and wet periods. Among these examples, the D5 dry period is particularly critical, as it is the longest and most persistent drought implied by most of the elemental ratios. Consequently, this interval can be effectively used to measure the strength of the various elemental ratios. Based on this, the Rb/Si and Rb/Ti ratios entirely failed to capture the D5 drought, instead indicating a comparatively wet period. While the K/Ti and Rb/Fe ratios captured the D5 event only partly. Yet, this drought period appears very

distinctly in the signal of the other proxy ratios so it could expect that all elemental ratios could capture this implied dry period.

In paleoclimatological reconstructions, precision is often considered a more critical factor than accuracy. In other words, the primary goal is not necessarily to precisely estimate the absolute amount of past precipitation, but rather to successfully capture the overall precipitation trend. From this perspective, variations in the exact precipitation amounts predicted by different elemental ratio reconstructions do not necessarily indicate that the statistical equations are incorrect. However, if elemental ratios intended for use as proxies show inconsistent trends, such as one proxy implying an increase in the precipitation trend over the last 600 years while another implies a decrease, this inconsistency suggests that those proxies may not provide reliable results.

CHAPTER 4

DISCUSSION

4.1 Element-ratio Profiles for the Past Precipitation Reconstruction

The 16 elemental ratio profiles obtained from the correlation matrices constructed by correlating winter precipitation data (average precipitation of October, November, December, January, February and March) taken from 4 meteorological stations (Muğla, Köyceğiz, Marmaris and Dalaman) with elemental data derived from geochemical data corresponding to the clastic rich layer's approximately middle point obtained from ITRAX. Although the correlations yielded R^2 values reaching up to 0.41, it was observed that the resulting precipitation reconstruction curves implied different trends, even for the same meteorological station, explained in the Results chapter. This demonstrated that the desired precision could not be achieved by using individual elemental ratios, so it can be concluded that reliable reconstructions cannot be constructed using single elemental ratios alone. Thus, it was determined that multiple elemental ratios could create better reconstruction rather than a single ratio. Consequently, 16 elemental ratios (S/1, Ca/cps, Ca/S, Ti/K, Mn/S, Fe/1, Fe/S, Ni/1, Ni/Ca, Cu/cps, Rb/Si, Rb/S, Rb/Ti, Rb/Fe, Sr/cps and Zr/cps) that showed the highest correlation with instrumental precipitation data and were deemed geochemically meaningful were selected for the application of Principal Component Analysis (PCA) to use all the ratios for more precise precipitation trend. 16 elemental ratios were imported to SPSS software, and the components were created. The software extracted 5 Principal Components (PCs) that compensate for 97% of the total variance in the dataset. The correlation coefficients (R) of each elemental ratio profile can be seen in the Figure 4.1. Muğla station was chosen for PCA because it has the longest period of precipitation measurement.

a)

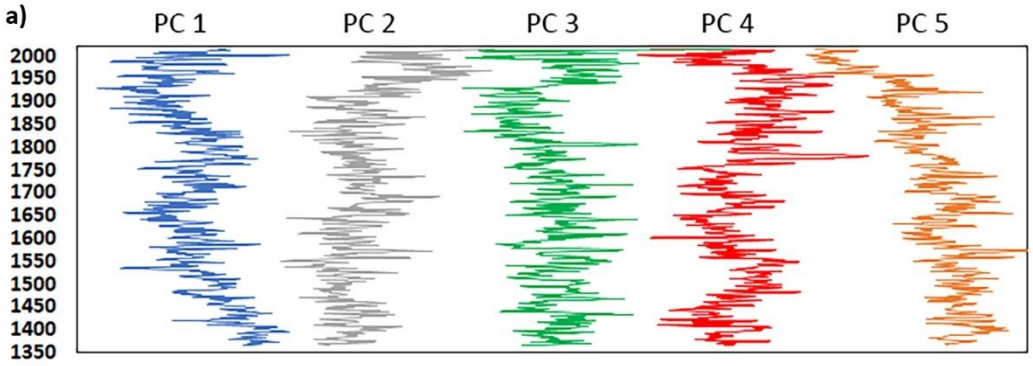

b)

	1	2	3	4	5
S	**0.864**	0.280	0.250	0.280	-0.047
Fe	**0.912**	0.226	0.276	-0.115	-0.015
Ni	**0.898**	0.249	0.274	-0.018	0.041
Ca_cps	**0.831**	-0.121	0.212	-0.143	**0.410**
Cu_cps	**0.403**	0.249	**0.813**	0.026	0.097
Sr_cps	**0.842**	-0.018	0.316	-0.193	0.218
Zr_cps	**0.515**	0.203	**0.740**	-0.068	0.099
Rb_Si	-0.386	**0.736**	-0.008	0.149	**-0.431**
Ca_S	**0.935**	0.084	0.153	0.049	0.217
Mn_S	**0.813**	-0.133	0.082	0.253	0.309
Fe_S	-0.059	0.132	-0.052	**0.974**	-0.073
Rb_S	0.188	**0.791**	0.135	**0.550**	0.018
K_Ti	0.318	0.039	0.109	-0.056	**0.912**
Ni_Ca	**0.927**	0.056	0.186	-0.085	0.267
Rb_Ti	0.098	**0.916**	0.137	-0.115	0.082
Rb_Fe	0.275	**0.905**	0.200	0.128	0.060

Figure 4.1. Results of PCA on 16 elemental ratios and winter precipitation of Muğla station. a) Precipitation reconstructions constructed by using single variable regression derived from PCs. Note that y-axis shows years while x-axis shows the precipitation amount. b) Correlation coefficients of each elemental ratios with 5 PCs.

Firstly, PC1 is highly positively correlated with S/1, Fe/1, Ni/1, Ca/cps, Sr/cps, Ca/S, Mn/S and Ni/Ca and moderately correlated with Zr/cps and Cu/cps. PC2 is highly positively correlated with Rb/Si, Rb/S, Rb/Ti and Rb/Fe. PC3 is highly positively correlated with Sr/cps and Zr/cps. PC4 is highly positively correlated with Fe/S and moderately correlated with Rb/S. Finally, PC5 is moderately positive correlated with Cu/cps and negatively with Rb/Si and highly positively correlated with K/Ti (Figure 4.1).

PCs derived from PCA were used as single variables in Linear Regression to construct precipitation reconstructions. Equation derived from PC5 implies a decrease in the upper parts whereas PC3's equation implies an increase for the same

part. Equation from PC4 implies a sharp fluctuation around the years 1600 and 1400 but in other 4 PCs' equations this fluctuation cannot be seen. PC1's equation implies an increase around the year 1800 whereas PC2's implies a decrease at that period and PC5's implies no changes around 1800. Overall trends of PC2's and PC3's imply approximately same pattern, but the equations derived from PC1 and PC5 imply different trends. In short, 5 different trends can be observed with 5 different equations derived from PCs. Thus, another statistical method should be applied for more precise trends while using multivariate elements rather than computing 16 elemental ratios. Since the estimation of a single variable (precipitation) was required using a multivariate dataset (geochemical data obtained from ITRAX), the Multiple Linear Regression (MLR) method was selected. For such multivariate datasets, multivariate statistical methods are routinely applied to effectively examine and understand the relationships that exist among the measured variables (Davis, 2002).

4.2 Multiple Regression Analysis for the Past Precipitation Reconstruction

Multiple Regression is employed because it may enhance the estimation ability compared to relying on a single elemental ratio. This can be achieved by utilizing multiple independent variables (proxies) simultaneously, allowing the model to create a more precise model. Multiple regression was applied to "winter" geochemical data with all elements obtained from ITRAX, varve thicknesses of the clastic-rich layers of the core (called as winter thickness) and the ratio of winter thickness to white colored carbonate layers thickness (called as summer thickness) as single independent variables and precipitation data as dependent variable. As precipitation data, 4 meteorological stations' "winter" precipitation amounts were used (Figure 4.2).

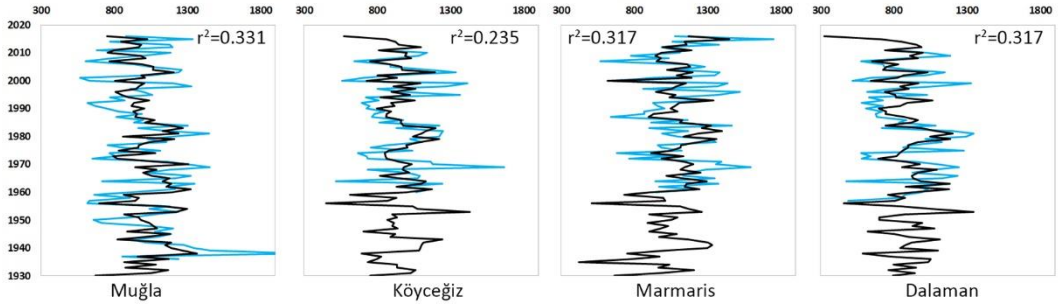

Figure 4.2. Results of MLR analysis for 4 meteorological stations' "winter precipitation data and "winter" geochemical data (17 elemental and 3 non-elemental data) and varve thicknesses. Blue lines are indication "winter" precipitations recorded in meteorological stations. Black lines are the trends created after MLR. The precipitation and geochemical data are not smoothed with 7-points moving average.

As it can be seen in the Figure 4.2 that, R^2 values derived from MLR that ranges between 0.331 (Muğla) and 0.235 (Köyceğiz). The R^2 value is 0.317 and equal for Marmaris and Dalaman station. The preliminary analysis (Figure 3.6 to Figure 3.9) revealed that the annual (unsmoothed) geochemical data correlated poorly with the instrumental "winter" precipitation, yielding generally low R^2 values across all stations. The average R^2 scores were extremely low, specifically recorded as 0.007 for both Muğla and Köyceğiz, 0.014 for Marmaris, and 0.011 for Dalaman. Similarly, the maximum R^2 values observed within the unsmoothed matrices were low: 0.061 for Muğla, 0.051 for Köyceğiz, 0.127 for Marmaris, and 0.080 for Dalaman. It can be concluded that the R^2 values are improved with Multiple Linear Regression analysis.

To test the formulas created using Multiple Linear Regression (MLR), rainfall reconstructions were created for periods where instrumental data records were unavailable. This method allows for determining the precision of the estimated long-term trends. Regression equations derived from the data of 4 meteorological stations were used to produce a time series extending back to approximately 1350 AD, to understand the trends in past precipitation regimes.

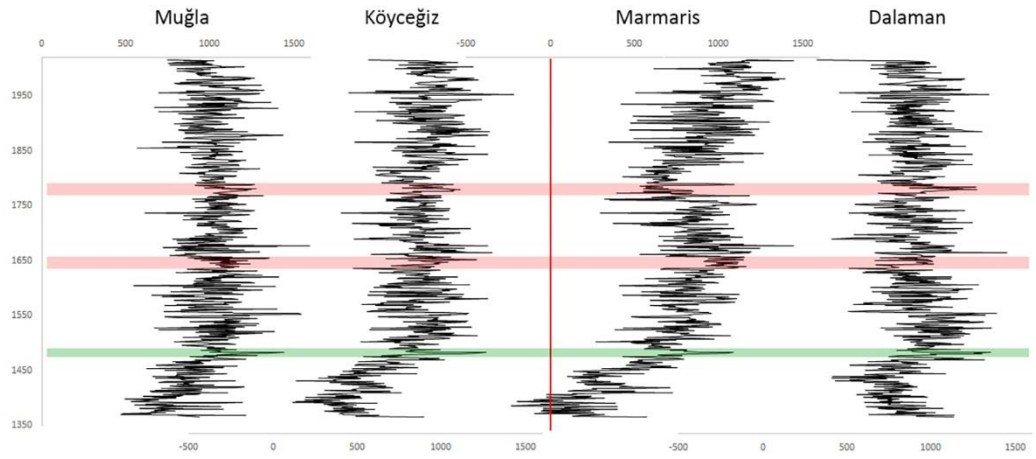

Figure 4.3. Precipitation reconstructions for 4 meteorological stations derived from the formulas obtained with MLR. Red horizontal layers are example periods which indicate the inconsistencies between trends and green horizontal layers are example periods which show a consistent period of the trends. Y- axis shows years and x-axis shows precipitation amount in mm. Note that Marmaris' trend is reaching negative precipitation values.

When the trends of reconstructions produced for 4 stations were examined, differences and similarities were identified in the trends. For example, an increase in precipitation around the year 1500 is implied by all 4 trends. On the other hand, around the year 1650, Dalaman trend implies a decrease in precipitation whereas in Muğla and Marmaris trends imply an increase in precipitation. Around the year 1700, Marmaris trend implies a decrease in precipitation but, all other 3 trends imply an increase. Furthermore, Marmaris trend implies negative precipitation regime around the year 1400. In short, although there are periods where these four trends imply similar trends, the fact that there are more periods where they imply different trends.

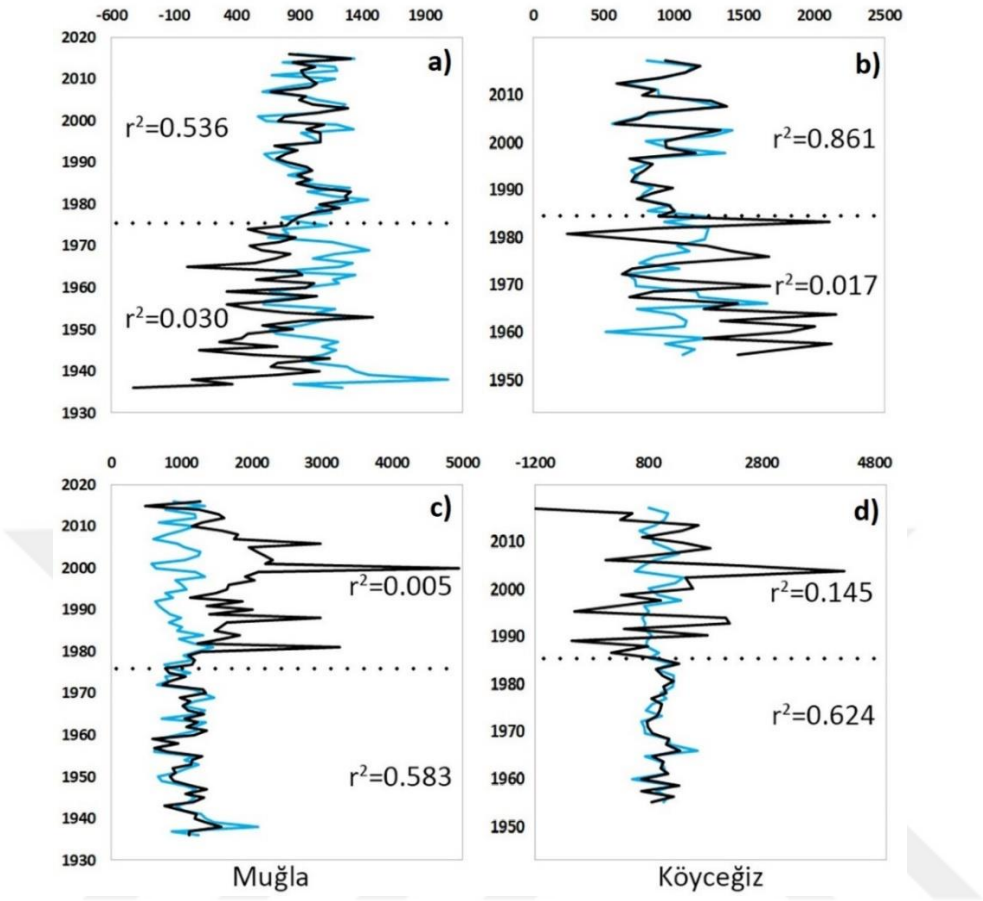

Figure 4.4. Upper Lower Operation results for Muğla and Köyceğiz stations. a) The upper half of the instrumental data is used for deriving equation, and the lower half is used for precipitation prediction for Muğla station. c) The lower half of the instrumental data is used for eqaution, and the upper half is predicted for Muğla station. b) The upper half of the instrumental data is used for equation, and the lower half is used for precipitation prediction for Köyceğiz station. d) The lower half of the instrumental data is used for equation, and the upper half is predicted for Köyceğiz station. Note that negative precipitation in a and d.

MLR created trends and tried to predict the precipitation trend for approximately 500 years, but since no precipitation record for past 500 years the implication cannot be controlled. Thus, to understand how accurately the equations work, 4 different

models were created based on Muğla and Köyceğiz meteorological stations (Figure 4.4).

Muğla meteorology station's 81 years of precipitation data divided into 2 groups with 40 years of precipitation. First, MLR applied for the 2016-1976 period and with that equation, 1935-1975 precipitation regime was predicted (Figure 4.4a). Second, with other half of the precipitation data (1986-1959) correlated with ITRAX data to predict first half of the precipitation data (2011-1985) (Figure 4.4c) This methodology is named as "Upper Lower Operation".

Same methodology was conducted for Köyceğiz station. Köyceğiz meteorology station's 52 years of precipitation data divided into 2 groups with 26 years of precipitation. Third, MLR applied for the 2011-1985 period and with that equation, 1986-1959 precipitation regime was predicted (Figure 4.4b). Fourth, with other half of the precipitation data (1986-1959) correlated with ITRAX data to predict first half of the precipitation data (2011-1985) (Figure 4.4d). Results were examined and it is found that the linear regression provides inaccurate results.

The Multiple Linear Regression (MLR) analysis demonstrated a strong statistical fit during the calibration phase, where actual precipitation values were known. Specifically, the R^2 scores obtained from the upper and lower halves of the Muğla and Köyceğiz datasets were high (Muğla: 0.536 and 0.583; Köyceğiz: 0.861 and 0.624). However, a significant drop in model performance was observed during the cross-validation (prediction) phase, where the equations were used to predict precipitation for the unmodeled half of the instrumental period. The predictive R^2 values decreased dramatically, falling to 0.005 (Muğla, upper half) and 0.030 (Muğla, lower half), and similarly low scores were noted for Köyceğiz (0.145 and 0.017). The reason this method was only tested for Muğla and Köyceğiz and not for Marmaris and Dalaman is to save time. Because, if a reconstruction technique fails

to perform reliably across two different stations, its successful application at a third station would still indicate that the method is unreliable.

To conclude, this considerable divergence between high calibration scores and near-zero prediction scores may be resulting from compaction effect or any other problem that arises when dividing the dataset into halves as upper and lower.

Since the results of the analyses (Upper Lower Operation) performed by splitting the dataset into two parts (upper and lower) were insufficient, another method should be used to divide the data. Due to changes in the upper and lower sections of the core resulting from compaction or other factors, the dataset was split into odd years (e.g., 1993, 1995, 1997) and even years (e.g., 1976, 1978, 1980). Subsequently, a correlation was established using Multiple Linear Regression (MLR) between the geochemistry and varve thickness of the even years and the "winter" precipitation of the corresponding even years from the meteorological stations. The resulting equation was then used to estimate the precipitation amounts for the odd years by inputting the geochemistry and varve thickness data of those odd years. The reverse operation was also performed, where an equation generated using the odd years was used to predict the even years and the method is called “Odd Even Operation”.

Firstly, “Odd Even Operation” method is used for Muğla station (Figure 4.5). The MLR equation derived from the even years is correlating with Muğla winter precipitation data’s even years with R^2 value of 0.448. Predicted odd years is correlating with Muğla winter precipitation data’s odd years with a low R^2 (0.072). When even and odd years (predicted) are merged and correlated with whole Muğla winter precipitation data, it has a R^2 value of 0.19. The reverse operation was performed, and it is found that the MLR formula derived from the odd years has a correlation with winter precipitation (odd years) 0.563 in terms of R^2 value. Predicted even years on the other hand correlates with precipitation of even years with an R^2

score of 0.058. Odd years and predicted even years are merged and the merged dataset is correlated with winter precipitation with R2 of 0.191.

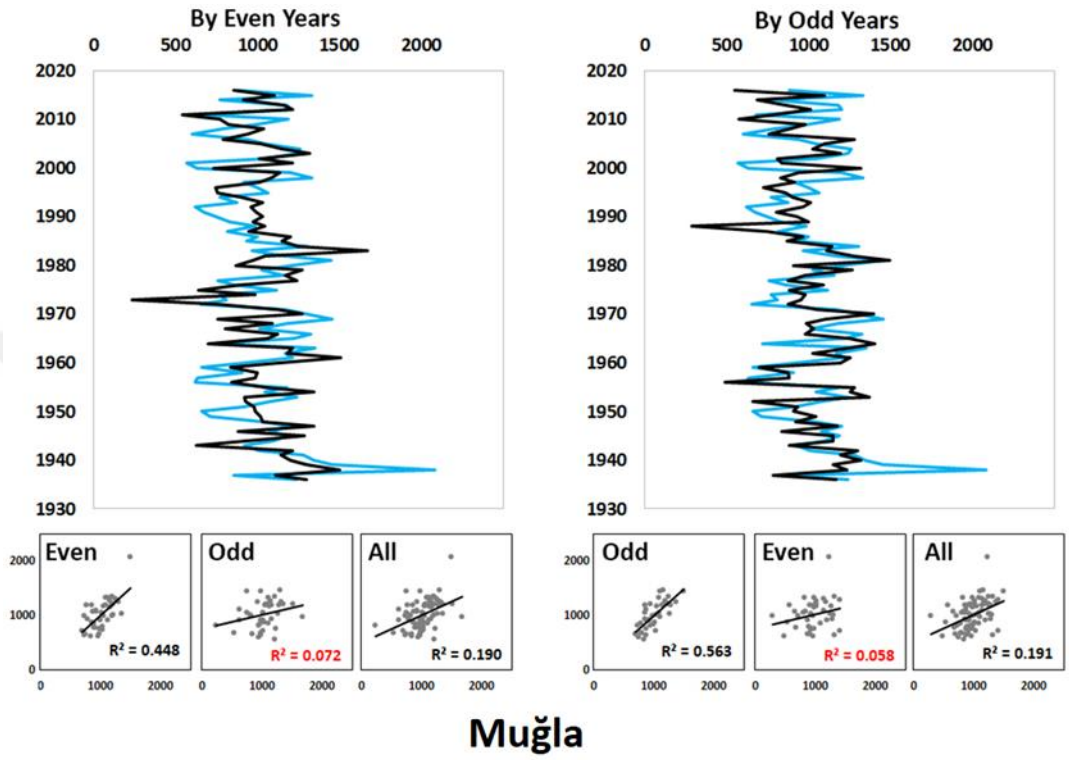

Figure 4.5. Graphs and R^2 values of the graphs are showing the results of "Odd Even Operation" performed for Muğla meteorological station's "winter" precipitation data. Blue lines are representing actual "winter" precipitation and black lines are showing the MLR results of the operation. X-axis and y-axis show precipitation (mm) and years respectively.

To examine the long-term precipitation trend prediction, an approximately 500-year precipitation regime trend was generated using the two equations produced after "Odd Even Operation".

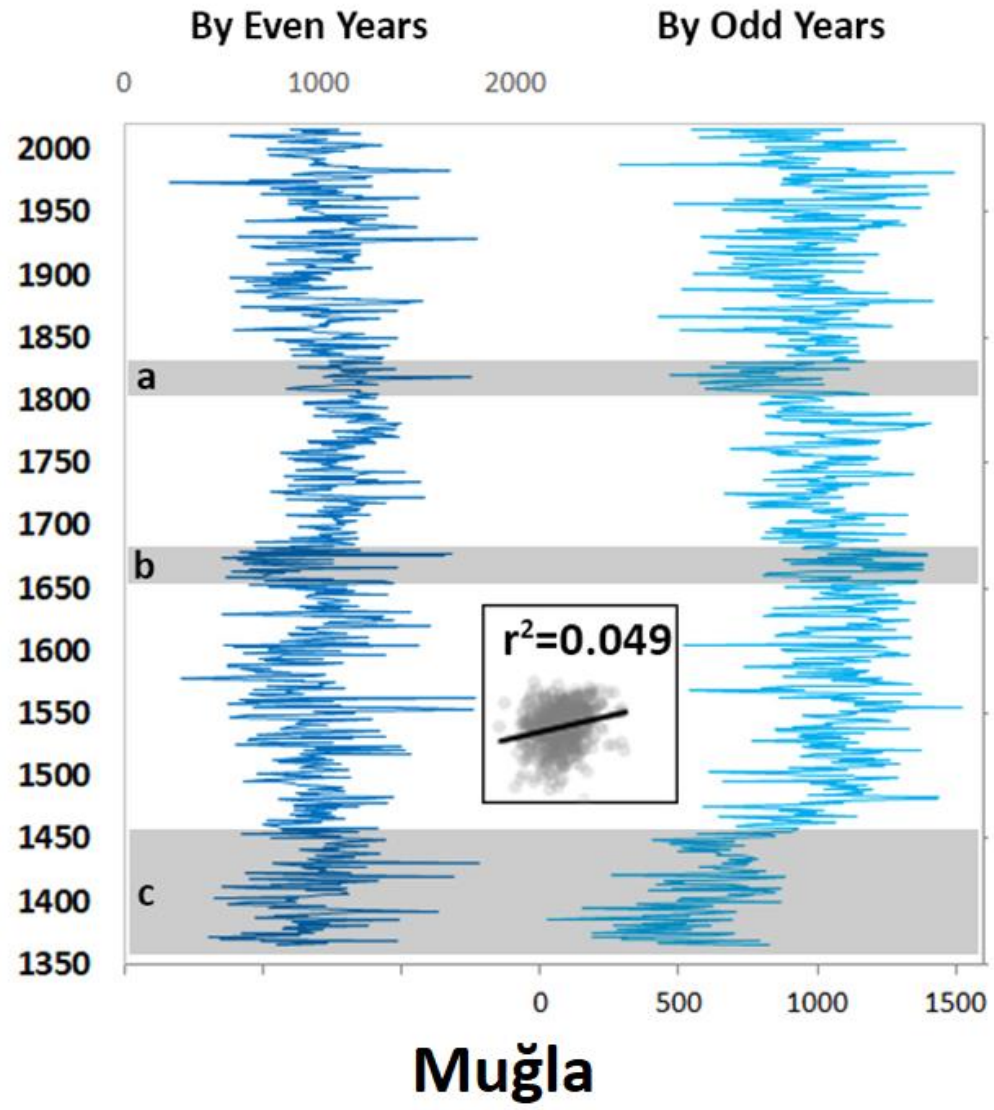

Figure 4.6. Graph showing the predicted trend derived from "Odd Even Operation" for Muğla station. Trend on the left (dark blue) representing the reconstruction derived from the formula obtained from even years (called as "by even years") and right trend (light blue) resulted from odd year's equation (called as "by odd years"). Time periods a, b and c are showing examples of inconsistencies between two trends.

When two generated reconstructions were examined, several inconsistencies were observed. Examples of these inconsistencies can be seen during periods a, b, and c (Figure 4.6). In period a, the "by even years" trend implies a wet phase, whereas the "by odd years" trend suggests arid conditions. During period b, the "by even years"

trend indicates a dry period, but the “by odd years” trend implies no such aridity. Finally, in period c, the “by odd years” trend suggests a gradual increase in precipitation, a finding that is not reflected in the “by even years” trend. Furthermore, the correlation coefficient (R^2) between the two trends was found to be low, at only 0.049.

Secondly, “Odd Even Operation” method is used for Köyceğiz station (Figure 4.7). The MLR equation derived from the even years is correlating with Köyceğiz winter precipitation data’s even years with R^2 value of 0.701. Predicted odd years is correlating with Muğla winter precipitation data’s odd years with a low R^2 (0.008). When even and odd years (predicted) are merged and correlated with whole Köyceğiz winter precipitation data, it has an R^2 value of 0.068. The reverse operation was performed, and it is found that the MLR formula derived from the odd years has a correlation with winter precipitation (odd years) 0.748 in terms of R^2 value. Predicted even years on the other hand correlates with precipitation of even years with an R^2 score of 0.102. Odd years and predicted even years are merged and the merged dataset is correlated with winter precipitation with R^2 of 0.000.

To examine the long-term precipitation trend prediction, an approximately 500-year precipitation regime trend was generated using the two equations produced after "Odd Even Operation" (Figure 4.8).

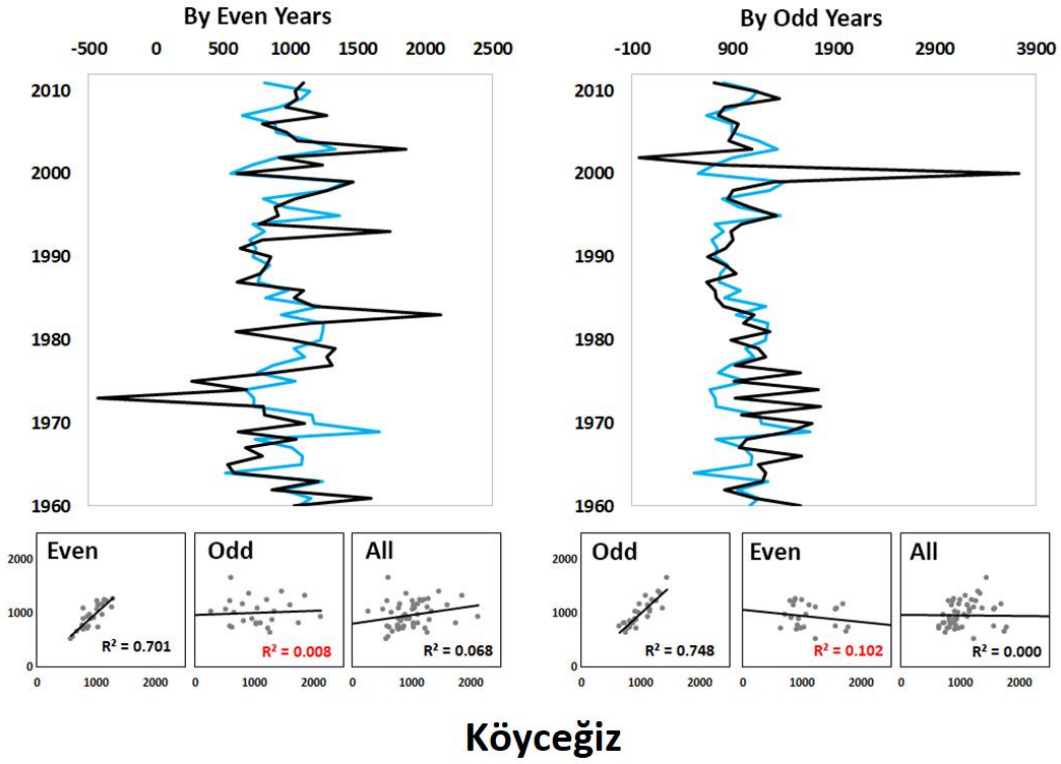

Figure 4.7. Graphs and R^2 values of the graphs are showing the results of "Odd Even Operation" performed for Köyceğiz meteorological station's "winter" precipitation data. Blue lines are representing actual "winter" precipitation and black lines are showing the MLR results of the operation. X-axis and y-axis show precipitation (mm) and years respectively.

When "by even years" and "by odd years" trends are examined, the most major inconsistency lies within the main precipitation trend over the last approximately 500 years. In other words, the "by even years" trend, despite minor fluctuations, implies a gradual increase in precipitation over this period. In contrast, the "by odd years" trend, while also showing fluctuations, suggests a gradual decrease in the precipitation trend over the exact same period. Furthermore, negative precipitation amounts are implied by the "by even years" trend. The correlation coefficient (R^2) between the "by even years" and "by odd years" trends were calculated to be notably low, at only 0.132 (Figure 4.8).

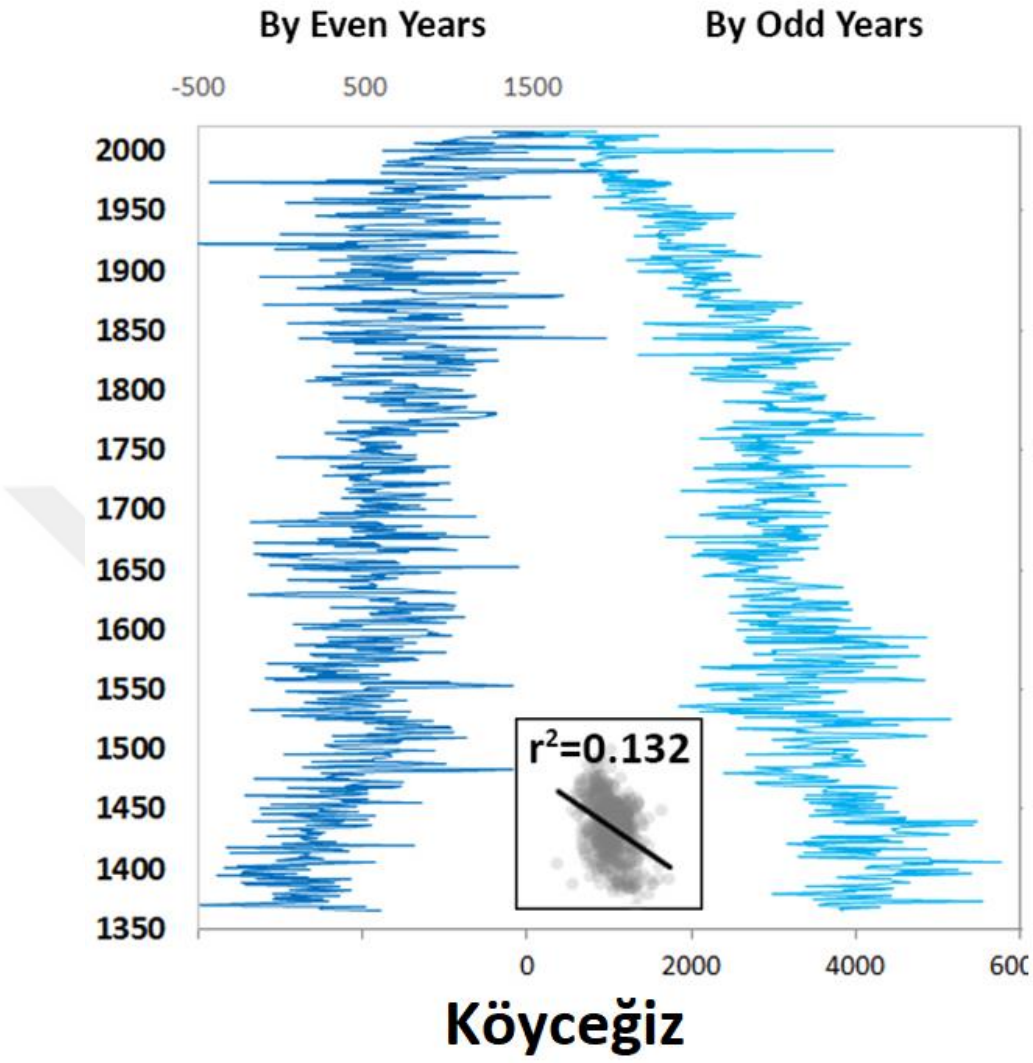

Figure 4.8. Graph showing the predicted trend derived from “Odd Even Operation” for Köyceğiz station. Trend on the left (dark blue) representing the reconstruction derived from the formula obtained from even years (called as “by even years”) and right trend (light blue) resulted from odd year’s equation (called as “by odd years”). Note that precipitation values implied by "by even years" trend has negative values.

The trends resulting from the MLR between the precipitation data from the Muğla and Köyceğiz stations (the dependent variable) and the ITRAX geochemical data and varve thicknesses (the independent variables) is insufficient in terms of required precision. This observation in the findings reported in the Results chapter, where

correlations utilizing smoothed data (by applying the 7-point moving average method) were shown to yield more precise results compared to unsmoothed data. Considering that the Multiple Linear Regression (MLR) method was applied to unsmoothed data in the Discussion chapter, it was reasoned that applying a smoothing procedure to the data used before the MLR method application would similarly increase the precision. Consequently, the precipitation, geochemistry, and varve thickness data were all subsequently smoothed using the 7-point moving average.

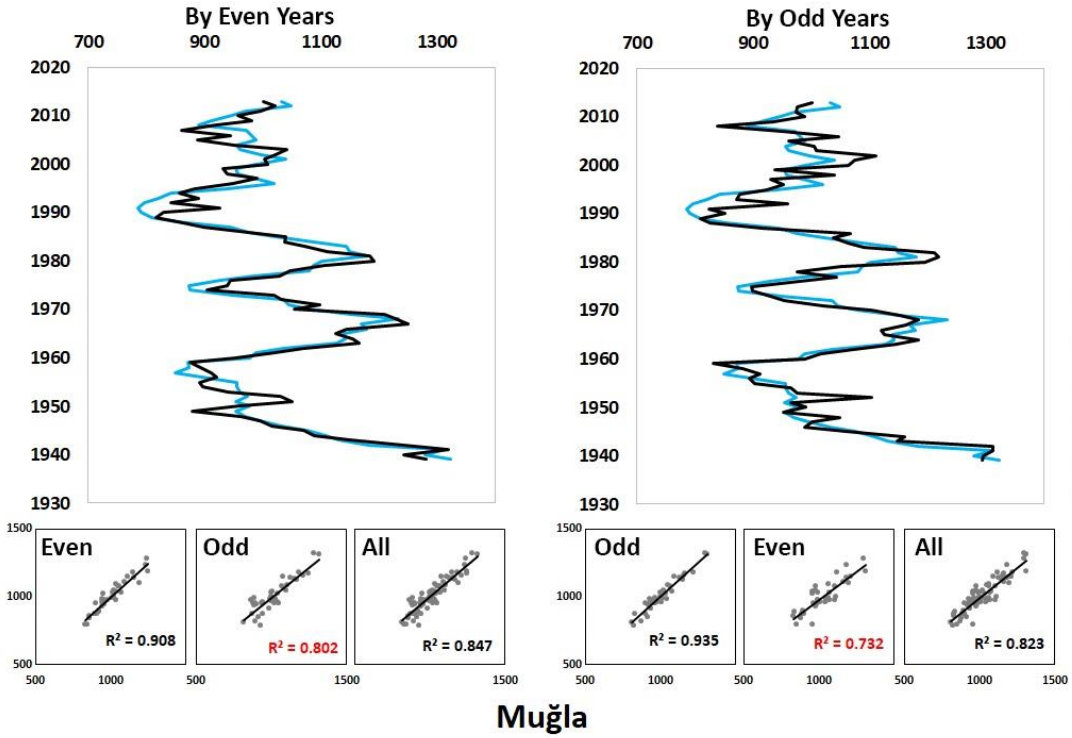

Figure 4.9. Graphs and R^2 values of the graphs are showing the results of "Odd Even Operation" performed for Muğla meteorological station's "winter" precipitation data. Note that the precipitation, geochemical and varve thickness data is smoothed with 7-point moving average method. Blue lines are representing actual "winter" precipitation and black lines are showing the MLR results of the operation. X-axis and y-axis show precipitation (mm) and years respectively.

“Odd Even Operation” method is used for Muğla station (Figure 4.9). The MLR equation derived from the even years is correlating with smoothed Muğla winter precipitation data’s even years with R^2 value of 0.908. Predicted odd years is correlating with smoothed Muğla winter precipitation data’s odd years with an R^2 of 0.802. When even and odd years (predicted) are merged and correlated with whole smoothed Muğla winter precipitation data, it has a R^2 value of 0.847. The reverse operation was performed, and it is found that the MLR formula derived from the odd years has a correlation with smoothed winter precipitation (odd years) 0.935 in terms of R^2 value. Predicted even years on the other hand correlates with smoothed precipitation of even years with an R^2 score of 0.732. Odd years and predicted even years are merged and the merged dataset is correlated with smoothed winter precipitation with R^2 of 0.823.

To examine the long-term precipitation trend prediction, an approximately 500-year precipitation regime trend was generated using the two equations produced after "Odd Even Operation" for smoothed data correlation (Figure 4.8).

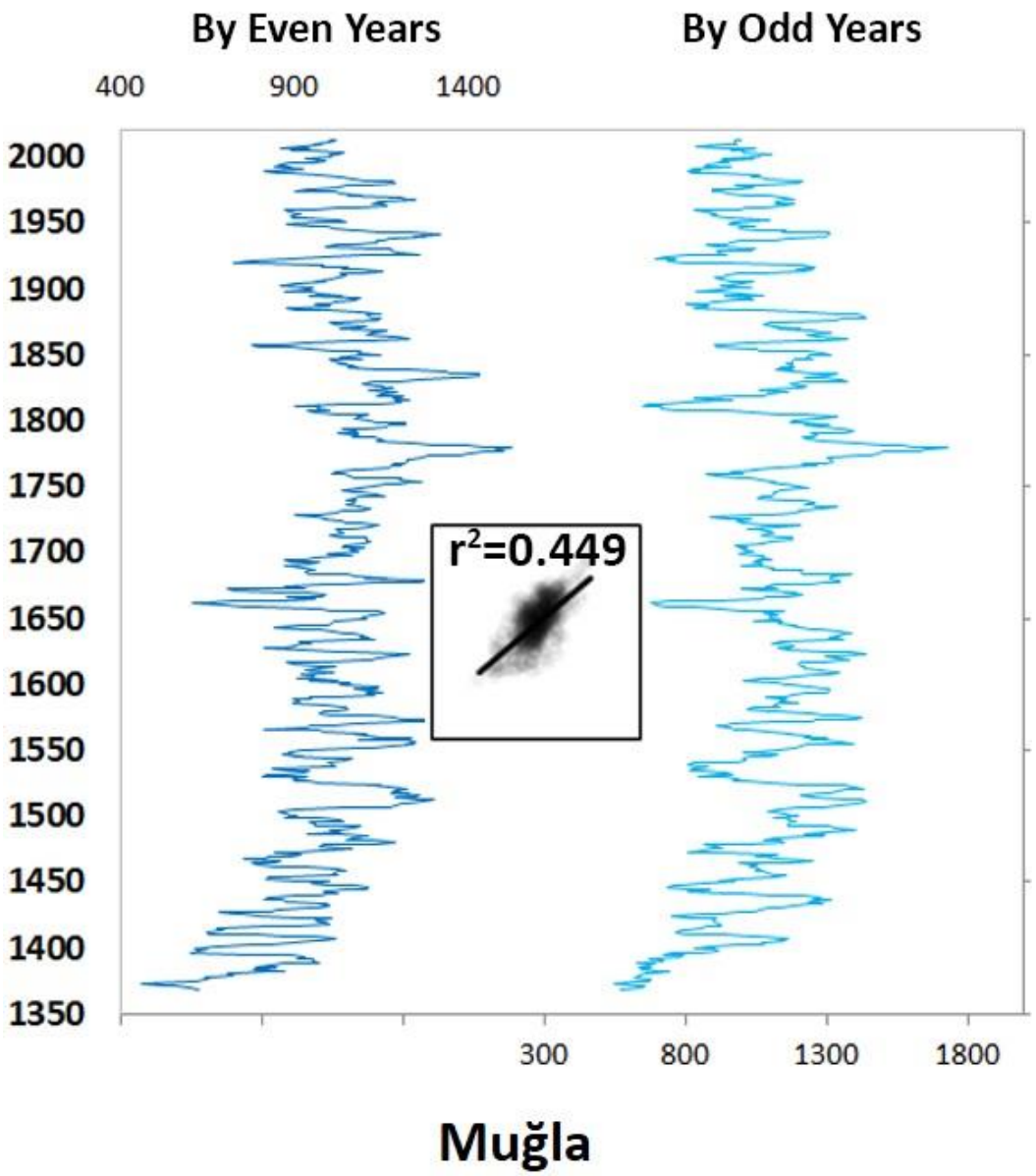

Figure 4.10. Graph showing the predicted trend derived from “Odd Even Operation” for Muğla station. Trend on the left (dark blue) representing the reconstruction derived from the formula obtained from smoothed even years (called as “by even years”) and right trend (light blue) resulted from smoothed odd year’s equation (called as “by odd years”).

The correlation coefficient (R^2) between the "by even years" and "by odd years" reconstructions for the Muğla station improved after the smoothing procedure.

Specifically, the R^2 value for the unsmoothed annual trends was low at 0.049; however, the R^2 value for the corresponding smoothed trends increased substantially to 0.449. Furthermore, an overall improvement in correlation was observed across all calculated R^2 values. The improvement observed in the trends generated for the Muğla station following the smoothing procedure is not sufficient to conclude that the methodology yields precise results. Consequently, these steps had to be repeated, and their results analyzed for a second station, Köyceğiz. To achieve this objective, the "odd-even operation" was performed using the smoothed geochemistry and varve thickness data, correlated against the smoothed Köyceğiz "winter" precipitation values.

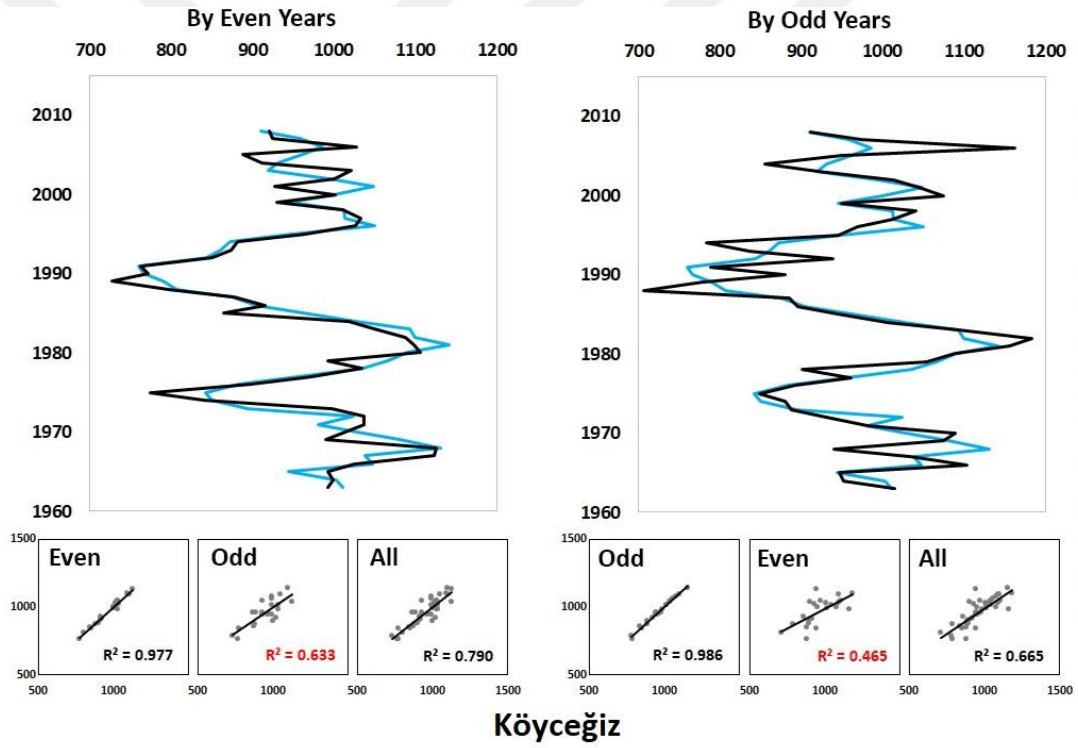

Figure 4.11. Graphs and R2 values of the graphs are showing the results of "Odd Even Operation" performed for Köyceğiz meteorological station's "winter" precipitation data. Note that the precipitation, geochemical and varve thickness data is smoothed with 7-point moving average method. Blue lines are representing actual "winter" precipitation and black lines are showing the MLR results of the operation. X-axis and y-axis show precipitation (mm) and years respectively.

“Odd Even Operation” method is used for Köyceğiz station (Figure 4.11). The MLR equation derived from the even years is correlating with smoothed Köyceğiz winter precipitation data’s even years with R^2 value of 0.977. Predicted odd years is correlating with smoothed Köyceğiz winter precipitation data’s odd years with an R2 of 0.633. When even and odd years (predicted) are merged and correlated with whole smoothed Köyceğiz winter precipitation data, it has a R^2 value of 0.790. The reverse operation was performed, and it is found that the MLR formula derived from the odd years has a correlation with smoothed winter precipitation (odd years) 0.986 in terms of R^2 value. Predicted even years on the other hand correlates with smoothed precipitation of even years with an R^2 score of 0.465. Odd years and predicted even years are merged and the merged dataset is correlated with smoothed winter precipitation with R^2 of 0.665. To examine the long-term precipitation trend prediction, an approximately 500-year precipitation regime trend was generated using the two equations produced after "Odd Even Operation" for smoothed data correlation (Figure 4.12).

The correlation coefficient (R^2) between the "by even years" and "by odd years" reconstructions for the Köyceğiz station improved after the smoothing procedure. Specifically, the R^2 value for the unsmoothed annual trends was low at 0.132; however, the R^2 value for the corresponding smoothed trends increased to 0.361. Furthermore, an overall improvement in correlation was observed across all calculated R^2 values.

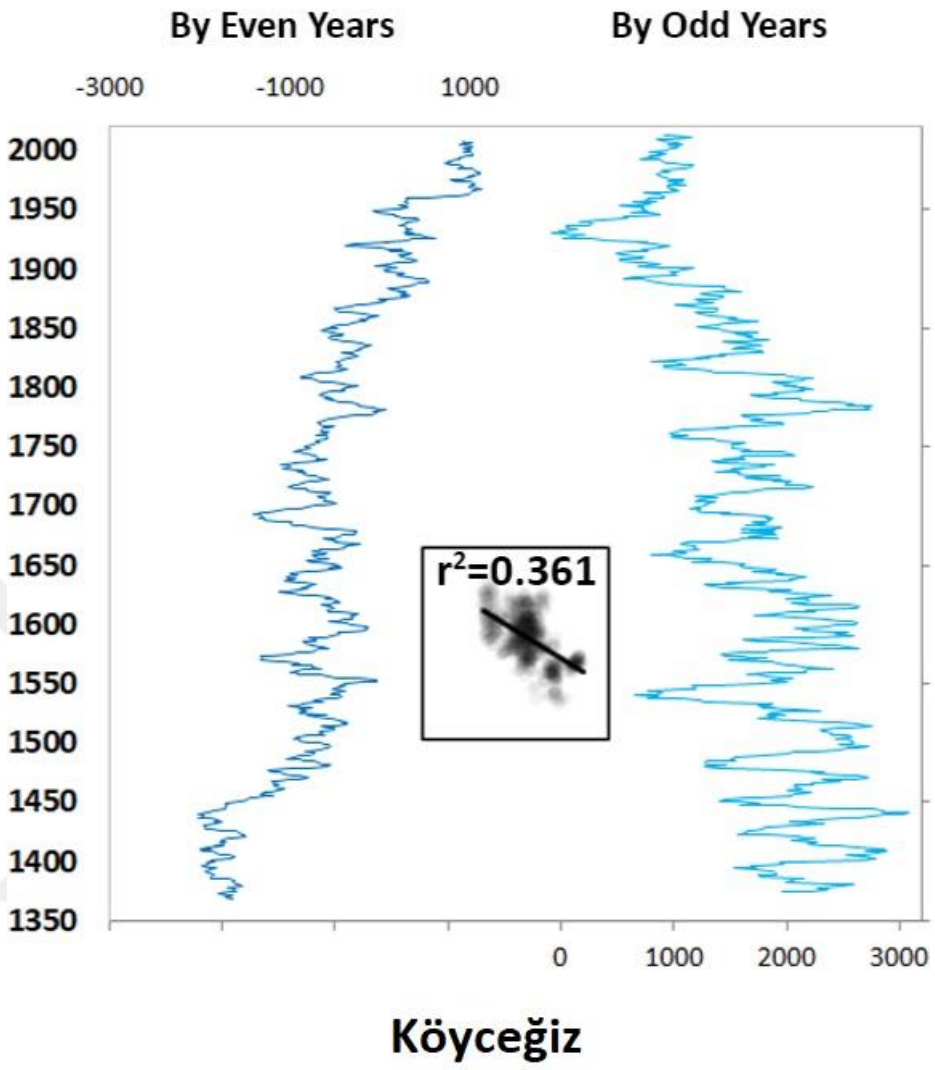

Figure 4.12. Graph showing the predicted trend derived from “Odd Even Operation” for Köyceğiz station. Trend on the left (dark blue) representing the reconstruction derived from the formula obtained from smoothed even years (called as “by even years”) and right trend (light blue) resulted from smoothed odd year’s equation (called as “by odd years”). Note that precipitation values implied by "by even years" trend has negative values.

Despite the similarity observed between the trends derived for the Muğla station after the smoothing operation, the trends derived for the Köyceğiz station were found to be inconsistent with each other. Although improvements in the R^2 values were noted after the smoothing procedure, major errors can be observed in the trends produced by this methodology. For instance, the "by even years" trend generated from the smoothed Köyceğiz station data implies the presence of negative precipitation values. Furthermore, while the "by even years" and "by odd years" trends produced from the smoothed Muğla data appear similar, a similarity cannot be observed in the same trends constructed for Köyceğiz. For example, in Köyceğiz, the trend derived "by even years" implies a gradual increase in precipitation over the approximately 500-year period, whereas the corresponding "by odd years" trend, despite showing fluctuations, implies no such gradual increase or decrease over the same period. Considering all these problems, it can be summarized that although the 7-point moving average smoothing applied to the data resulted in more precise trends and higher R^2 values compared to the unsmoothed data, the produced trends still lack sufficient precision. Consequently, the MLR method, even when applied to smoothed data, was deemed inadequate for the reconstruction.

When Multiple Linear Regression (MLR) is applied to datasets featuring a high number of elements and inter-correlated variables, certain problems may arise during the equation generation process, with multicollinearity being the primary concern. The problem of multicollinearity is a significant challenge encountered in Multiple Linear Regression (MLR) when two or more explanatory variables in a model are closely linearly associated or can be used to predict each other. When variables exhibit this high degree of correlation, they are referred to as collinear. If multicollinearity is present, the linear regression assumption of limited multicollinearity is violated, causing the model itself to become unstable. Since the correlated variables essentially convey redundant information, the model struggles to accurately distinguish between the strength of the different effects each individual variable has on the response variable (Tranmer et al., 2020).

4.3 Principal Component Analysis and Multiple Regression Analysis for the Past Precipitation Reconstruction

The outputs of this study so far clearly demonstrate the necessity of applying an additional statistical method to the dataset before applying MLR, to mitigate these issues. Consequently, this established the requirement for utilizing Principal Component Analysis (PCA). PCA extracts the important information from these inter-correlated variables and re-expresses it as a set of new orthogonal variables called principal components, thereby reducing the dependency and high correlation (multicollinearity) inherent in the original measurements (Abdi & Williams, 2010).

To overcome all these problems, Principal Component Analysis (PCA) was performed using the smooth (with 7-point moving average) geochemical and varve thickness datasets within the SPSS statistical software package. The subsequent PCA application yielded 5 Principal Components (PCs) that compensate for 88% of the total variance in the dataset.

Figure 4.13 presents the matrix of Component Coefficients (R) for the 5 principal components (PC1 to PC5). The figure displays the correlation between each of the original 20 variables (elemental and non-elemental proxies) and the constructed PCs. PC1 exhibits strong positive correlation for, including Zr (0.905), Cu (0.866), Br (0.832), Cl (0.742), and the moderately correlated with counts per second (cps) (0.643); it shows strong negative correlation with Mn (-0.823) and Si (-0.764). PC2 is characterized by high positive correlations with S (0.914), Ni (0.913), Fe (0.852), and moderately correlated with Ti (0.635) and V (0.598). PC3 showing strong positive correlations for Zn (0.844) and K (0.825), alongside a moderate negative correlation with Cl (-0.509). PC4 is highly correlated with Cr (0.806) and moderately correlated with Rb (0.575), while negatively and moderately with Sr (-0.681). Finally, PC5 is dominated by the varve thickness variables. W_S is representing the ratio of Winter/Summer varve thickness and TW means varve thickness of winters. PC5 is highly correlated with W_S (0.922) and moderately correlated with TW (0.643).

	Component				
	1	2	3	4	5
Zr	0.905	0.028	0.089	0.032	0.089
Cu	0.866	0.256	0.078	0.198	0.193
Br	0.832	0.034	-0.438	-0.097	0.140
Cl	0.742	-0.015	-0.509	-0.213	0.100
Mn	-0.823	-0.146	-0.043	-0.308	0.037
Si	-0.764	0.198	0.354	-0.237	0.072
Ca	-0.592	-0.523	-0.103	-0.541	-0.175
cps	0.643	0.689	0.067	0.162	0.167
S	-0.043	0.914	0.209	0.109	0.066
Ni	0.095	0.913	0.220	0.247	0.115
Fe	0.094	0.852	0.394	0.298	0.091
Ti	0.139	0.635	0.605	0.374	0.096
V	0.184	0.598	0.550	0.367	0.078
Zn	-0.188	0.286	0.844	-0.007	0.123
K	-0.272	0.386	0.825	0.137	-0.021
Rb	0.367	0.396	0.513	0.575	0.209
Cr	0.298	0.304	0.075	0.806	0.174
Sr	0.130	-0.440	-0.175	-0.681	-0.316
W_S	0.057	0.091	0.053	0.143	0.922
TW	0.428	0.218	0.071	0.372	0.643

Figure 4.13. Component Coefficients for the 5 principal components derived from PCA. This table displays the correlation between each of the original 20 variables (elemental and non-elemental proxies) and the constructed PCs. High absolute values (highlighted in green) indicate a strong statistical relationship between the variable and the corresponding principal component. Note that cps is counts per second, "W_S" is the ratio of Winter/Summer thickness of the varves and "TW" is winter varve thickness.

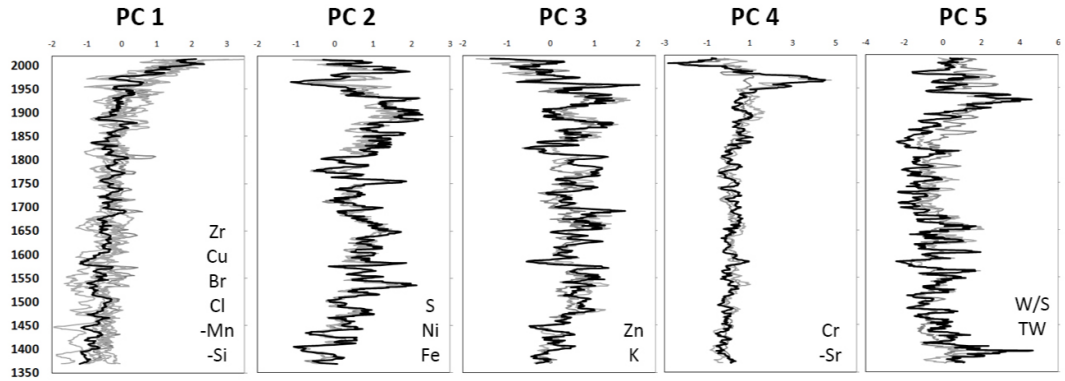

Figure 4.14. Graphs showing the PCs and their correlations with most dominant components. Black lines are PCs' trends and gray lines are component's trends.

It was hypothesized that the trends obtained from an MLR procedure applied to the resulting Principal Components (PCs) would exhibit improved precision. Consequently, the Upper Lower Operation and Odd-Even Operation should be performed to understand if the methodology provides more precise results. Thus, Upper Lower Operation is initiated with applying MLR to these Principal Components. Firstly, MLR is conducted between PCs and smoothed Muğla "winter" precipitation datasets.

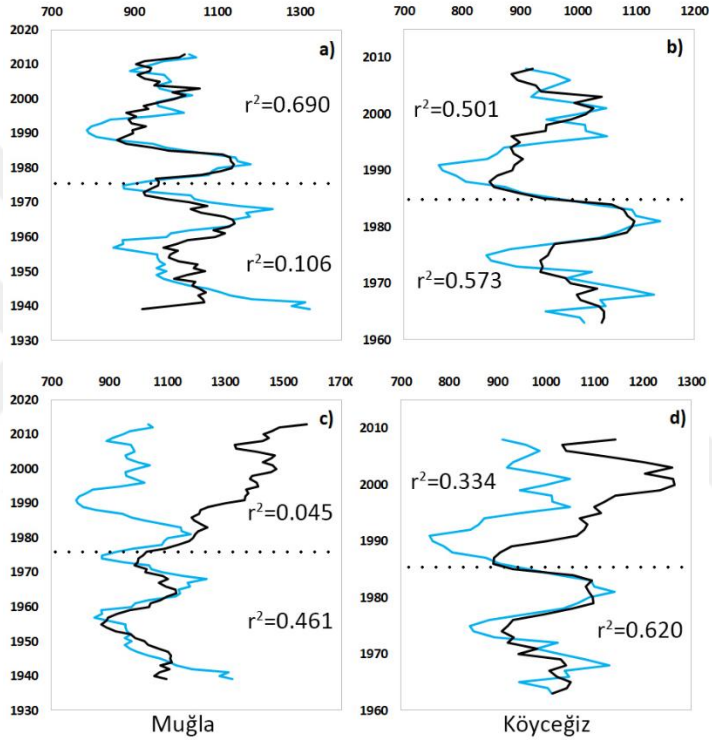

Figure 4.15. Upper Lower Operation results for Muğla and Köyceğiz stations. The operation is conducted with PCs and equations are derived from MLR. a) The upper half of the instrumental data is used for deriving equation, and the lower half is used for precipitation prediction for Muğla station. c) The lower half of the instrumental data is used for equation, and the upper half is predicted for Muğla station. b) The upper half of the instrumental data is used for equation, and the lower half is used for precipitation prediction for Köyceğiz station. d) The lower half of the instrumental data is used for equation, and the upper half is predicted for Köyceğiz station.

The R^2 scores obtained from the calibration phase of Muğla and Köyceğiz datasets are as follows: Muğla upper half is 0.690 and lower half is 0.461; Köyceğiz upper half is 0.501 and lower half is 0.620. However, a decrease in model performance was observed during the cross-validation (prediction) phase, where the equations were used to predict precipitation for the unmodeled half of the instrumental period. The predictive R^2 values decreased, falling to 0.045 (Muğla, upper half) and 0.106 (Muğla, lower half), but relatively high scores were noted for Köyceğiz (0.573 and 0.334). When the upper half of the precipitation record was reconstructed using the equations derived from the lower half of the core data, the resulting predictions showed low precision. Conversely, using formulas generated from the upper half to predict the lower half resulted in higher precision. This difference suggests that precipitation records prior to the 1980s may contain more errors compared to contemporary records. Furthermore, although the estimated upper half precipitation trends derived from lower-half formulas showed a visible absolute value shift due to misestimation, their overall trend patterns were observed to be consistent. The trends (Figure 4.15) obtained after MLR analysis with PCs show higher R^2 in prediction phase than the trends created with only MLR analysis (Figure 4.4). After "Upper Lower Operation", "Odd Even Operation" initiated to test the methodology's precision.

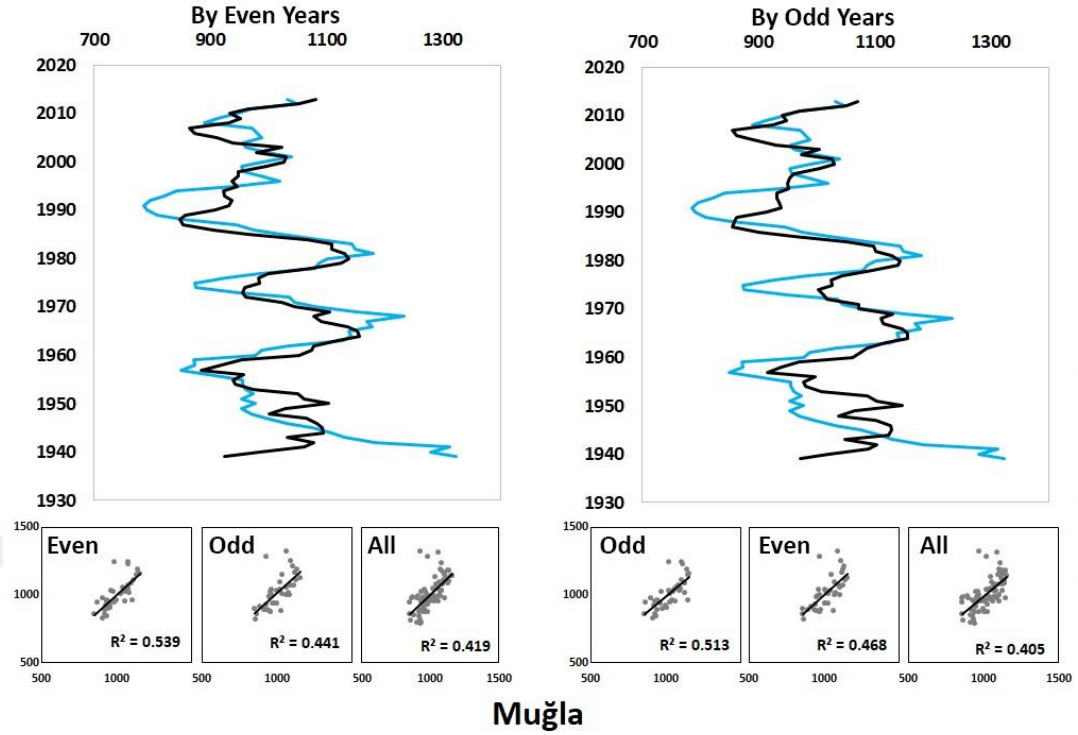

Figure 4.16. Graphs and R^2 values of the graphs are showing the results of "Odd Even Operation" performed for Muğla meteorological station's smoothed "winter" precipitation data with PCs. Blue lines are representing actual "winter" precipitation and black lines are showing the MLR results of the operation. X-axis and y-axis show precipitation (mm) and years respectively.

"Odd Even Operation" method is used between PCs and Muğla station (Figure 4.16). The MLR equation derived from the even years is correlating with smoothed Muğla winter precipitation data's even years with R^2 value of 0.539. Predicted odd years is correlating with smoothed Muğla winter precipitation data's odd years with an R^2 of 0.441. When even and odd years (predicted) are merged and correlated with whole smoothed Muğla winter precipitation data, it has a R^2 value of 0.419. The reverse operation was performed, and it is found that the MLR formula derived from the odd years has a correlation with smoothed winter precipitation (odd years) 0.513 in terms of R^2 value. Predicted even years on the other hand correlates with smoothed precipitation of even years with an R^2 score of 0.468. Odd years and predicted even

years are merged and the merged dataset is correlated with smoothed winter precipitation with R^2 of 0.405.

To examine the long-term precipitation trend prediction, an approximately 500-year precipitation regime trend was generated using the two equations produced after "Odd Even Operation" data correlation (Figure 4.17).

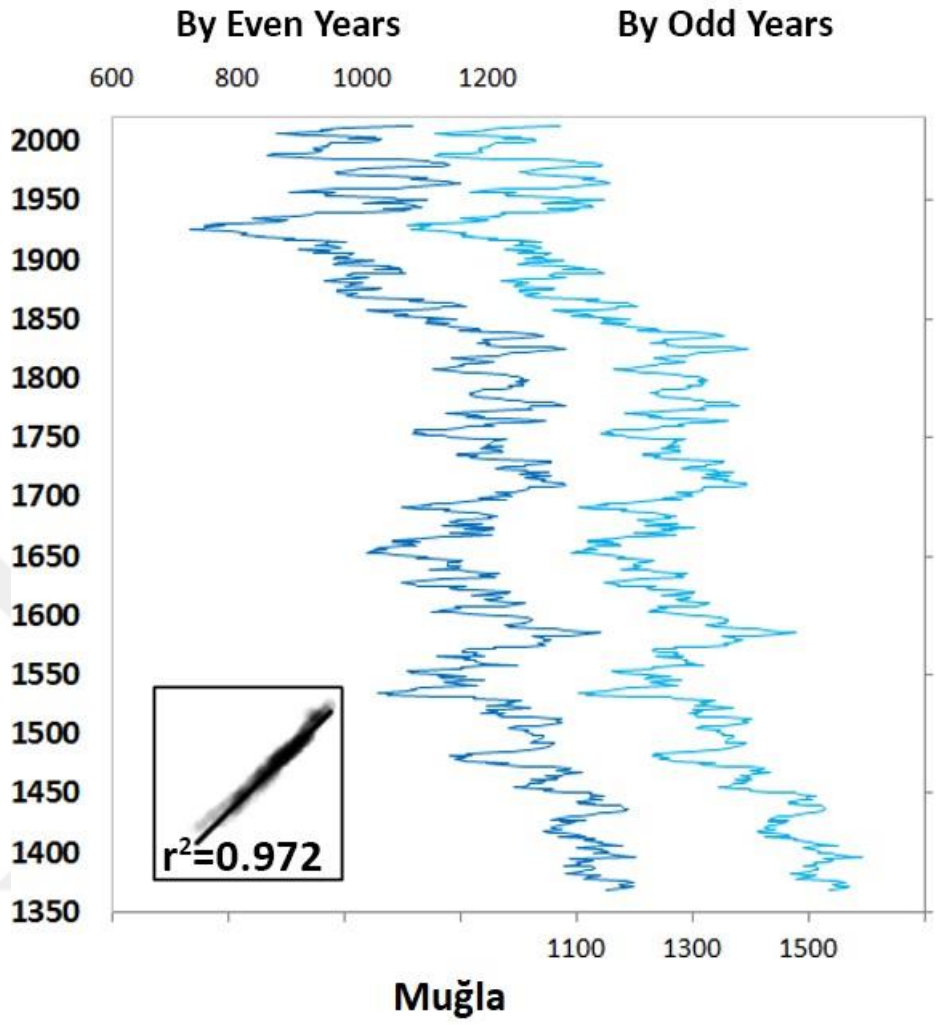

Figure 4.17. Graph showing the predicted trend derived from "Odd Even Operation" between PCs and Muğla station. Trend on the left (dark blue) representing the reconstruction derived from the formula obtained from smoothed even years (called as "by even years") and right trend (light blue) resulted from smoothed odd year's equation (called as "by odd years").

The R^2 value for the trends for Muğla station constructed only with MLR was at 0.449; however, the R^2 value for the trends created by the new method, which is application of PCA before MLR, increased dramatically to 0.972. However, an overall decrease in correlation was observed across R^2 values derived while performing "Odd Even Operation".

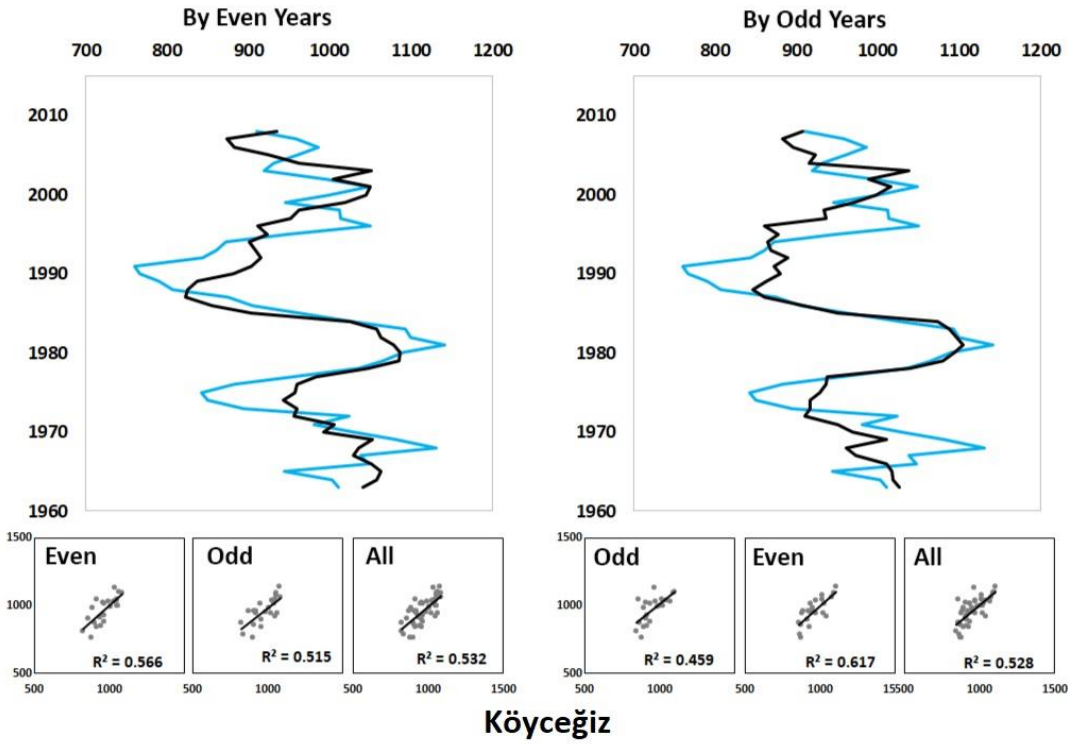

Figure 4.18. Graphs and R^2 values of the graphs are showing the results of "Odd Even Operation" performed for Köyceğiz meteorological station's smoothed "winter" precipitation data with PCs. Blue lines are representing actual "winter" precipitation and black lines are showing the MLR results of the operation. X-axis and y-axis show precipitation (mm) and years respectively.

"Odd Even Operation" method is used between PCs and Köyceğiz station (Figure 4.19). The MLR equation derived from the even years is correlating with smoothed Köyceğiz winter precipitation data's even years with R^2 value of 0.566. Predicted odd years is correlating with smoothed Köyceğiz winter precipitation data's odd years with an R^2 of 0.515. When even and odd years (predicted) are merged and correlated with whole smoothed Köyceğiz winter precipitation data, it has a R^2 value of 0.532. The reverse operation was performed, and it is found that the MLR formula derived from the odd years has a correlation with smoothed winter precipitation (odd years) 0.459 in terms of R^2 value. Predicted even years on the other hand correlates with smoothed precipitation of even years with an R^2 score of 0.617. Odd years and

predicted even years are merged and the merged dataset is correlated with smoothed winter precipitation with R^2 of 0.528.

To examine the long-term precipitation trend prediction, an approximately 500-year precipitation regime trend was generated using the two equations produced after "Odd Even Operation" for smoothed data correlation (Figure 4.19).

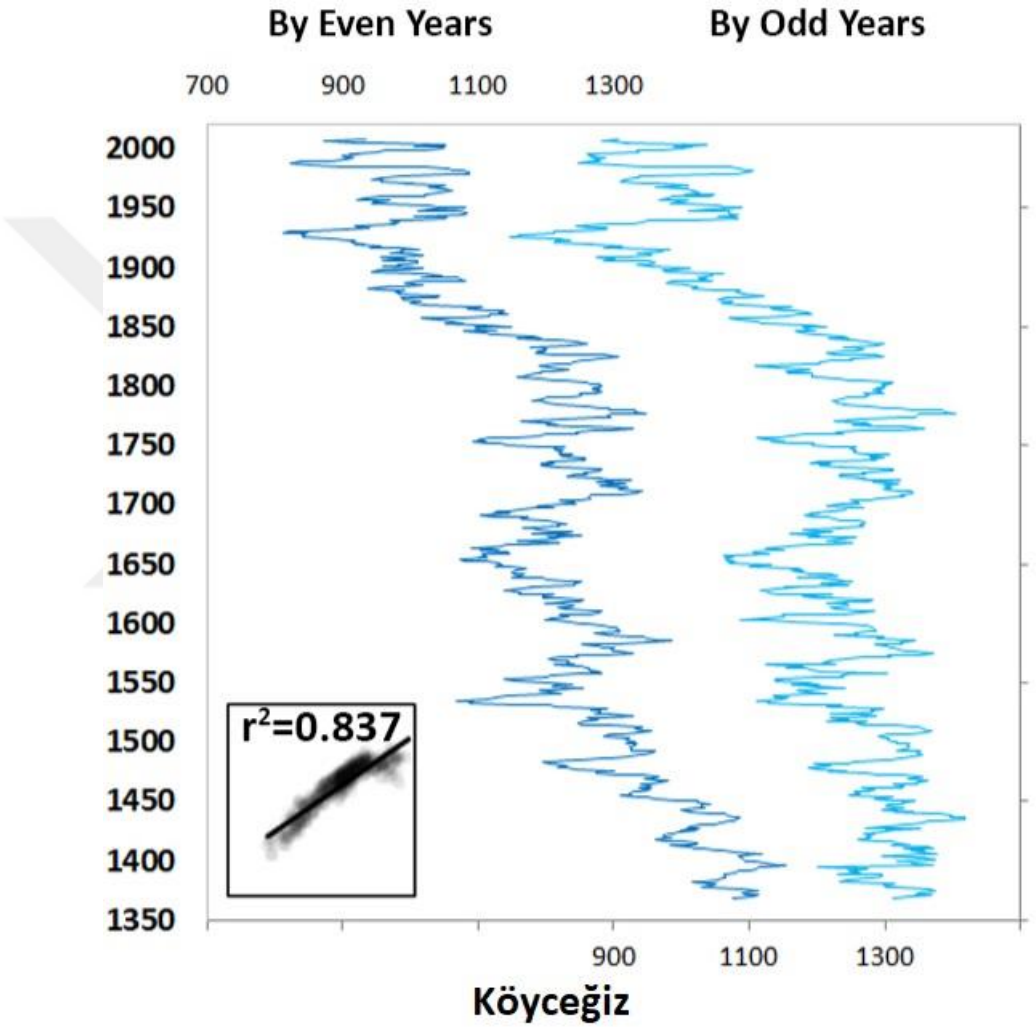

Figure 4.19. Graph showing the predicted trend derived from “Odd Even Operation” between PCs and Köyceğiz station. Trend on the left (dark blue) representing the reconstruction derived from the formula obtained from smoothed even years (called as “by even years”) and right trend (light blue) resulted from smoothed odd year’s equation (called as “by odd years”).

The R^2 value for the trends for Köyceğiz station constructed only with MLR was at 0.361; however, the R^2 value for the trends created by the new method, which is application of PCA before MLR, increased dramatically to 0.837. However, an overall decrease in correlation was observed across R^2 values derived while performing "Odd Even Operation".

To sum up, when the long-term reconstruction trends -derived from correlating ITRAX geochemical data with instrumental precipitation data using only element-based data and Multiple Linear Regression (MLR)- were examined, significant inconsistencies were observed across the different meteorological stations. However, consistent trends were subsequently achieved across these stations when the MLR analysis was performed using the Principal Components (PCs) generated after the application of Principal Component Analysis (PCA) to the geochemical data. MLR equations' coefficients and constants are listed in Figure 4.21.

Element-based Multiple Regression

	Muğla	Köyceğiz	Dalaman	Marmaris	Fethiye
Constant	1201.96	539.36	398.22	380.09	1313.64
cps	23.13	115.48	176.37	53.12	-69.49
Si	-93.66	23.87	94.69	-556.20	118.19
S	-404.10	-650.69	-618.81	-107.42	-406.63
Cl	137.17	-70.30	-187.47	133.81	160.35
K	-71.64	-839.43	-589.46	84.30	-107.41
Ca	128.07	-43.69	-51.35	-439.97	324.93
Ti	-375.20	539.53	-36.57	479.84	-367.10
V	-86.59	-259.46	-201.08	-327.80	-32.44
Cr	5.46	27.96	26.80	53.86	6.19
Mn	-103.92	-153.14	-183.73	-169.13	15.70
Fe	1989.67	1964.85	2649.90	-206.34	1873.84
Ni	-966.16	-1022.91	-1669.98	450.92	-921.00
Cu	13.41	18.63	-0.69	-38.41	121.11
Zn	-48.98	-27.93	41.45	-43.43	-143.78
Br	-178.30	-9.12	62.82	-99.77	-148.51
Rb	-76.99	-170.87	-214.12	79.67	-105.22
Sr	-115.54	50.28	25.36	175.53	-114.47
Zr	86.53	-95.06	-65.38	-102.52	10.07
TW	-4680.16	-2701.65	-67.57	-5176.75	-1443.56
W_S	78.60	-5.11	2.24	4.78	17.92
r^2	**0.884**	**0.891**	**0.953**	**0.858**	**0.898**

PC-based Multiple Regression

	Muğla	Köyceğiz	Dalaman	Marmaris	Fethiye
Constant	1189.29	1177.02	1221.40	1216.87	1010.70
PC 1	-89.64	-88.04	-136.91	-79.99	-96.48
PC 2	-81.15	-76.94	-104.93	-75.68	-90.22
PC 3	-35.27	-20.29	-25.91	-60.51	-13.84
PC 4	-42.32	-49.42	-64.89	-42.37	-53.80
PC 5	-58.54	-53.39	-77.66	12.80	-55.69
r^2	**0.426**	**0.556**	**0.743**	**0.520**	**0.588**

Figure 4.20. Table of element coefficients from the equation generated by element-based MLR and table of PC coefficients from the equation generated by PC-based MLR for 5 different precipitation data from 5 different meteorological stations.

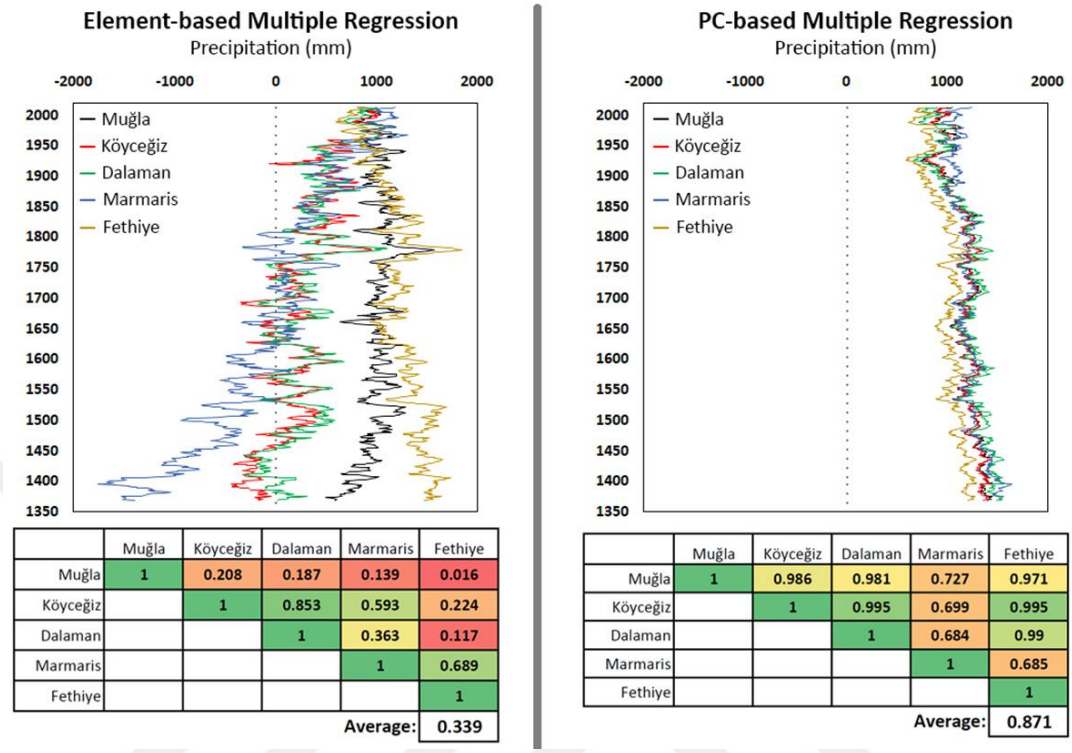

	Muğla	Köyceğiz	Dalaman	Marmaris	Fethiye
Muğla	1	0.208	0.187	0.139	0.016
Köyceğiz		1	0.853	0.593	0.224
Dalaman			1	0.363	0.117
Marmaris				1	0.689
Fethiye					1
				Average:	0.339

	Muğla	Köyceğiz	Dalaman	Marmaris	Fethiye
Muğla	1	0.986	0.981	0.727	0.971
Köyceğiz		1	0.995	0.699	0.995
Dalaman			1	0.684	0.99
Marmaris				1	0.685
Fethiye					1
				Average:	0.871

Figure 4.21. Figure showing the comparison of Element-based MLR and PC-based MLR methodologies applied to varve thickness and geochemical data to obtain long term precipitation reconstructions for 5 different meteorological stations. Note that negative precipitation values are implied by Element-based MLR results. Tables below the graphs show R^2 values of the correlations between reconstructions produced for different stations using the same methodology.

When the reconstructions generated by the two distinct methodologies are examined, significant inconsistencies regarding accuracy and precision were observed among the 5 stations created with the element-based approach. Furthermore, negative precipitation values were observed in the reconstructed trends for Köyceğiz, Dalaman, and Marmaris. On the other hand, the trends produced using the PC-based method (PCA + MLR) were consistent in terms of precision across all five stations. Although the R^2 table shows that the Marmaris trend shows differences in accuracy compared to the others, the correlation for the Marmaris station is still more precise

when compared to trends produced by the element-based methodology. Since, average R^2 value (0.339) obtained by element-based MLR lower than the average value (0.871) calculated from PC-based MLR (Figure 4.21).

The reconstructions generated by the proposed methodology (the PCA-followed-by-MLR analysis) within this study were found to yield the most precise trends obtained throughout the entire research. Furthermore, to validate the precision of these reconstructions, their consistency with studies conducted by various proxies across Türkiye such as a speleothem study (Fleitmann et al., 2009), a varve lake (Jones et al., 2006) as well as with a prior study performed on Köyceğiz Lake (Akçer-Ön, 2017), is demonstrated in the Figure 4.22.

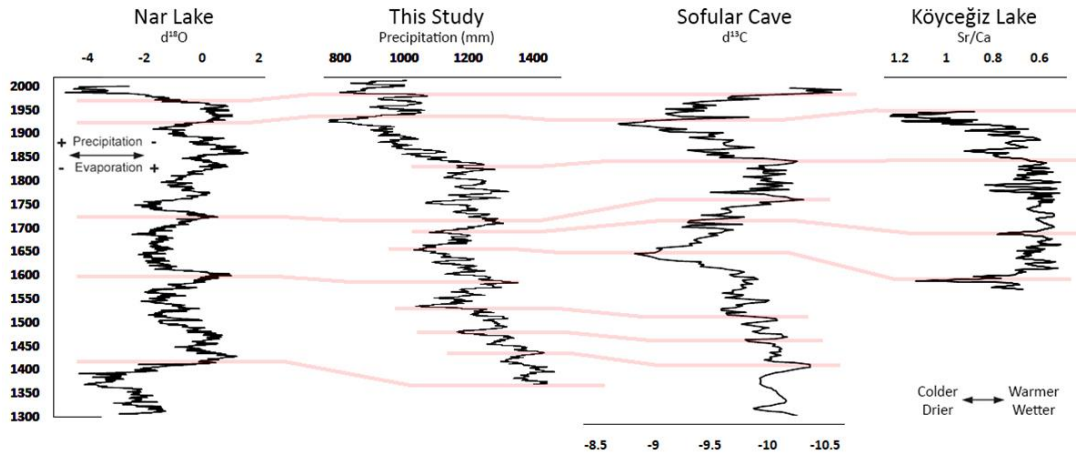

Figure 4.22. The figure compares 4 precipitation reconstructions that have been conducted in Türkiye. The reconstruction labeled Nar Lake originates from a varved lake study, utilizing the O^{18} ratio (Jones et al., 2006). The Sofular Cave record was obtained from a speleothem study dated using C^{13} (Fleitmann et al., 2009). The trend labeled Köyceğiz Lake represents a prior paleoclimate study carried out at Köyceğiz (Akçer-Ön, 2017). Red lines indicate similar events implied by different trends. Note that drier and wetter axis are reversed in Nar Lake graph.

The reconstruction produced in this study is observed to be highly consistent with the Sofular Cave record (approximately 600 km away from Köyceğiz Lake), displaying only 20-year discrepancies. These minor time discrepancies are considered acceptable, as the Sofular Cave study utilized Uranium-Thorium (U-Th) dating on a speleothem archive, which differs fundamentally from a varved lake chronology. Overall, the current study is highly consistent with the Sofular Cave record in terms of both event timing and general trend. Furthermore, the reconstruction exhibits consistency with a prior Köyceğiz Lake study (Akçer-Ön, 2017) across four main events and similar general trends, although the core used in that earlier study covered a narrower time window. The trend obtained in the Nar Lake (approximately 600 km away from Köyceğiz Lake) study is also observed to be consistent with the trend produced in the current work; however, it must be emphasized that the reconstruction shown in the figure is the exact mirror image of the one produced here. This distinction can be explained by the difference in proxy utilization: in the study completed by Jones et al. (2006), O^{18} measurements were taken from sediments within the whitish carbonate layers corresponding to summer levels. Periods where the O^{18} ratio decreased were interpreted as summers of increased evaporation. Therefore, the rainfall reconstructions were based on the assumption that winter precipitation increased during periods when the O^{18} ratio decreased. The resulting trend exhibits a complete visual opposition to the trend obtained in this study. In other words, the reconstruction within the scope of the present study was created using geochemical measurements taken from the clastic-rich layers corresponding to the winter months, whereas the other study used O^{18} measurements taken from the carbonate-rich layers corresponding to the summer months. Therefore, a symmetric reversal (mirror image) between the reconstructions of the two studies is highly probable.

Moreover, to validate the accuracy and reliability of the final reconstruction, a comprehensive review of historical drought events documented in the literature was conducted. One of the most prominent features in the resulting reconstruction is the severe drought observed during the 1920s. In a study conducted by van der Schrier

et al. (2021), it is stated in the 1921 European drought stands out as the most severe and widespread drought event on the continent since the beginning of the 20th century, affecting a vast geographic area stretching from Ireland to the Ukraine and the Volga region. In another study conducted by Nicault et al it is stated that reconstructions of the Palmer Drought Severity Index (PDSI) over the last 500 years reveal that the sixteenth and early seventeenth centuries constituted the driest historical period in the Mediterranean basin, characterized by intense and prolonged dry episodes such as the 1540–1575 event, the 1620–1640 and 1645-1665 droughts. While the subsequent Little Ice Age generally introduced wetter conditions, particularly during the first half of the eighteenth century, this stability was interrupted by significant anomalies like the 1760–1780 drought (Nicault et al., 2008). The pointed droughts can also be seen from the final reconstruction. Furthermore, The Celali Rebellions (1596–1610) were inextricably linked to the climatic anomalies of the Little Ice Age, specifically a period of extreme aridity known as the "Great Drought" that afflicted the Eastern Mediterranean from 1591 to 1596. This ecological catastrophe, recorded as the most severe drought in six centuries, occurred simultaneously with a widespread epizootic that decimated the livestock populations essential for the empire's economy and food supply (White, 2011). In the reconstruction, it can be observed that from the beginning of the sixteenth century, a major drought is affecting Anatolia so that this drought leads to a series of rebellions. In addition, from the beginning of nineteenth century, a decrease can be observed in precipitation trend. It can be linked with the industrial revolution and recent global warming.

In conclusion, the reconstruction method created by the methodology proposed in that study can produce precise results because the trends constructed in the study is consistent with both historical records and other paleoclimate studies across Türkiye.

CHAPTER 5

CONCLUSION AND RECOMMENDATIONS

The conclusions and recommendations from the study can be listed as follows:

- Varve records are extremely valuable archives for lake studies, and this study demonstrates that robust reconstructions can be achieved using the proposed methodology.
- The span of the instrumental meteorological station records utilized for this methodology is highly critical to obtain more robust and reliable results from the reconstructions.
- If the variables employed in the reconstruction analysis are not statistically independent, the resulting R^2 values may appear artificially high, leading to totally arbitrary results. Therefore, the application of Principal Component Analysis (PCA) is essential.
- The use of smoothing techniques, such as a 7-point moving average, is crucial for ensuring that the resulting correlations are statistically meaningful.
- When performing precipitation reconstructions from varved lakes, utilizing the geochemical data from the clastic-rich winter layers (brownish, grayish darker layers) yield superior results compared to using the carbonate-rich summer layers (whitish, light-colored layers).
- By counting the yellowish laminae, with confirmation from visual checks and alignment with the peaks of the Ca/Ti ratio, a sedimentary record spanning 609 years was established within the 124.95 cm-long core. This result shows an average sedimentation rate of 0.205 cm/yr.
- The application of Principal Component Analysis (PCA) to the ITRAX data derived from the winter laminae resulted in 5 Principal Components (PCs), which compensate for 88% of the total variance in the dataset. Subsequently,

the Multiple Regression (MLR) analysis performed using these independent (PCs) produced consistent precipitation trends across the different meteorological stations.

- Precipitation reconstruction effectively captures major historical dry periods, such as the severe 1921 European drought, which is recognized as one of the most widespread climatic anomalies of the 20th century.
- A significant decline in precipitation observed at the end of the 16th century aligns with the "Great Drought" (1591–1596), providing high-resolution geochemical evidence for the climatic triggers behind the socio-economic upheavals of the Celali Rebellions.
- The identified dry periods in the 16th and 17th centuries, followed by the relatively wetter conditions of the early Little Ice Age and subsequent anomalies (e.g., 1760–1780), demonstrate a strong consistency with Mediterranean-wide Palmer Drought Severity Index (PDSI) reconstructions.
- The decrease trend in precipitation observed from the early 19th century onwards suggests a link to the onset of the Industrial Revolution and the escalating effects of recent global warming on the Eastern Mediterranean hydroclimate.

REFERENCES

Abdi, H., & Williams, L. J. (2010). Principal component analysis. *WIREs Computational Statistics, 2*, 433–459. https://doi.org/10.1002/wics.101

Akçer-Ön S. (2017). Küçük Buz Çağı'nda Güneş etkisine bağlı iklim değişimleri: Köyceğiz Gölü çökel kayıtları (GB Anadolu). Türkiye Jeoloji Bülteni 60 (4): 569-588 (in Turkish) doi:10.25288/tjb.370616.

Akkemik, Ü., & Aras, A. (2005). Reconstruction (1689–1994) of April-August precipitation in southwestern part of central Türkiye. Int J Climatol 25:537–548.

Akkemik, Ü., Dağdeviren, N., Aras, A. (2005). A preliminary reconstruction (A.D. 1635–2000) of spring precipitation using oak tree rings in the western Black Sea region of Türkiye. Int J Biometeorol 49:297–302. doi:10.1007/s00484-004-0249-8.

Akkemik, Ü, D'Arrigo, R., Cherubini, P., Köse, N., Jacoby, G.C., (2008). Tree-ring reconstructions of precipitation and streamflow for north-western Türkiye. Int J Climatol 28:173–183.

Anderson, R.Y., Dean, W.E., Bradbury, J.P., Love, D. (1985). Meromictic lakes and varved lake sediments in North America. U.S. Geological Survey Bulletin 1607. Retrieved June 22, 2022, from https://pubs.usgs.gov/bul/1607/report.pdf.

Avşar, U., Jónsson, S., Avşar, Ö, and Schmidt, S. (2016). Earthquake-induced soft-sediment deformations and seismically amplified erosion rates recorded in varved sediments of Köyceğiz Lake (SW Türkiye). Journal of Geophysical Research: Solid Earth, 121(6), 4767-4779. doi:10.1002/2016JB012820.

Avşar, Ö., & Kurtuluş, B. (2017). Distribution of water and bottom sediment temperature of Köyceğiz Lake. J. Geol. Eng. 41, 117–136.

Avşar, U., Akar, M., Pearson, C. (2019). Geoarchaeological investigations in the Amuq valley of Hatay: sediment coring project in the environs of Tell Atchana. in H. Sözbilir, Ç. Özkaymak, B. Uzel, Ö. Sümer, M. Softa, Ç. Tepe, S. Eski (eds), The Proceedings and Abstracts Book: 72nd Geological Congress of Türkiye, January 28 – February 1, 2019. Ankara, TMMOB Jeoloji Mühendisleri Odası: 798–802.

Adıyaman, Ö. And Chorowicz, J. 2002. Late Cenozoic tectonics and volcanics in the northwestern corner of the Arabian plate: a consequence of the strike-slip Dead Sea Fault Zone and lateral escape of Anatolia, Journal of Volcanology and Geothermal Research, 117. 327-345.

Amrouch, K., Lacombe, O., Bellahsen, N., Daniel, J. M. and Callot, J. P. 2010. Stress and strain patterns, kinematics and deformation mechanisms in a basement cored anticline: Sheep Mountain Anticline, Wyoming. Tectonics, 29, TC1005, doi:10.1029/2009TC002525.

Anderson, R.Y., Dean, W.E., Bradbury, J.P., Love, D. (1985). Meromictic lakes and varved lake sediments in North America. U.S. Geological Survey Bulletin 1607. Retrieved June 22, 2022, from https://pubs.usgs.gov/bul/1607/report.pdf.

Arger, J., Michel, J. and Westaway, R.W.C. 2000. Neogene and Quaternary volcanics of southeastern Türkiye. The Geological Society, London, Special Publications, 173,459-487

Bayarı, C. S., Kazancı, N., Koyuncu, H., Çağlar, S.S. and Gökçe, D., (1995). Determination of the origin of the waters of Köyce¤iz Lake, Türkiye, J. Hydrol.166: 171-191.

Danladi, I. B., Akcer-Ön, S., Z. B. Ön, Z.B, and Schmidt, S. (2021). High-resolution temperature and precipitation variability of southwest Anatolia since 1730 CE from Lake Gölcük sedimentary records, Turkish Journal of Earth Sciences, 30(5), 601-610, doi:10.3906/yer-2008-14.

Davis, J.C. (2002). Statistics and Data Analysis in Geology. John Wiley & Sons, New York.

Dean, J.R., Jones, M.D., Leng, M.J., Noble, S.R., Metcalfe, S.E., Sloane, H.J., Sahy, D., Eastwood, W.J., and Roberts, N. (2015). Eastern Mediterranean Hydroclimate over the late Glacial and Holocene, reconstructed from the Sediments of Nar Lake, Central Türkiye, Using Stable Isotopes and Carbonate Mineralogy. Quaternary Science Reviews, 124, 162–174.

Fleitmann, D., Cheng, H., Badertscher, S., Edwards, R.L., Mudelsee, M., Gokturk, O.M., Fankhauser, A., Pickering, R., Raible, C.C., Matter, A., Kramers J., Tuysuz, O. (2009). Timing and Climatic impact of Greenland Interstadials Recorded in Stalagmites from Northern Türkiye. Geophysical Research Letters, 36, L19707.

Eastwood, W.J., Leng, M.J., Roberts, N., Davis, B. (2007). Holocene climate change in the Eastern Mediterranean Region: A Comparison of Stable Isotope and Pollen Data from Lake Gölhisar, Southwest Türkiye. Journal of Quaternary Science, 22(4), 327–341.

El Ouahabi, M., Hubert-Ferrari, A., & Fagel, N. (2017). Lacustrine clay mineral assemblages as a proxy for land-use and climate changes over the last 4 kyr: The Amik Lake case study, Southern Türkiye. Quaternary International, 438, 15–29. doi: 10.1016/j.quaint.2016.11.032

El Ouahabi, M., Hubert-Ferrari, A., Lebeau, H., Karabacak, V., Vander Auwera, J., Lepoint, G., Dewitte, O., Schmidt, S. (2018). Soil erosion in relation to land-use changes in the sediments of Amik Lake near Antioch antique city during the last 4 kyr. The Holocene, 28(1), 104–118. doi :10.1177/0959683617715702.

Environmental Science. (n.d.). Dendrochronology: What Tree Rings Tell Us. Retrieved November 20, 2025, from https://www.environmentalscience.org/dendrochronology-tree-rings-tell-us

Heinrich, I., Touchan, R., Dorado Liñán, I., Vos, H., & Helle, G. (2013). Winter-to-spring temperature dynamics in Türkiye derived from tree rings since AD 1125. Climate Dynamics, 41(7-8), 1685–1701. doi:10.1007/s00382-013-1702-3.

Jacobson, M. J., Flohr, P., Gascoigne, A., Leng, M. J., Sadekov, A., Cheng, H., et al. (2021). Heterogenous late Holocene climate in the Eastern Mediterranean—The Kocain Cave record from SW Türkiye. Geophysical Research Letters, 48, e2021GL094733. https://doi.org/10.1029/2021GL094733.

Jex, C. N., Baker, A., Eden, J. M., Eastwood, W. J., Fairchild, I. J., Leng, M. J., … Sloane, H. J. (2011). A 500 yr speleothem-derived reconstruction of late autumn–winter precipitation, northeast Türkiye. Quaternary Research, 75(03), 399–405. doi: 10.1016/j.yqres.2011.01.005

Jones, M.D., Leng, M.J., Roberts, C.N., Türkeş, M., and Moyeed, R. (2005). A coupled calibration and modelling approach to the understanding of dry-land lake oxygen isotope records: Journal of Paleolimnology, v. 34, p. 391–411, doi: 10.1007/s10933-005-6743-0.

Jones, M.D., Roberts, N.C., Leng, M.J., Türkes, M. (2006). A high-resolution late Holocene Lake isotope record from Türkiye and links to North Atlantic and monsoon climate. Geology 34, 361e364.

Kalugin, I., Daryin, A., Smolyaninova, L., Andreev, A., Diekmann, B., & Khlystov, O. (2007). 800-yr-long records of annual air temperature and precipitation over southern Siberia inferred from Teletskoye Lake sediments. Quaternary Research, 67(3), 400–410. https://doi.org/10.1016/j.yqres.2007.01.007

Karadaş, Ö. (2022). Paleoclimate reconstruction from varved sediments in Köyceğiz Lake, Southwest Anatolia [Master's thesis, Middle East Technical University].

Kazancı, N., Plasa, R.-H., Neubert, E., & İzbirak, A. (1992). On the limnology of Köyceğiz Lake (SW Anatolia). Zoology in the Middle East, 6(1), 109–126. doi:10.1080/09397140.1992.10637619.

Kazancı, N., Muzaffer D., Sonmez, G. (2008). The physico-chemical and biological characteristics of Köyceğiz Lake in southwestern Türkiye between 1991 and 1993 and future management proposals. Rev Hydrobiol 2:165–205.

Köse, N., Akkemik, Ü., Dalfes, HN, Özeren, M.S. (2011) Tree-ring reconstructions of May–June precipitation of western Anatolia. Quat. Res 75:438–450. doi: 10.1016/j.yqres.2010.12.005.

Köse, N., Akkemik, Ü., Güner, H. T., Dalfes, H. N., Grissino-Mayer, H. D., Özeren, M. S., & Kındap, T. (2013). An improved reconstruction of May–June precipitation using tree-ring data from western Türkiye and its links to volcanic eruptions. International Journal of Biometeorology, 57(5), 691–701. doi:10.1007/s00484-012-0595-x.

Köse, N., Güner, H. T., Harley, G. L., & Guiot, J. (2017). Spring temperature variability over Türkiye since 1800 CE reconstructed from a broad network of tree-ring data. Climate of the Past, 13(1), 1–15. doi:10.5194/cp-13-1-2017.

Kylander, M. E., Ampel, L., Wohlfarth, B., & Veres, D. (2011). High-resolution X-ray fluorescence core scanning analysis of Les Echets (France) sedimentary sequence: new insights from chemical proxies. Journal of Quaternary Science, 26(1), 77–88.

Kurtuluş, T., Kurtuluş, B., Avşar, Ö., & Avşar, U. (2019). Evaluating the thermal stratification of Köyceğiz Lake (SW Türkiye) using in-situ and remote sensing observations. Journal of African Earth Sciences, 103559. doi: 10.1016/j.jafrearsci.2019.103559.

Meydan, A. F., Kalugin, I. A., Darin, A. V., Babich, V. V., Markovich, T. I., Rogozin, D. Y., Çağatay, M. N., Gülyüz, E., & Akkol, S. (2024). Paleoenvironmental reconstruction of Lake Van and Lake Erçek over the last millennium using varved sediments (Eastern Türkiye). Quaternary International, 714, Article 109581. https://doi.org/10.1016/j.quaint.2024.10.013

NASA Earth Observatory. (2005). Paleoclimatology: Ice Cores. https://earthobservatory.nasa.gov/features/Paleoclimatology_IceCores

NASA Earth Observatory. (2005). Paleoclimatology: Speleothems. https://earthobservatory.nasa.gov/features/Paleoclimatology_Speleothems

National Oceanic and Atmospheric Administration (NOAA) National Centers for Environmental Information (NCEI). (n.d.). How Can Corals Teach Us About Climate? Retrieved November 20, 2025, from https://www.ncei.noaa.gov/news/how-can-corals-teach-us-about-climate

National Weather Service (NWS). (n.d.). Downtown Charleston Weather Observing Station Recognized as a Centennial Site and Second Longest Station Record

Worldwide. Retrieved November 20, 2025, from https://www.weather.gov/news/212503-press-release

Nicault, A., Alleaume, S., Brewer, S., Carrer, M., Nola, P., & Guiot, J. (2008). Mediterranean drought fluctuation during the last 500 years based on tree-ring data. *Climate Dynamics*, *31*(2-3), 227–245. https://doi.org/10.1007/s00382-007-0349-3

Ocakoğlu, F., Dönmez, E. O., Akbulut, A., Tunoğlu, C., Kır, O., Açıkalın, S., … Leroy, S. A. (2015). A 2800-year multi-proxy sedimentary record of climate change from Lake Çubuk (Göynük, Bolu, NW Anatolia). The Holocene, 26(2), 205–221. doi :10.1177/0959683615596818.

O'Sullivan, P. E. (1983). Annually laminated lake sediments and the study of Quaternary environmental changes – a review. Quaternary Science Reviews 1:245 – 313.

Ön, Z.B., Akçer-Ön, S., Özeren, M.S., Eriş, K.K., Greaves, A.M., Çağatay, M.N. (2018). Climate Proxies for the Last 17.3 ka from Lake Hazar (Eastern Anatolia), Extracted by Independent Component Analysis of m-XRF data, Quaternary International, 486, 17-28.

Roberts, N., Allcock, S. L., Barnett, H., Mather, A., Eastwood W. J., Jones, M., Primmer, N., Yiğitbaşıoğlu, H., Vannière, B. (2018). Cause-and-effect in Mediterranean erosion: The role of humans and climate upon Holocene sediment flux into a central Anatolian Lake catchment. Geomor. https://doi.org/10.1016/j.geomorph.2018.11.016

Şenel, M., 1997. Geological Map Series of Türkiye 1:100 000 Scale. No. 1, Geologic Map of Fethiye L7 Quadrangle. General Directorate of Mineral Research and Exploration, Geological Research Department, Ankara (in Turkish).

Şenel, M., 1997. Geological Map Series of Türkiye 1:100 000 Scale. No. 2, Geologic Map of Fethiye L8 Quadrangle. General Directorate of Mineral Research and Exploration Geological Research Department, Ankara (in Turkish).

Şimşek, F. B., & Çağatay, M.N. (2018). Late Holocene high resolution multi-proxy climate and environmental records from Lake Van, eastern Türkiye. Quaternary International. doi: 10.1016/j.quaint.2017.12.043.

Touchan, R., Garfin, G.M., Meko, D.M., Funkhouser, G., Erkan, N., Hughes, M.K., Wallin, B.S. (2003). Preliminary reconstructions of spring precipitation in southwestern Türkiye from tree-ring width. Int J Climatol 23:157–171.

Touchan, R., Akkemik, Ü., Hughes, MK., Erkan, N. (2007). May–June precipitation reconstruction of southwestern Anatolia, Türkiye during the last 900 years from tree-rings. Quat Res 68:196–202.

Tranmer, M., Murphy, J., Elliot, M., & Pampaka, M. (2020). Multiple linear regression (2nd Edition; Cathie Marsh Institute Working Paper 2020-01).

Cathie Marsh Institute. https://hummedia.manchester.ac.uk/institutes/cmist/archive-publications/working-papers/2020/2020-1-multiple-linear-regression.pdf

Tylmann, W., Enters, D., Kinder, M., Moska, P., Ohlendorf, C., Poręba, G., & Zolitschka, B. (2013). Multiple dating of varved sediments from Lake Łazduny, northern Poland: Toward an improved chronology for the last 150 years. Quaternary Geochronology, 15, 98–107. doi: 10.1016/j.quageo.2012.10.001.

Ülgen, U. B., Franz, S. O., Biltekin, D., Çagatay, M. N., Roeser, P. A., Doner, L., & Thein, J. (2012). Climatic and environmental evolution of Lake Iznik (NW Türkiye) over the last ~4700 years. Quaternary International, 274, 88–101. doi: 10.1016/j.quaint.2012.06.016.

Weinheimer, A., & Biondi, F. (2003). PALEOCLIMATOLOGY | Varves. Encyclopedia of Atmospheric Sciences, 1680–1685. doi:10.1016/b0-12-227090-8/00305-5.

White, S. (2011). *The climate of rebellion in the early modern Ottoman Empire*. Cambridge University Press.

Wick, L., Lemcke, G., Sturm, M. (2003). Evidence of Late glacial and Holocene climatic change and human impact in eastern Anatolia: high-resolution pollen, charcoal, isotopic and geochemical records from the laminated sediments of Lake Van, Türkiye. The Holocene, 13, 665-675.

Van der Schrier, G., Allan, R. P., Ossó, A., Sousa, P. M., Van de Vyver, H., Van Schaeybroeck, B., Coscarelli, R., Pasqua, A. A., Petrucci, O., Curley, M., Mietus, M., Filipiak, J., Štěpánek, P., Zahradníček, P., Brázdil, R., Řezníčková, L., van den Besselaar, E. J. M., Trigo, R., & Aguilar, E. (2021). The 1921 European drought: impacts, reconstruction and drivers. Climate of the Past, 17(6), 2201–2221. https://doi.org/10.5194/cp-17-2201-2021

Zolitschka, B. (1991). Absolute dating of late Quaternary Lacustrine sediments by high resolution varve chronology. Hydrobiologia, 214(1), 59–61. doi:10.1007/bf00050932.

Zolitschka, B. (2003). Dating based on freshwater and marine laminated sediments. In: Mackay, A., Battarbee, R., Birks, J., Oldfield, F. (Eds.), Global Change in the Holocene. Edward Arnold Publishers, London, pp. 92-106.

Zolitschka, B., & Enters, D. (2009). Lacustrine sediments. In: Gornitz, V. (Ed.), Encyclopedia of Paleoclimatology and Ancient Environments. Springer, Dordrecht, pp. 485-488.

Zolitschka, B., Francus, P., Ojala, A. E. K., and Schimmelmann, A. (2015). Varves in lake sediments- A review, Quat. Sci. Rev., 117, 1–41. doi: 10.1016/j.quascirev.2015.03.019.

APPENDICES

Varve counting methodology with profiles of R/G, Ca/Ti and [R/G]x[Ca/Ti]. Taken from Karadaş (2022). Full image of the core KYC-J used in the study.

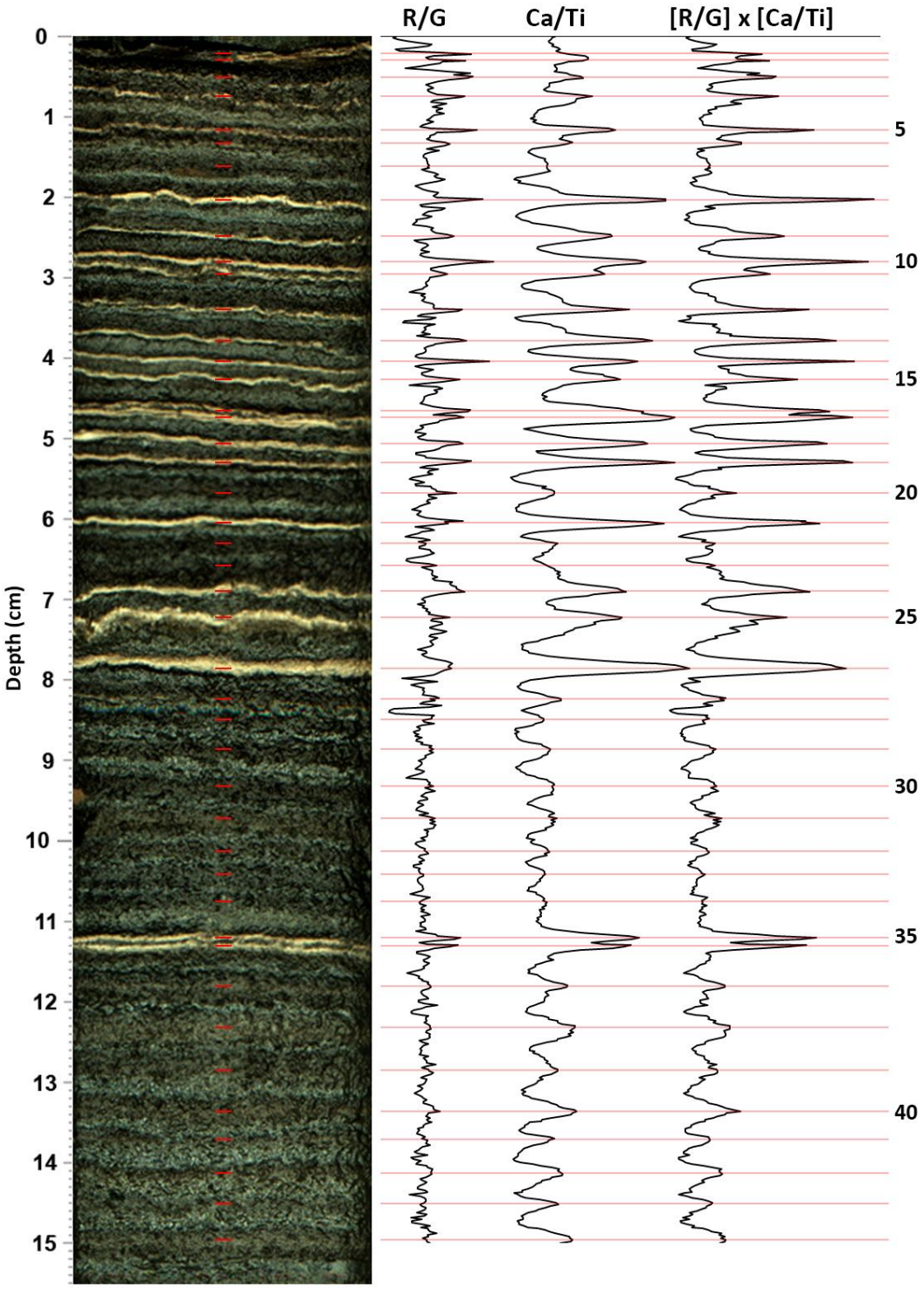
R/G
Ca/Ti
[R/G] x [Ca/Ti]
Depth (cm)
0
1
2
3
4
5
6
7
8
9
10
11
12
13
14
15
5
10
15
20
25
30
35
40

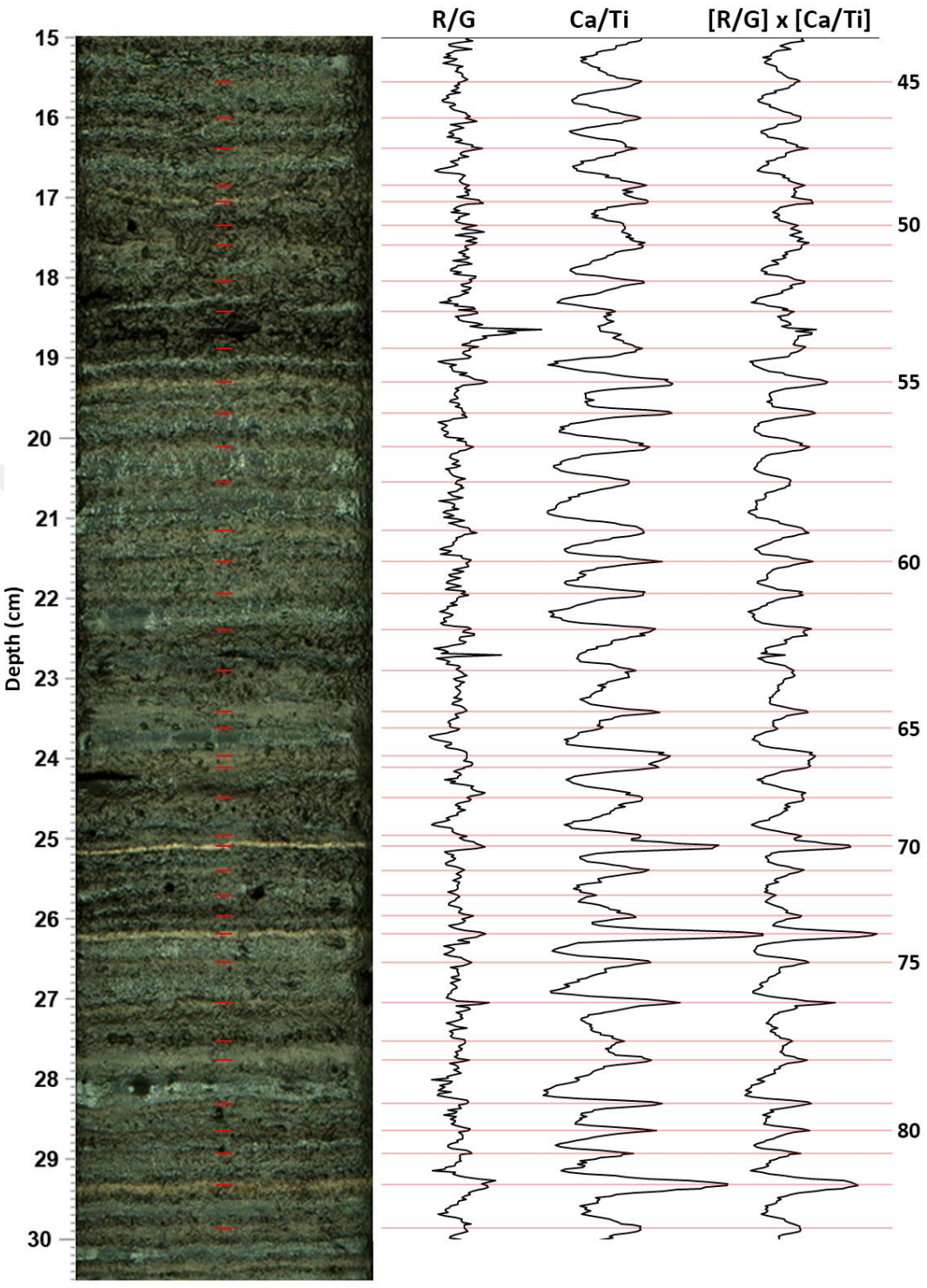
R/G
Ca/Ti
[R/G] x [Ca/Ti]
Depth (cm)
15
16
17
18
19
20
21
22
23
24
25
26
27
28
29
30
45
50
55
60
65
70
75
80

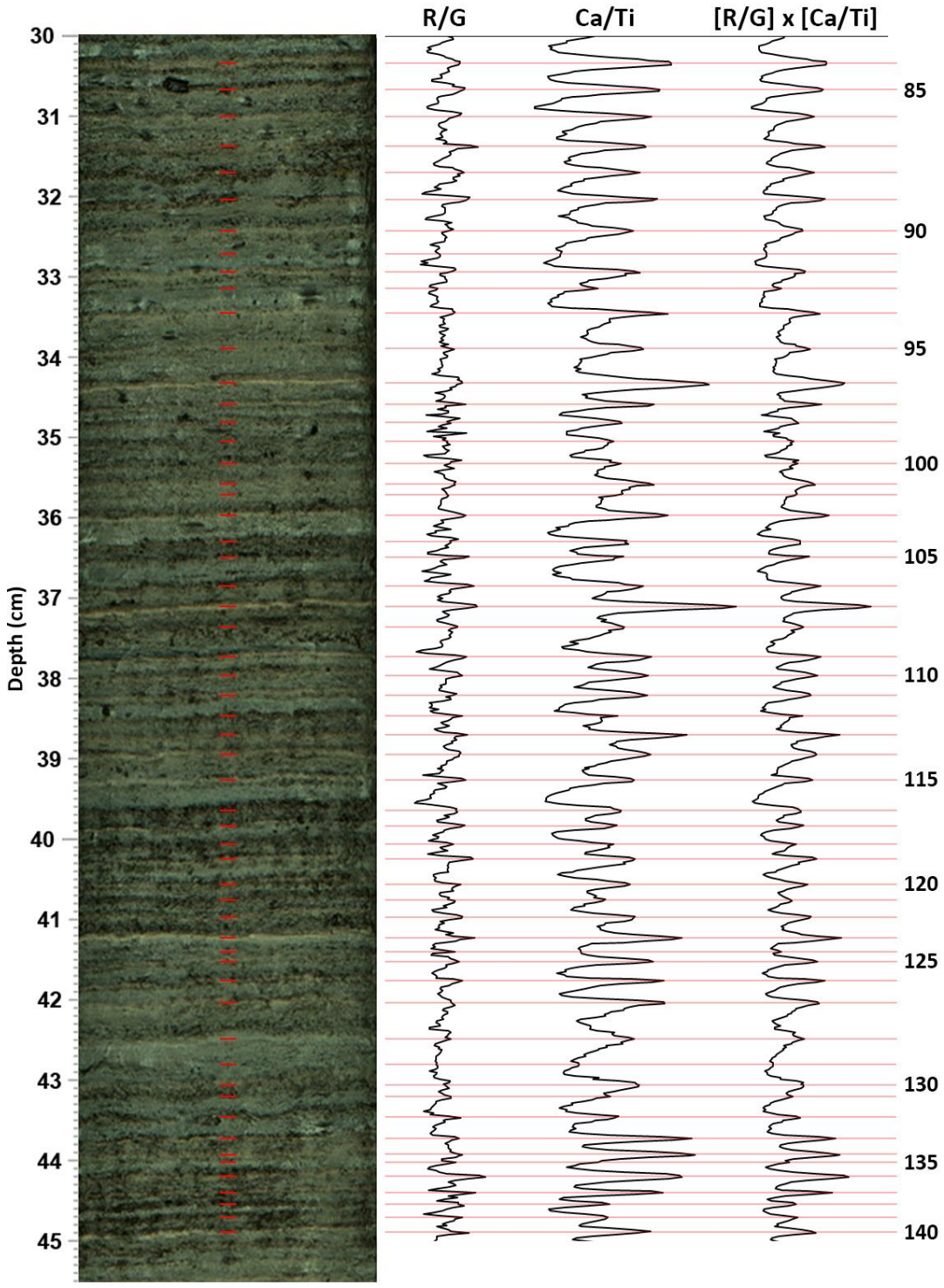
R/G
Ca/Ti
[R/G] x [Ca/Ti]
Depth (cm)
30
31
32
33
34
35
36
37
38
39
40
41
42
43
44
45
85
90
95
100
105
110
115
120
125
130
135
140

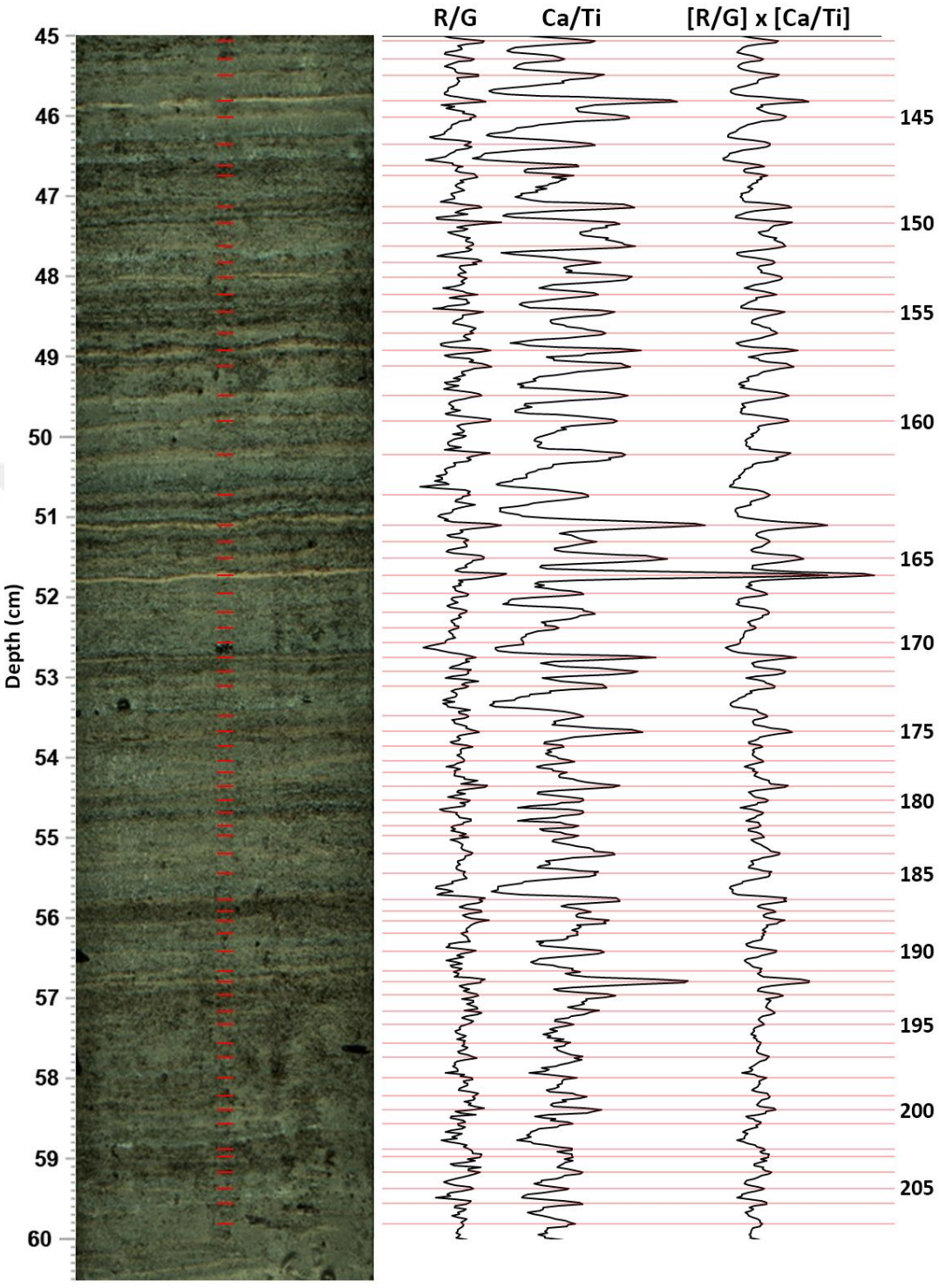
R/G
Ca/Ti
[R/G] x [Ca/Ti]
Depth (cm)
45
46
47
48
49
50
51
52
53
54
55
56
57
58
59
60
145
150
155
160
165
170
175
180
185
190
195
200
205

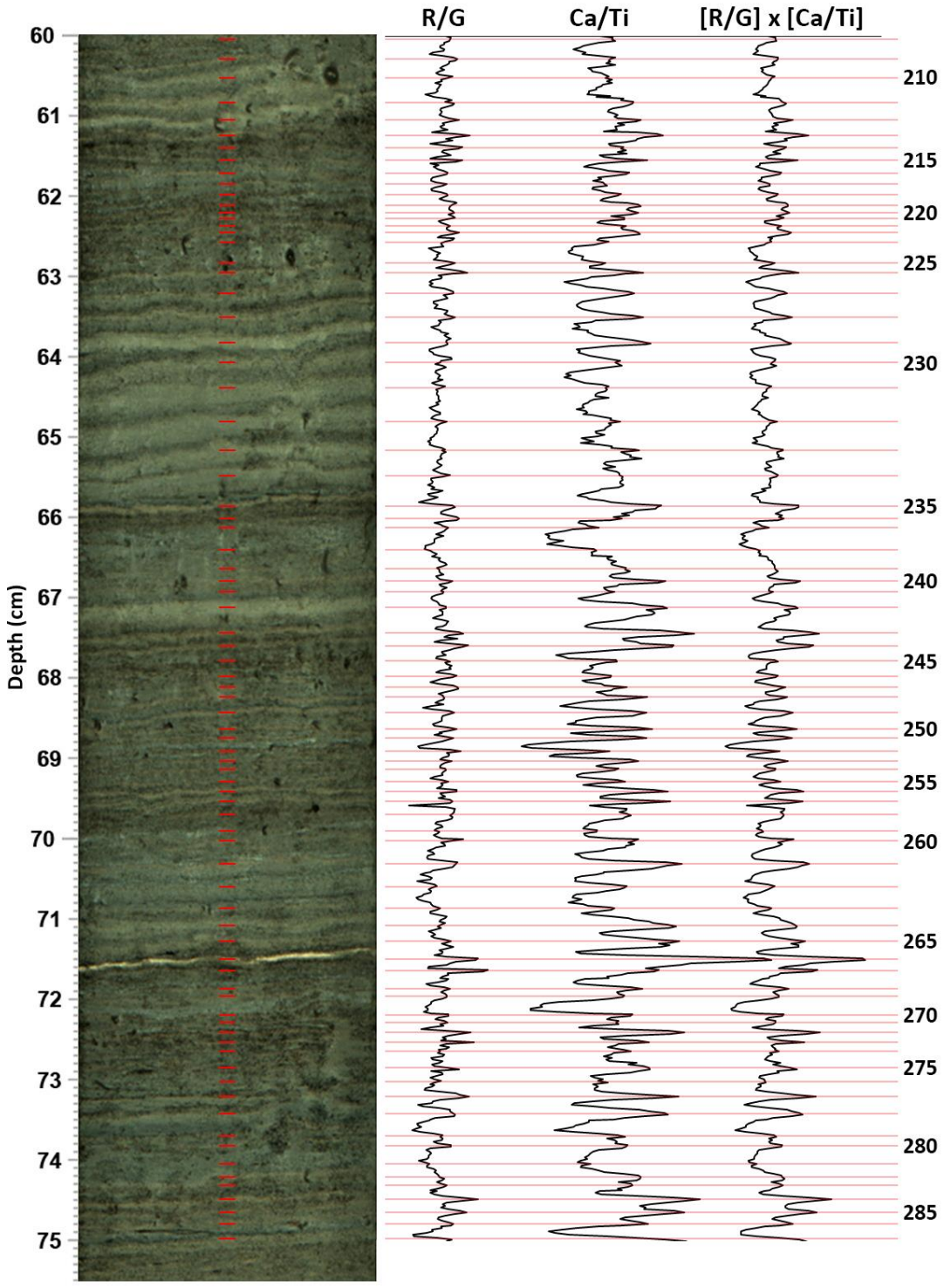
R/G
Ca/Ti
[R/G] x [Ca/Ti]
Depth (cm)
60
61
62
63
64
65
66
67
68
69
70
71
72
73
74
75
210
215
220
225
230
235
240
245
250
255
260
265
270
275
280
285

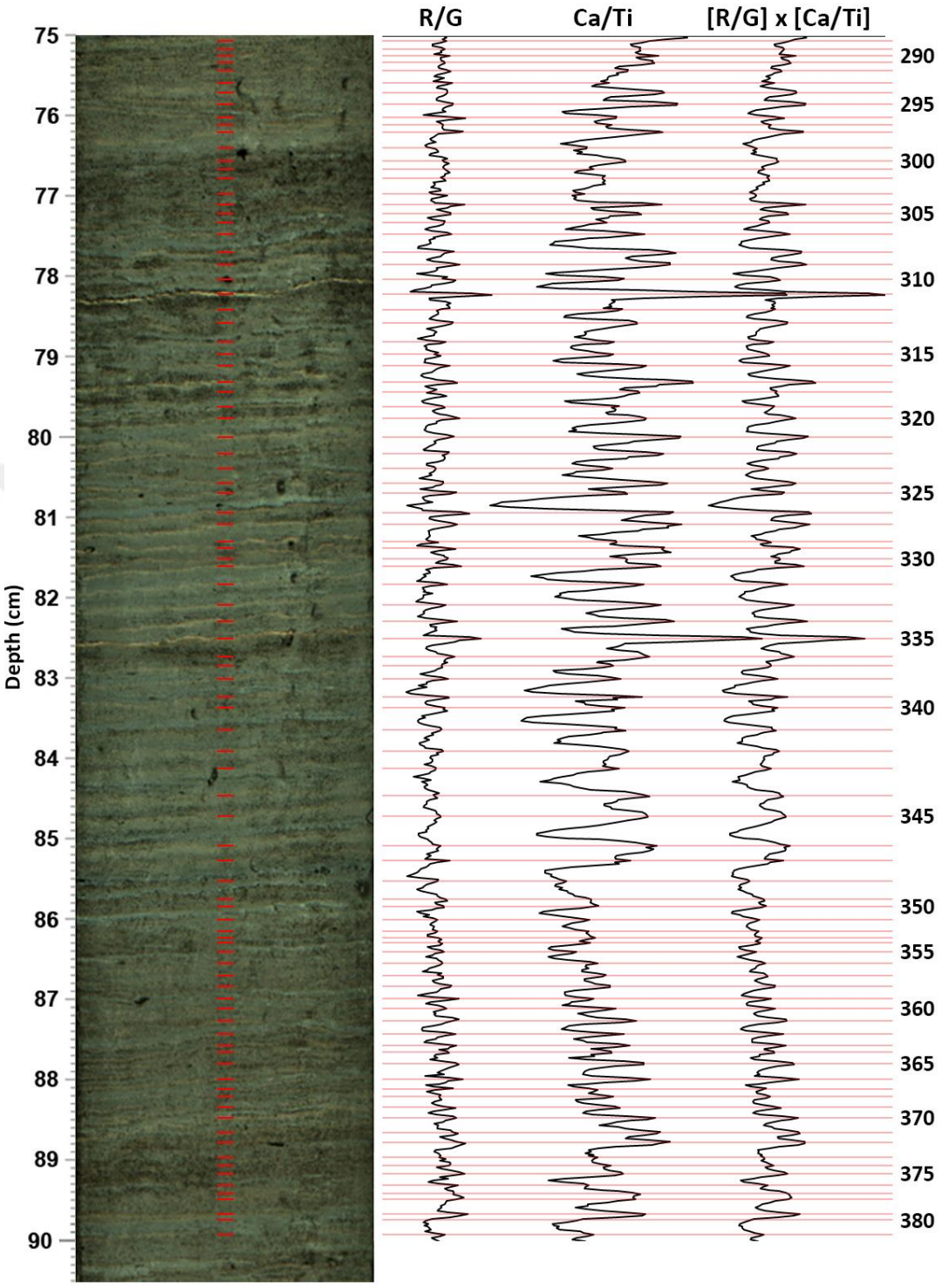
R/G
Ca/Ti
[R/G] x [Ca/Ti]
Depth (cm)
75
76
77
78
79
80
81
82
83
84
85
86
87
88
89
90
290
295
300
305
310
315
320
325
330
335
340
345
350
355
360
365
370
375
380

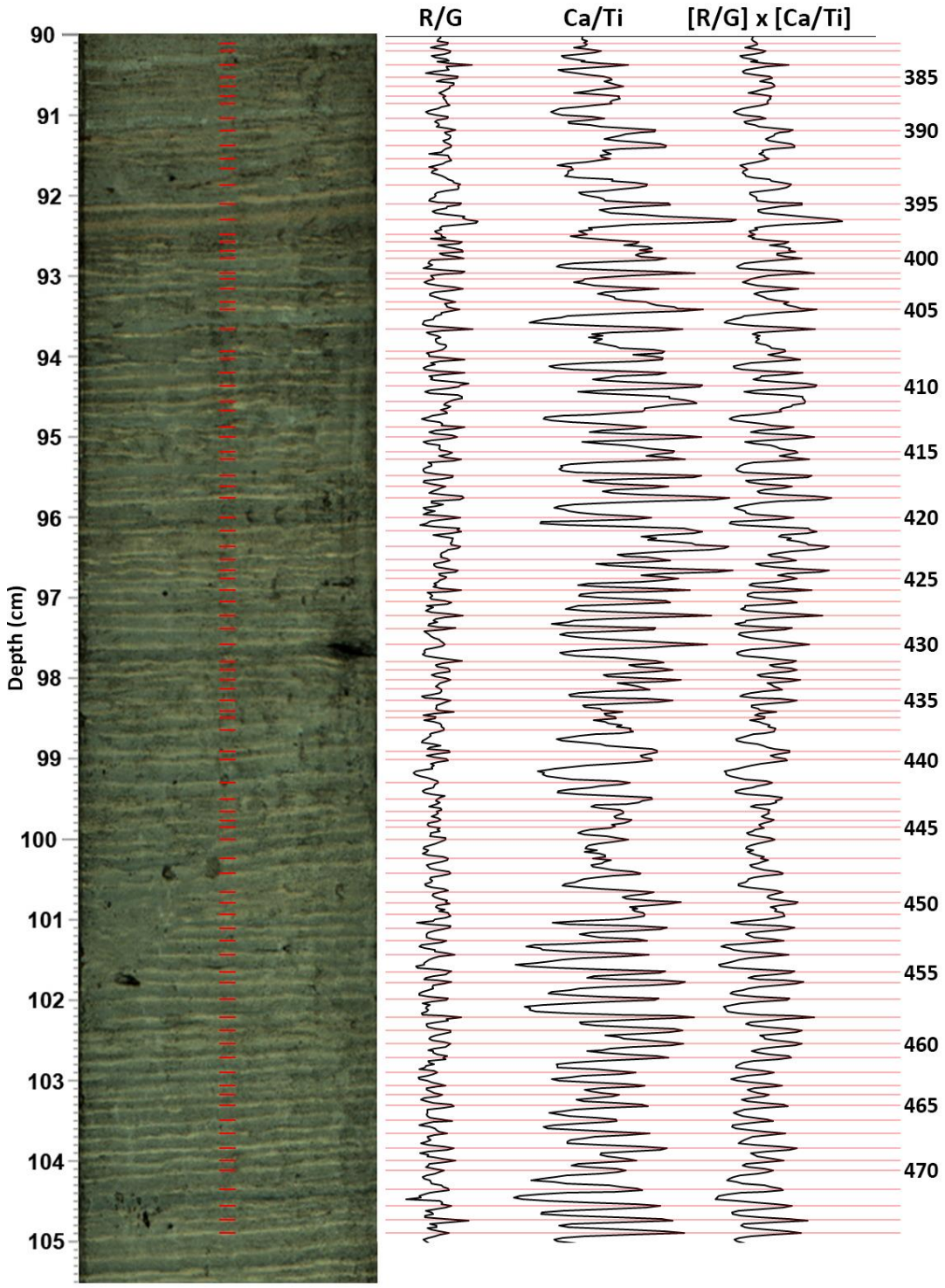
R/G
Ca/Ti
[R/G] x [Ca/Ti]
Depth (cm)
90
91
92
93
94
95
96
97
98
99
100
101
102
103
104
105
385
390
395
400
405
410
415
420
425
430
435
440
445
450
455
460
465
470

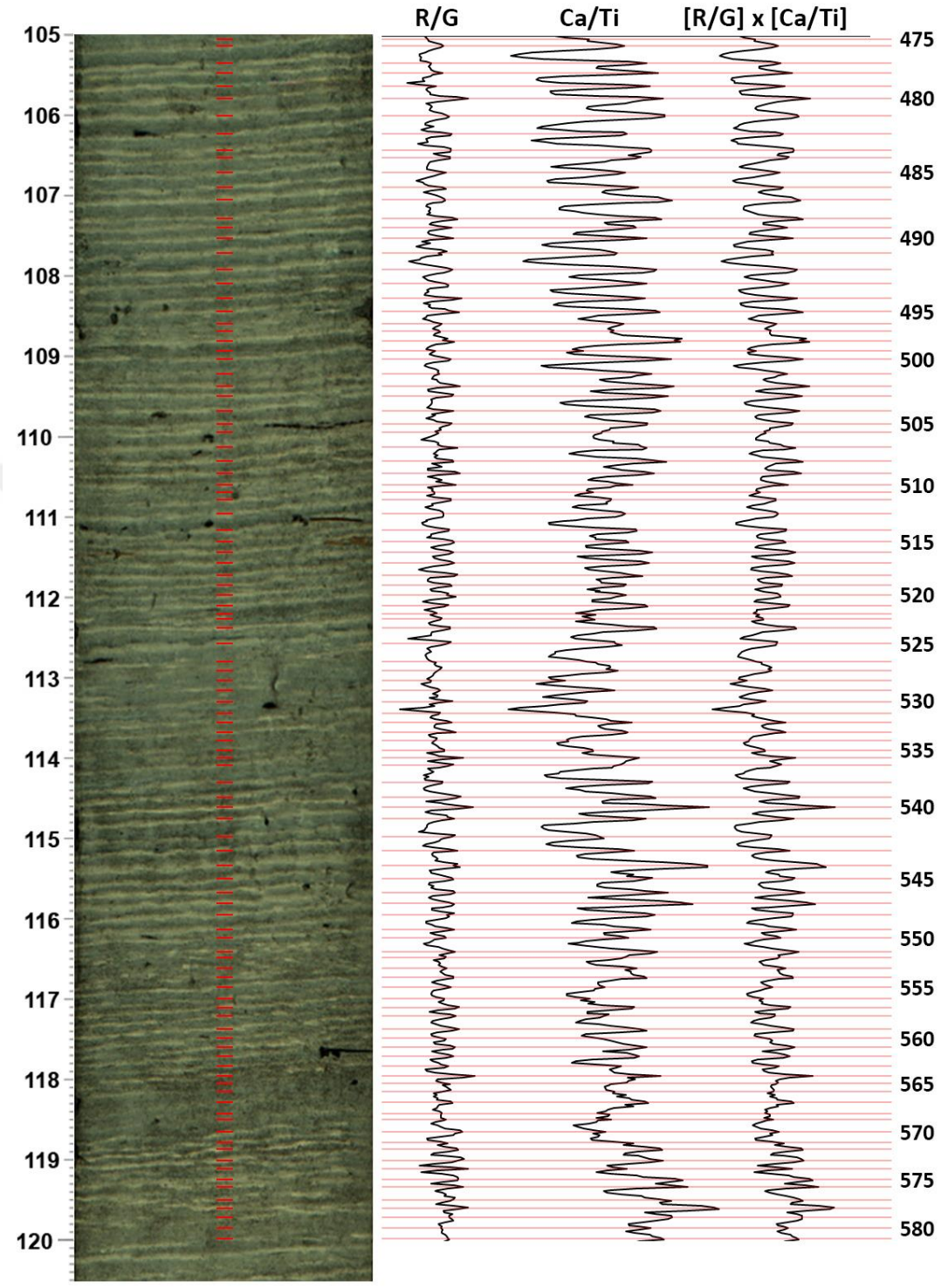
R/G
Ca/Ti
[R/G] x [Ca/Ti]
105
106
107
108
109
110
111
112
113
114
115
116
117
118
119
120
475
480
485
490
495
500
505
510
515
520
525
530
535
540
545
550
555
560
565
570
575
580

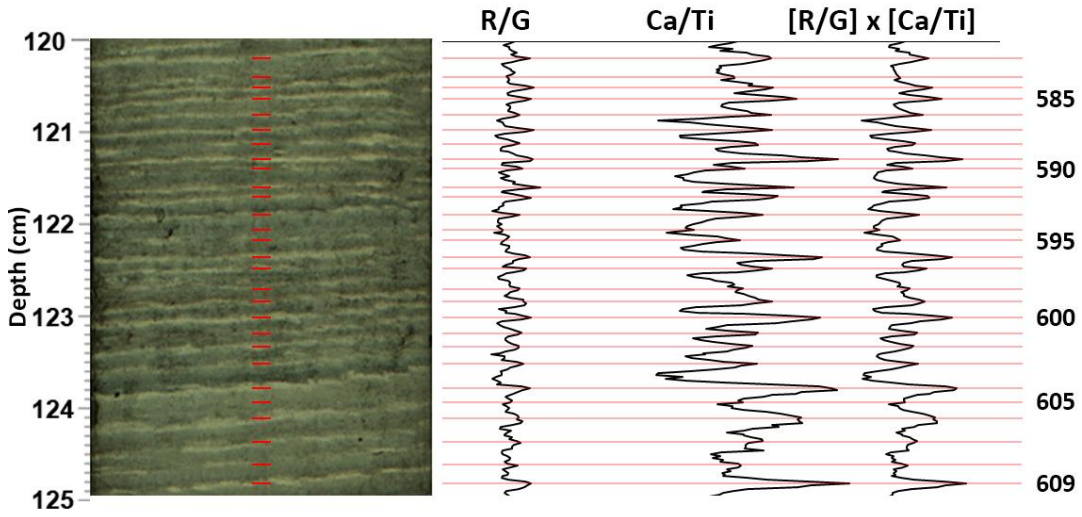
R/G
Ca/Ti
[R/G] x [Ca/Ti]
Depth (cm)
120
121
122
123
124
125
585
590
595
600
605
609